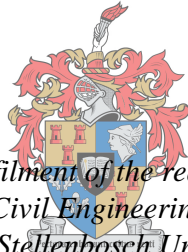# The Liquefaction potential of soils on the Cape Flats established by means of empirical correlation

by

Jurgens Johannes Schoeman

*Thesis presented in fulfilment of the requirements for the degree of
Master of Engineering in Civil Engineering in the Faculty of Engineering
at Stellenbosch University*

UNIVERSITEIT
iYUNIVESITHI
STELLENBOSCH
UNIVERSITY

100
1918·2018

Supervisor: Ms N. Fouche

December 2018

# Declaration

By submitting this thesis electronically, I declare that the entirety of the work contained therein is my own, original work, that I am the sole author thereof (unless to the extent explicitly otherwise stated), that reproduction and publication thereof by Stellenbosch University will not infringe any third-party rights and that I have not previously in its entirety or in part submitted it for obtaining any qualification.

*Date: December 2018*

i

# Abstract

Soil Liquefaction is a problem associated mostly with earthquakes and occurs in areas with relatively shallow water tables. During an earthquake, the soil loses strength and stiffness due to the shaking. This results in settlement of silty sands, forcing groundwater out of its pores and up to the surface. The soil is put into a temporary state where the structure of the soil is distressed, resulting in soil particles losing contact and ultimately behaving like a liquid. The Cape Flats, situated in the Western Cape of South Africa, is an area known for flooding in low lying areas during the winter months, especially in informal settlements. The majority of the area is characterised by flat plains, and heavy winter rain cannot drain away due to the soil being saturated and draining canals usually blocked or absent. The soil in this area is also predominantly fine and medium grained silty sand, mostly cohesionless and uncemented, and potentially prone to liquefaction if ground shaking occurs. The Milnerton Fault Line runs through the Cape Flats and was the cause of the large destructive earthquake that struck Cape Town in 1809 and the years thereafter. Volcanoes of bursting sand and mud were reportedly seen all over the low-lying areas. Therefore, it is important to know whether liquefaction can occur in the Cape Flats during seismic events.

Empirical correlation methods from proven studies were used to determine if the soils from the Cape Flats are susceptible to liquefaction during shear, induced by earthquakes. The testing methods used were the Piezocone Penetrometer and the Standard Penetration Test. Critical State concepts were also applied. Determining areas where the soils might be potentially dilative or contractive were established from literature. Soils that are potentially contractive are generally loose and potentially liquefiable. Soils that are dilative in nature are generally dense and should resist flow liquefaction. The use of the Dynamic Probe Super Heavy (DPSH) test was also included in the study due to limited access of SPT testing done on sands within the study area. The DPSH test also provides an equivalent SPT-N value and was essentially used in the same calculations. Results from the SPT and CPT tests indicated that the majority of soils in the study area are susceptible to liquefaction within the first 1.0 – 2.0 metres below ground.

Soil samples obtained from within the study area as well as pre-graded soil samples were tested on a custom made vibrating table. Samples were graded to form uniformly graded, gap graded and well graded samples. The soils were saturated to 100% and vibrated at accelerations of 0.15g and 0.25g. These are Peak Ground Accelerations that can be expected for an earthquake in South Africa. The fact that denser soils have a larger or longer resistance to liquefaction was also proven in the laboratory on the vibrating table. Samples that were in a loose state liquefied much quicker compared to samples that were compacted and denser. Well graded and gap graded samples also resisted liquefaction for longer compared to that of uniformly graded samples.

# Opsomming

Grondvervloeïng is 'n probleem wat meestal gepaardgaan met aardbewings en gebeur in areas met redelike vlak watertafels. Sanderige grond verloor sterkte tydens `n aardbewing. Dit veroorsaak dat sanderige grond versak en lei daartoe dat water uit die porieë forseer word. Die grond gaan dan deur `n tydelike fase waar dit soos `n vloeistof reageer. Die Kaapse Vlaktes, geleë in die Wes-Kaap van Suid Afrika, is `n area alombekend vir vloede in laagliggende dele tydens winter. Die grond in die area is ook meestal fyn en medium gegradeerde sand, los en moontlik vatbaar vir vervloeiing tydens `n aardbewing. Die Milnerton-foutlyn strek deur die Kaapse Vlaktes en was die oorsaak van een van Kaapstad se grootse aardbewings in 1809. Vulkane van sand was glo gesien, en dit is dus belangrik om te bevestig of  grondvervloeiing hier kan plaasvind.

Empiriese vergelykings van erkende studies was gebruik om te bepaal of grond op die Kaapse Vlaktes grondvervloeiing kan ondergaan tydens `n aardbewing. Die toets metodes was die van die Standaard Penetrasie Toets (SPT) en die die Keël Penetrasie Toets (CPT). Kritiese fase konsepte was ook toegepas. Dig en goed gekompakteerde grond kan uitsit en moontlik vervloeiing weerstaan. Los grond kan inkrimp of versak tydens `n aardbewing en moontlik vervloeiing ondergaan. Beide die twee fases was ook ondersoek. Dinamiese Penetrasie Super Swaar toetse (DPSH) was ook ingesluit by die SPT data omdat net n beperkte hoeveelheid van SPT data beskikbaar was. Die DPSH lewer `n soortgelyke waarde as die van die SPT, sodat altwee die toetse se data in die tesis gebruik was. Data dui daarop aan dat al die studie areas grondvervloeiing kan ondervind tydens `n aardbewing, veral in die eerste 2 meter onder grondvlak.

Grondmonsters was getoets op n vibrasie tafel, spesiaal gebou vir die studie. Monsters was gegradeer om verskillende verhoudings van fyn tot grof te kry. Die monsters was dan tot 100% versadig, met water, en gevibreer teen n versnelling van 0.15 en 0.25g. Laasgenoemde is die verwagte Piek Grond Versnelling (PGA) wat verwag kan word tydens 'n aardbewing in Kaapstad en Suid-Afrika. Digter grond het tydens toetse langer vervloeiing weerstaan. Monsters met a groter aantal fyn en growwer verhouding het ook langer vervloeiing weerstaan vergelykend met medium grote eenvormige gegradeerde sand.

# Acknowledgments

This thesis would not have been possible without the support of my study leader, Ms N. Fouche, my co-supervisor Professor P. Day, and my employer, Mr J. Yates at Core Geotechnical Consultants.

Professor P. Day also helped considerably towards making CPT testing possible and made valuable contributions towards this project.

Mr R. Briedenhann, Collin and Gavin from the geotechnical laboratory for helping with much needed testing and recommendations.

I would also like to thank Mari Scott, who continuously helped with graphs and data management.

Working with Visual Basic Applications and iteration calculations was made easy with the help of Justin Schietekat, a dear friend.

Acknowledgement is also owed to Core Geotechnical Consultants and Fairbrother Geotechnical Engineering, both in Cape Town, that supplied valuable data for use in this project.

Lastly, thanks to my parents and God who gave me the opportunity and continuous support.

# Table of Contents

# LIST OF TABLES

# LIST OF FIGURES

# LIST OF EQUATIONS

# LIST OF SYMBOLS AND ABREVATIONS

CD                Contractive/Dilative (for boundary)

CPT               Cone Penetration Test

CRR               Cyclic Resistance Ratio

CSR               Cyclic Stress Ratio

CSL               Critical State Line

DCP               Dynamic Cone Penetrometer

DPSH              Dynamic Penetrometer Super Heavy

Fr                Normalised friction ratio

Fs                Factor of Safety

Ic                Soil Behaviour Type Index

MSF               Magnitude Scaling Factor

PGA               Peak Ground Acceleration

Qtn               Normalised cone penetration ratio

SBT               Soil Behaviour Type

SPT               Standard Penetration Test

$a_{max}$         Peak ground surface (horizontal) acceleration.

$g$               Acceleration of gravity.

$\tau_{max}$      Maximum earthquake induced shear strength.

$\sigma_v$        Total overburden stress at depth of investigation

$\sigma'_v$       Initial effective overburden stress (vertical) at depth of investigation

$r_d$             Shear stress reduction coefficient to adjust for the flexibility of the soil

xiii

# 1  Introduction

## 1.1  Background

Soil Liquefaction is a problem associated mostly with earthquakes and occurs in areas with relatively shallow water tables. During an earthquake, the soil loses strength and stiffness due to the seismic movement. This results in settlement of soils such as silty sands, forcing pore water out of its pores and up to the surface. The soil is placed into a temporary state where the structure of the soil is distressed, causing grains to lose contact and ultimately behaving like a liquid (Sarsby, 2000).

Liquefaction of soils has been observed in almost all large earthquakes. The first time it was noted on an engineering level, with empirical correlations in mind, was during the 1964 earthquake in Niigata, Japan. This earthquake caused serious problems to nuclear power stations, dam walls and underground services. Sand boils are one of the most common observed effects of liquefaction. It has a volcanic form and is the result of excess pore water pressure within the soil. A channel is formed by the pore water pressure and this carries soil upwards where it sometimes breaches the surface and forms a sand boil (Sarsby, 2000). Earthquakes aren't the only source of liquefaction. Heavy ground movement caused by construction machinery or other geological events can also cause the ground to liquefy. Heavy traffic movement has been noted to cause liquefaction at some major road crossings and bridges where the water table is virtually at ground level (Terzaghi et al., 1996).



*Figure 1.1: Sand Boil at a rail yard in the United States (Davids, 2001)*

The Cape Flats, situated in the Western Cape of South Africa, is an area known for flooding in low lying areas during the winter months, especially in informal settlements. The majority of the area is characterised by flat plains, and heavy winter rain cannot drain away due to the soil being saturated and draining canals usually blocked or absent. The soil in this area is also predominantly fine and medium grained silty sand, mostly cohesionless and uncemented, and potentially prone to liquefaction if ground shaking were to occur. There is a considerable number of low-cost, government-funded houses on the

Cape Flats. These low-cost houses have been built with cost saving in mind and in most cases, have not considered the effects of natural disasters. The flats are also home to Khayelitsha, one of the largest informal settlements in the country (NKuna, 2016).



*Figure 1.2: Informal Houses in Khayelitsha (Hutchings, 2015)*



*Figure 1.3: Government Subsidised House in Delft (NKuna, 2016)*

Earthquakes are mostly associated with fault lines, and the Milnerton fault line runs through the densely populated Milnerton area, south towards the Cape Flats and Mitchells Plain. It runs close to the Koeberg Nuclear power station and Cape Town's city centre. The city centre itself is in part built on reclaimed land. Reclaimed land has a bad reputation when it comes to liquefaction due to the nature of soils being used in construction and the relatively loose state it is deposited in. Large scale liquefaction within reclaimed land was recently seen in the earthquakes that occurred in Christchurch, New Zealand, and Tokyo, Japan.

## 1.2    Problem statement

Soil Liquefaction has been studied thoroughly in developed countries such as Japan, and methods have been created to indicate if a soil is susceptible to soil liquefaction. Soil properties and conditions are however not the same everywhere. For soil to liquefy, several requirements must be met. Normally a

saturated or partially saturated soil with fine graded silty sand is the ideal combination for liquefaction, combined of course with an earthquake or considerable vibration from some source (Rauch, 1997).

Soil that is uncemented, loosely packed, uniformly graded, and/or have large grain sizes (or similar grain sizes) does not compact very well and leaves space for water in the pores. During shaking, loose soil tends to contract. This results in an increase in pore water pressure (in saturated soil), and the pressure that cannot be dissipated fast enough becomes the excess pore water pressure build up. Since water is not compressible, and the surrounding soil is also saturated, it forces the water to move upwards. The main effect is not water movement but an increase in pore water pressure.

On level ground, this can lead to lateral spreading and sand boils, which could ultimately lead to bearing capacity failures and large differential settlements. On uneven ground, slope failures can occur resulting in landslides and in both cases considerable financial damage. The effects of liquefaction within the Cape Flats have been studied only partially, and a better understanding of possible risks and associated complications is needed, hence this study.

## 1.3    Objectives

The primary objective of this study is to determine whether:

1.  The sands of the Cape Flats are potentially liquefiable during a seismic event, with the use of:
    a.  SPT and CPT testing and correlating the results with known empirical formulas.
    b.  Laboratory testing, by testing saturated soil samples on a vibration table to simulate an earthquake.

The secondary objectives of this study are to:

1.  Determine, through available literature and empirical correlations, what the minimum density and soil properties would have to be to minimise the risk of a soil liquefying during a seismic event.
2.  Determine the ideal density for a soil to resist liquefaction during testing on a vibration table and what effect soil grading has on liquefaction.

## 1.4    Contribution of Research

Liquefaction is studied around the world in developed countries. New and updated work is frequently published, and research is continuous. In South Africa, limited research has been done on liquefaction, mostly within mine tailings (Puri & Kostecki, 2013), and even less research towards the sands on the Cape Flats. Work that has been done in South Africa is outdated, mostly because these studies used methods that were last updated in the 1970s (Parker, 1991). Since then, these methods were continuously updated and improved, and new techniques were developed to better determine the

3

liquefaction potential of soils (Andrus & Stokoe, 2000; Idriss & Boulanger, 2010; Robertson, 2010; Seed, et al., 2003).

This study, as far as the author knows, is also the first one to test sand from the Cape Flats on a vibrating table to simulate actual earthquakes. An accelerometer was used to test samples at various ground accelerations. Testing methods such as the SPT and CPT are the most common when using the results in empirical correlations with soil liquefaction. This study attempted to incorporate more widely used testing methods such as the DPSH. The DPSH is more cost effective and mobile, meaning they could be used in many more markets and areas where conventional testing methods, such as the SPT and CPT, are not affordable.

## 1.5    Limitations

Several limitations and constraints were present throughout the research and practical work of this thesis. The following are general limitations, and if any further research is proposed, this will have to be addressed.

- A larger amount of testing could have been carried out with additional funding. These tests include more SPT and CPT (in-situ) testing as well as more large-scale vibration table testing in the laboratory.
- Location, access and safety. A major setback was that of finding suitable areas for sampling within the Cape Flats that were safe and allowed access for sampling and measurements.
- Small cost-effective plastic containers were used in the vibration table testing. This meant that several assumptions had to be made, such as the effect of friction on the container walls and a potential increase in pore water pressure due to water being unable to dissipate during shear.

## 1.6    Report Layout

This thesis consists of six chapters and are set out as follows:

- Chapter 1: Introduction. This chapter summarises the objectives, contribution to research and limitations encountered during this project.
- Chapter 2: Literature Review. This chapter aims to summarise the basic and necessary knowledge and background data needed in understanding this thesis. This explains the use of actual testing methods and their empirical correlation.
- Chapter 3: Methodology. The process followed with actual testing, data gathering and implementation. This chapter also includes assumptions made due to limitations and complications encountered.

- Chapter 4: Results and Discussions. This chapter includes the actual data obtained during testing, sampling and calculations. The data obtained during the research is also reviewed and compared to that of literature studies.
- Chapter 5: Conclusions and Recommendations. The final chapter summarises and concludes observations made throughout the study. It also highlights suggested recommendations for future research and testing within the field of liquefaction and with empirical correlations.

# 2   Literature Review

## 2.1   Introduction

This chapter will present the reader with the necessary background about soil liquefaction and the geology of the area investigated. It will further provide information regarding the empirical correlations as used to determine the susceptibility of a soil to undergo liquefaction. Some of the various testing methods used for liquefaction determination and how they relate are also discussed.

## 2.2   The Cape Flats

### 2.2.1   Location

The area of investigation forms part of the greater Cape Town Metropolitan City. Figure 2.1 indicates the predominantly sand-covered areas over much of the Peninsula. The majority of the Cape Flats is situated south of the Bellville-Cape Town railway line, and between the Muizenberg-Cape Town and Bellville-Eersterivier railway lines (Segun  et al., 2010).
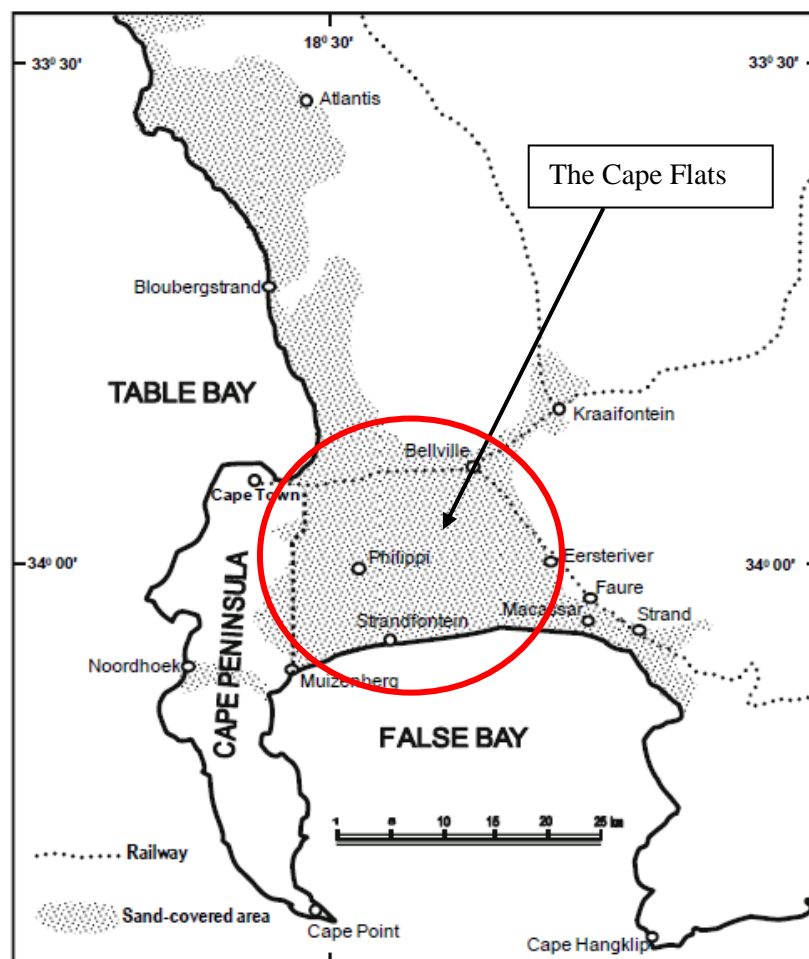


*Figure 2.1: General location of the Cape Flats (Segun  et al., 2010)*

6

### 2.2.2    Geological Setting

#### 2.2.2.1    Geological History

To better understand the properties of the sediments within the Cape Flats, one needs to know the origin and depositional history of the area. The events that led to the geology of greater Cape Town and its surroundings occurred over millions of years and went through various geological changes. The area as we know it today was once under water, frozen beneath a glacier and heated by intrusive volcanism (Norman & Whitfield, 2006).

Most of the continents and land masses observed today in the southern hemisphere were derived from the breakup of the super continent Gondwana millions of years ago. The resulting rift separated southern Africa from the Falkland Plateau. The Agulhas Sea developed from large graben structures, and the resulting sediments that accumulated in this rift consolidated to form the Cape Supergroup (Norman & Whitfield, 2006). The Karoo Supergroup is not present in the area, but its development played a crucial role in the sediments found around Cape Town today. The Karoo Supergroup came into existence during the early Permian Period, when the Paleo–Pacific plate was subducted under the Falkland Plateau. The subduction of the Paleo-Pacific plate created a series of mountains that later eroded into the Karoo Sea. The Falkland Mountains weathered to an extent where the originally deposited Cape Supergroup became visible again. The Cape Supergroup resisted weathering, by being covered with an upper layer rich in quartz and consisting of mostly quartzitic sandstones (Thamm & Johnson, 2009).

Much of the Cape Flats consists of fine, uniform sand with shallow water tables. The sands are aeolian, meaning they were transported by wind, and blown all over the area, mostly from beaches over thousands of years. The sand itself originated from marine environments, as most of southern Africa was once under water. Beneath the sand the bedrock mostly consists of Malmesbury shale, and Cape Granite exist in smaller western regions of the area (Roberts  et al., 2006; Nichols, 2009). Weathering and erosion over time formed the contemporary landscape, leaving fine, uniform sediment behind.

The Malmesbury group ranges from sandstone to shale and is the oldest known formation in the Cape Town region. Sediments from strong turbidity currents and marine slumping sediments settled, and over time they became metamorphosed due to the pressure of overlying newer formations. These rocks became the Malmesbury Group (Norman & Whitfield, 2006). By the end of the Precambrian, around 620 million years ago, the Peninsula granite intruded into the Malmesbury shale as a batholith. Over time the granite weathered and eroded. This, along with the Malmesbury group, became the basement layer for younger Table Mountain Group sandstones.

At around 450 million years ago, sediments started settling in the shallow marine environment that was present at that time. Environments consisted of delta flats and tidal streams. After lithification by pressure, these sediments became folded to form part of the Cape Fold Belt. This was followed by the

Graafwater Formation, consisting of pale, dark coloured sandstones, silt and light-coloured shale. Deposition of the Graafwater Formation was followed by the Peninsula Formation, containing current-bedding (e.g. water-formed) pebbles and conglomerates. This is an indication of faster flowing water and high energy environments.

By the end of the Peninsula Formation, a small ice age was developing. At the time, the continent was much further south, and the deposition of the Pakhuis Formation, a tillite, took place. The Pakhuis Formation now forms the highest part of Table Mountain (Roberts et al., 2006; Thamm & Johnson, 2009). Over the years many of these formations either eroded away to the basement rocks of the Malmesbury Group, mostly shale and sandstone, or granite of the Peninsula Pluton. During the early years of the Cenozoic Era, approximately 66.0 to 2.0 million years ago, calcareous silty sands and limestones were deposited while most of the area was a shallow marine environment. During this time, peat lenses formed, and marine clays settled on the basement. By the end of the Neogene Period, 23 to 2.6 million years ago, the area became drier and aeolian sediments settled during the Quaternary Period, 2.3 million years ago to present. Most of these sediments were derived from weathered sandstones and shales. Figure 2.2 indicates the general geology of greater Cape Town and the location of the Cape Flats. The Cape Flats primarily consists of sediments from the Quaternary Period.
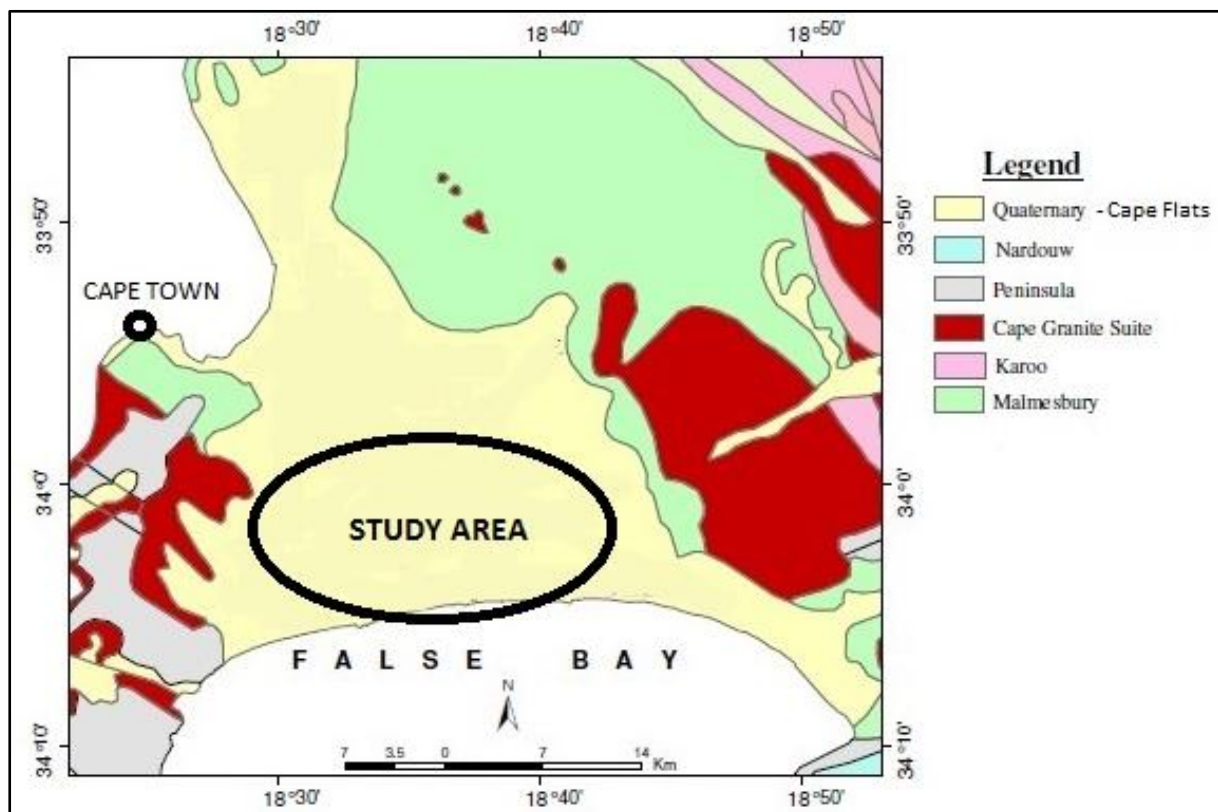


*Figure 2.2: Cape Town Geology and location of the Cape Flats (Segun et al., 2010).*

8

### 2.2.2.2    Geology of the Cape Flats

Sands from the Cape Flats are mainly derived from two sources. These are weathering and beach sands (Segun  et al., 2010). Sands weathered away from rocks derived from the quartzitic sandstones of the Malmesbury Group and Table Mountain Group. With time, these weathered materials deposited within a shallow marine environment. Today, fish fossils and calcretized sands can be found within these Formations.

Beaches in the area consist of aeolian dune sands that move continuously. These were mostly deposited after the formation of the marine sands and are generally loose and less cemented (Segun  et al., 2010). Two prominent Formations exists within the Cape Flats, namely the Springfontein and Witzand Formations. The Springfontein Formation comprises well sorted, fine to medium grained, quartz sand. Near the coast, it is light greyish and white to buff in colour. Cross-bedding, calcrete and marine fossils are also observed sporadically throughout the Formation. The Springfontein Formation exhibits a thickness of up to 25 m in places, and borehole data indicates up to 65 m near Atlantis (Theron  et al., 1992). Atlantis is however outside of the Cape Flats area and sands are believed to be up to 35 m thick in the Cape Flats area (Theron  et al., 1992). The number of organic fines increases further away from the coast (Roberts  et al., 2006). The Springfontein Formation overlies the Witzand Formation in areas towards the west. The Springfontein Formation is characterised as having intermittent peat layers of 3 to 5 metres thick. Near the area of Fishhoek, the Springfontein Formation overlies the Elandsfontein Formation. The latter has been identified through borehole data and consist of coarse grained quartz-rich sands that is underlined by weathered granites of the Cape Granite Suite (Theron  et al., 1992). The Witzand Formation is primarily the product of calcrete rich dune sands and is essentially aeolian. These soils are cemented in places and appear as dense calcrete lenses due to the presence of the calcrete rich sands. The prominent dunes along False Bay are from the Witzand Formation. These dunes are rich in shell fragments and mostly loose in consistency. However, dense cemented calcrete zones exist throughout (Theron  et al., 1992).

### 2.2.3    Seismic Activity and Earthquakes

South Africa does not lie near any major plate boundaries. Tectonically speaking, Cape Town, and even the rest of South Africa, is stable and large earthquakes are not very common. Nevertheless, the area has a history, Table 2.1, of relatively minor earthquakes and some have caused considerable damage to infrastructure and services leading to financial losses.

Earthquakes are measured either by a magnitude scale or an intensity scale. The magnitude scale is obtained by physically measuring the energy released during a seismic event, whereas the intensity scale uses a ranking system by profiling observed damages from a seismic event. The magnitude is measured commonly on the Richter Scale, while Intensity uses the Modified Mercalli Scale. The Richter scale, invented by Charles F. Richter in 1934, measures the seismic waves from an earthquake, adjusting

them to the depth and distance from the epicentre. In 1902 Giuseppe Mercalli invented the Mercalli scale, and since being modified (after observing larger earthquakes) it is called the Modified Mercalli Scale. The scale uses twelve different levels of earthquake damage observed (De La Harpe, 2015). Table 2.1, adapted from De La Harpe (2015) summarises some of the earthquakes around the Cape area in the last 200 years.

*Table 2.1: Some of the earthquakes in the greater Cape area (Toerien, 2014)*

| Date | Region | Magnitude (Richter) | Intensity (Mercalli) |
|---|---|---|---|
| 4/12/1809 | Cape Town | 6.3 | VIII |
| 2/6/1811 | Cape Town | 5.7 | VII |
| 19/6/1811 | Cape Town | 5 | VI |
| 14/8/1857 | Western Cape | 5 | VI |
| 13//9/1899 | Cape Town | 5 | VI |
| 9/10/1921 | Tulbagh | 5 | VI |
| 27/8/1963 | Worcester-Ceres | 5 | VI |
| 29/9/1969 | Tulbagh | 6.3 | VIII |
| 2/3/1977 | South Western Cape | 5.3 | VI |
| 31/10/1991 | Ceres | 5 | VI |

Many earthquakes in South Africa are near mines in the northern part of the country and are the result of mining activity (Hartnady, 2003), because of underground blasting that releases tension in the earth, regional stresses, and acid mine drainage that dissolves dolomite. The latter is however mostly associated with small, locally-felt earthquakes.

Earthquakes are triggered by various activities and natural earth movements. Regional stress is the driving force of seismic activity in southern Africa, which originates mostly from continental drift and mid-oceanic ridges (Cichowicz & Kijko, 2006). Figure 2.3 indicates the dominant seismic active areas in South Africa. The blue dots in the northern part of the country are mostly associated with the Kaap-Vaal Craton and mining. The blue dots in the southern part of the country can be related to the Cape Fold belt syntaxis and regional stresses associated with the fold belt (Guzman & Fernandez, 1978).
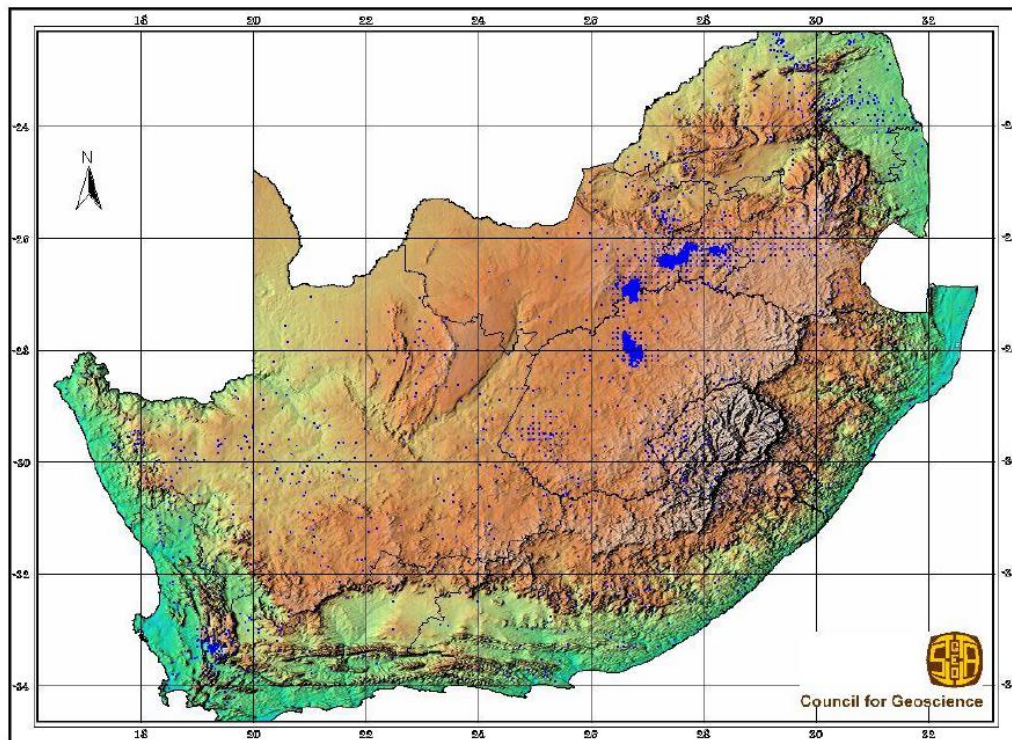
*Figure 2.3: Map of Seismic activity in South Africa (Guzman & Fernandez, 1978)*

Locally, the Milnerton Fault Line runs through the Greater Cape Town and Cape Flats (Hartnady, 2003). Figure 2.4 is a map of the Cape Town region, showing the location of the Milnerton Fault relative to other, previously mapped, faults and dolerite dykes. The point JB marks the area of maximum destruction at Jan Biesjes Kraal during the earthquake of 4 December 1809. This was one of South Africa's largest earthquakes that took place as result of tension relief along the fault line and regional stress surrounding it (Hartnady, 2003).

The earthquake that occurred during the night of 26 September in 1969 is known as the most destructive earthquake to ever hit South Africa. Large scale damage was reported in the towns of Wolseley, Tulbagh, Ceres and Worcester. Seismic stations in this area were not operational yet, and a magnitude of 6.3 on the Richter scale was estimated from the Modified Mercalli Scale. In later years, the Peak Ground Acceleration (PGA) was determined at approximately 0.22g. The Saron-Groenhof Fault, associated with the Cape Fold-belt, was blamed for this earthquake (Hartnady, 2003).
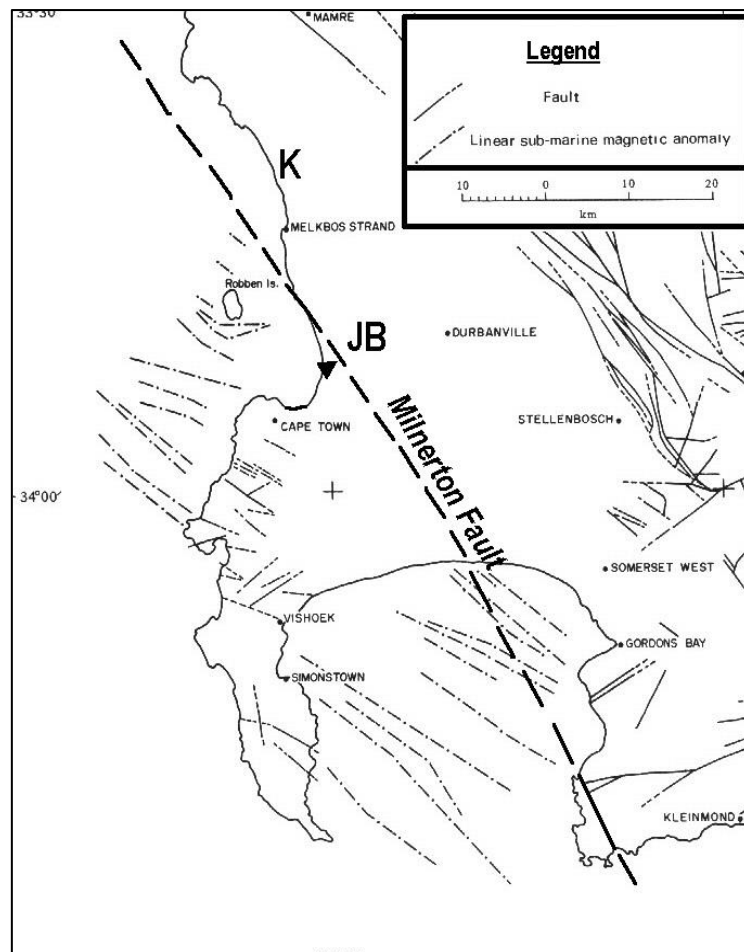
*Figure 2.4: Location of the Milnerton Fault Line in Cape Town (Hartnady, 2003)*



*Figure 2.5: Destruction in Tulbagh after the 6.3 Magnitude earthquake in 1969 (Toerien, 2014)*

12

The Council for Geoscience in South Africa published ground acceleration maps for South Africa after a series of seismic hazard assessments.

Figure 2.6 indicate the probable Peak Ground Acceleration (PGA) for areas in southern Africa, which is measured in units of gravity acceleration (g). The PGA is equal to the maximum ground acceleration during a seismic event and is the same as the amplitude of the largest recorded acceleration on an accelerogram measuring device. Richter scale generally measures total energy, whereas the PGA is an indication of how hard or fast the earthquake shakes the earth. It can be inferred from this PGA map (Figure 2.6), that the earthquake that took place in 1969, with a PGA of 0.22, is relatively accurate for the examined area. This assumption is also confirmed by comparing the earthquake that occurred near Cape Town in 1809, to that of PGA values with the same magnitude.
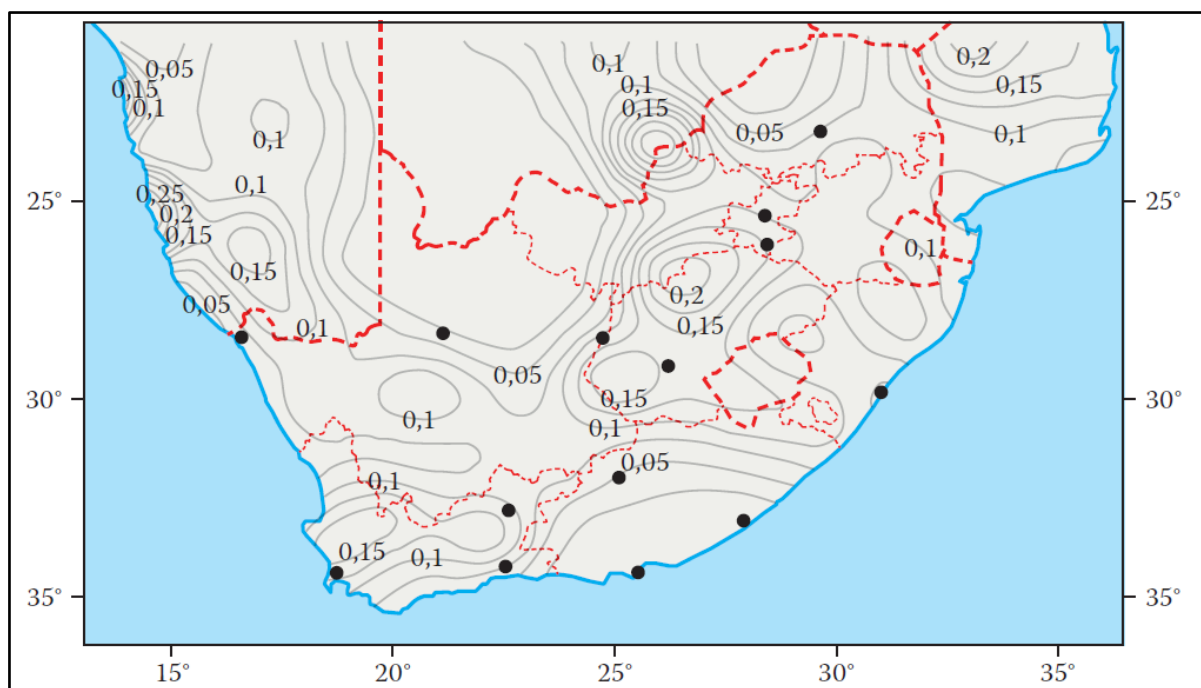


*Figure 2.6: PGA map for southern Africa (Wium, 2010)*

The maps can be used to determine the maximum destruction that is possible after a potentially large seismic event. The PGA values can also be used in simulations and laboratory testing to observe what effect such a PGA value will have. The PGA map in Figure 2.6 will be used in this study as a reference point for the probable PGA's to be expected in the Cape Town area.

## 2.3    Liquefaction

"*The sudden drop of shear strength under undrained conditions from the yield strength to the substantially smaller critical state strength is known as liquefaction*" (Terzaghi  et al., 1996).

Liquefaction is defined differently by various authors and industry specialists. When a saturated or partly saturated and unconsolidated soil undergoes vibration, it tends to liquefy or act as a fluid under the right circumstances. More technically, cohesionless and saturated soils lose strength and shear resistance during vibration, due to pore water pressure build-up within the pores (Rauch, 1997). A soil that has zero effective stress because of the hydraulic gradient that has been reached due to seepage, is said to be liquefied (Craig, 2010). In addition, liquefaction can be defined as the temporary transformation of a soil into a liquid state. This could be due to a sudden loss in shearing resistance, caused by the collapse of the grain structure, which is associated with temporary increase in pore fluid pressure (Allaby, 2008). Liquefaction can be initiated from either shock, such as an earthquake, or sudden loading of the soil due to landslides or structural failure. In general, any failure that arises due to an increase in pore water pressure and a loss of shear strength in the soil can be termed liquefaction (Robertson, 2010). Wei and Yang (2015) define liquefaction as a flow failure because of soil loosening during an earthquake, causing large cyclic shear deformations. This can result in landslides on steep slopes, lateral spreading on near level ground or sand boils, and formation of grabens on level ground. Flow liquefaction also primarily occurs in loose to moderately loose soils (Wei & Yang, 2015).

Cyclic mobility can be described as a certain type of liquefaction, and occurs while an earthquake or shear is taking place. After the earthquake soil will densify and pore water pressure will dissipate, ending liquefaction. Cyclic mobility may occur in both loose and dense soils. Cyclic mobility can also lead to lateral spreading that causes deformations and differential settlement beneath foundations (Idriss & Boulanger, 2010). Cyclic liquefaction can occur during an earthquake, resulting in flow liquefaction. Flow liquefaction can happen during or after the triggering event (Rauch, 1997). As a tremor or earthquake occurs, a form of compaction starts to take place due to seismic loading. This decreases the void spaces and increases pore water pressure within the voids of an undrained soil. Water cannot be compressed, and the only other place for a shallow water table to move is upwards and out of the pores. The resulting effect is water seepage above level ground, and a subsidence of near surface soil. This will cause buildings with shallow foundations to experience large differential settlement (see Figure 2.7).

*Figure 2.7: Differential Settlement due to liquefaction (Yamaguchi  et al., 2012)*

### 2.3.1   Causes and types of soil susceptible to Liquefaction

Several events can cause liquefaction. The most noticeable one is that of earthquakes. Earthquakes can either be in the form of plate movements, or other geological events such as the movement of water, regional stresses, plumes or geysers.

Liquefaction could be initiated by the dynamic input of a single large event, such as a large increment of shear strength from the toe failure of a slope, or continuous shear waves from an explosion (Terzaghi et al., 1996). Heavy construction machinery has also been claimed to be the reason for small scale liquefaction events near building sites. These events are however small and normally do not last long due to the shearing event only being in one area and water pressures dissipating quickly enough to halt the process (Craig, 2010).

Liquefaction has mostly been observed in relatively young soils, younger than the Holocene Age (younger than approximately 1 million years), and in non-plastic or slightly plastic soils. These relatively young soils are also uncemented, silica-based sandy soils. Furthermore, liquefaction events occur in areas with shallow water tables, relatively flat ground and generally within 12m of ground surface (Idriss & Boulanger, 2010; Gandomi  et al., 2013).

The physiognomy of the soil is defined by the size, gradation, shape and arrangement of the grains. These properties are determined by the geological history of the area and depositional environments (Terzaghi  et al., 1996). Clean sands containing less than 5% fines, when passed through the No.200 sieve (0.075mm) are the most susceptible to liquefaction. This is because they are most likely deposited in an uncompacted condition with a permeability just low enough to restrict drainage during a seismic event (Terzaghi  et al., 1996; Craig, 2010). Therefore, soils with a higher fines content will resist the

15

separation of grains and provide a stronger resistance to soil liquefaction. On the other hand, coarse grained sands and gravels are less likely to reach equilibrium at very high void ratios. Furthermore, they can drain much more easily and quickly to avoid an excess of pore water pressure being built up (Terzaghi et al., 1996). During the shaking or vibration process (shearing), bonding stresses between the grains are weakened, causing the soil to lose frictional strength and the ability to carry load. When undergoing shear deformation, a soil will either dilate or contract. Loose soils will start to decrease or contract in volume, and in some cases dense soils will dilate or expand with enough shearing energy.

With insufficient or slow draining of water in the surrounding soil, the decrease in volume or settlement will trigger a rise of pore water pressure (u). The pore water pressure will keep rising until it equals the level of total stress (σ) in the soil. This will lead to the effective stress (σ') becoming less and less until it equals zero. Ultimately, the shear strength (τ) becomes zero as well, resulting in the soil losing all strength and carrying capacity (Schofield & Wroth, 2005; Gandomi et al., 2013) . See Equation 2.1 and Equation 2.2 below for effective stress and shear strength respectively.

$$\sigma' = \sigma - u$$

*Equation 2.1: Effective stress*

$$\tau = \sigma'. \tan u$$

*Equation 2.2: Shear strength*

The boundary between the dilative and contractive behaviour is known as the critical state line. When the shear strength reaches zero, the soil will lose its cohesion and ability to maintain form, resulting in a state of liquefaction.

Rauch (1997) summarised the observed affects resulting from various stress conditions in Table 2.2. The table describes the visual observations after an earthquake and how varying stress conditions could lead to different types of liquefaction.

*Table 2.2: Observed effects for various stress conditions (Rauch, 1997)*

| In-Situ Stress Condition | Observed Soil Behaviour | Observed Observation in field Conditions |
|---|---|---|
| No active driving shear stress (Such as flat ground) | Volume decreases – contract  Pore pressure rises | Ground settlement  Soils boils |
| Active driving shear stress more than residual soil strength | Loss of soil stability  Liquefaction occurs | Flow slides  Sinking and differential settlement of buildings  Underground pipes and light structures start to float |
| Active driving shear stress lower than residual soil strength | Limited shear distortion  Soil mass remains stable and moistly intact | Slumping and failures of slopes  Settlement of buildings  Lateral spreading |

16

### 2.3.2    Critical State Concept and the Steady State Line

Critical State Soil Mechanics (CSSM) is the area within the study of soil mechanics that includes theoretical models that represents the structural and mechanical behaviour of undrained soils based on the critical state concept.

The critical state concept is based on the observed soil behaviour of undrained, saturated clays and sands in triaxial compression tests, and applies to undisturbed soils or soils with the same properties it would have had in-situ. The concept states that when a continuous shear stress is applied to a soil, it will eventually flow as a highly viscous fluid until it reaches a defined state, called the critical state. Each soil has its own unique critical state line (CSL). The critical state idea or concept is an additional way of estimating liquefaction potential. It states that when a soil with an average effective stress "p'' and a void ratio "e" plots above the CSL, that the soil will contract while under drained loading conditions, or generate excess pore water pressure during undrained loading conditions, reducing the effective stress until it reaches the critical state line. The opposite is also true, where a soil with "p" and "e" plots below the CSL it will dilate during drained loading conditions or decrease in pore water pressure during undrained loading conditions that increases the effective stress until it reaches the CSL (Puri & Kostecki, 2013). When the CSL is reached, the soil will no longer change in effective stress or void ratio. Furthermore, contractive behaviour is related to strain softening, while dilative conditions are related to strain hardening (Seed et al., 2003).

Each soil body will have a different density, with dense soils generally being stronger and dilatant, while loose soils are weak and contractive. It is however impossible to characterise a soil by just looking at density, as it will behave differently at various densities.

With CSSM, the idea is to characterise the never-changing properties of soil, separate to that of variable properties such as the current density or void ratio.

The *state parameter* (Ψ) concept can be described as the difference between the void ratio at the critical state ($e_{cs}$) and the in-situ void ratio ($e_o$). A soil will be dilative and will strain harden during undrained shear if the soil is denser than the critical state Ψ < 0. If the soils are however looser than the critical state (Ψ > 0), it will strain soften and be contractive in undrained shear. If a soil has a state parameter of Ψ > - 0.05 then strain softening and strength loss can be expected in undrained shear. The critical state is the final state a soil will reach if sheared continuously (Figure 2.8).

17
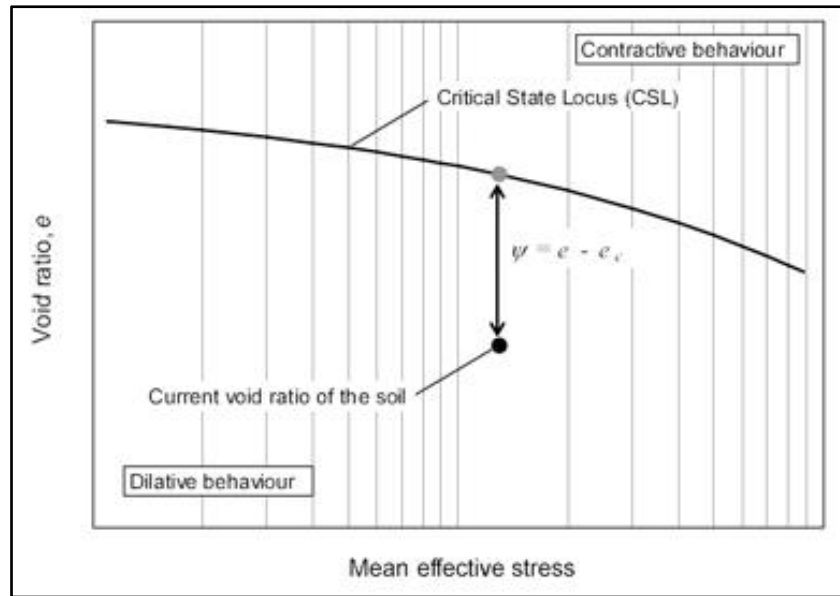
*Figure 2.8: State Parameter and Critical State Line (Jefferies & Shuttle, 2011)*

Ground movement becomes the main driving factor when empirical correlations are idealised for liquefaction as result of earthquakes. The cyclic stress ratio (CSR) is determined from the average horizontal shear waves from the earthquake likely expected and the vertical overburden stress within the soil. The likelihood for liquefaction to occur can be determined by looking at in-situ ground conditions and soil properties. The cyclic resistance ratio (CRR) of the soil can then be determined. The values for the CSR and the CRR are then plotted along with other known liquefaction case studies to determine whether the soil in question will also liquefy during a seismic event. The concept of the CSR and CRR are discussed further in the following sections.

To conclude, whether a body of soil will liquefy or not depends on the state of the soil relative to the critical state line. If the soil is dense and plots below the CSL the soil will dilate on shear and should not liquify. If it is loose and plots above the CSL, it will contract on shear and the pore water pressures will increase leading to the loss of strength. This could then possibly lead to liquefaction.

### 2.3.3    History of liquefaction disasters

Over the years, many large-scale soil liquefaction events have occurred, resulting in serious financial and structural complications. Probably one of the largest documented cases was the liquefaction that took place on 16 June 1964 in Niigata, Japan (Figure 2.9). The Niigata earthquake of 1964 had a magnitude of 7.5 with the epicentre 50km away to the north-west of the city, and at a depth of 34km. As a result, large scale liquefaction and sand boils were experienced all over the city.  Most of the city is underlain by recent deltaic deposits and consist of unconsolidated sand (Rothe, 1969).



*Figure 2.9: Large scale settlement due to liquefaction in Niigata, Japan (Earthquaketrack, 2016)*

Inspection of soils and foundations after the disaster indicated that the major cause was poor subsoil conditions. Most of the damage observed was due to settlement and very little structural damage took place due to the vibration itself. The lower part of the town was built on thick layers of recently deposited sand. The reason for the settlement is due to an increase in pore water pressure in saturated sands, resulting in the loss of soil strength and the soil's bearing capacity (Rothe, 1969).

The earth is met with large destructive earthquakes almost on a yearly basis and many of them have seen some sort of liquefaction as a result. Examples of liquefaction around the world are that of the 1989 San Francisco Bay earthquake, the Port Kobe earthquake of 1995 and more recently in New-Zealand that of Christchurch earthquakes in 2010 and 2011. The series of earthquakes that hit the Canterbury region in New-Zealand in 2010 and 2011 had a magnitude of 6.3 to 7.1. The epicentre of these earthquakes was determined to be very close to Christchurch at a depth of 5km for the first earthquake, and about 10km for the second major earthquake (Earthquaketrack, 2016). Engineers

19

estimate that more than 200 000 tons of silt and sand where pushed up in the form of sand boils all over the city (Figure 2.10).



*Figure 2.10: Sand boils in Christchurch (Earthquaketrack, 2016)*

The city of Christchurch is underlain by Quaternary alluvial deposits from rivers and streams in the area. Large areas of where the city is today, was once swamps, shallow marine estuaries and lagoons. Silty sands were left behind after the water bodies drained over years. These silty sands are uncemented and loose in consistency (Chih-Chieh  et al., 2017).

The earthquakes that hit the city in 2010 and 2011 lead to large scale destruction and loss of life. Liquefaction caused underground services such as water lines to float to the surface, leading to flooding and limiting access to people in need of rescue. The loss of water lines further constrained firefighting and water needed to extinguish fires. Aftershocks that hit the city resulted in more liquefaction and subsidence as the soils were weakened by the previous shocks. Landslides, due to weakened surface soils and loss of shear strength, were observed in the hills and mountains surrounding the city (Wei & Yang, 2015).

A more recent and deadly liquefaction disaster is the one that took place during the Meinong earthquake, on the 6th of February 2015. The epicentre was near the town of Meinong, in southern Taiwan. The earthquake, with a magnitude of 6.4, did surprisingly little damage to the town of Meinong. Instead, large scale damage was reported 30km west of the epicentre, in Tainan City (Chih-Chieh  et al., 2017). The Wei Guan apartment building of 16 storeys collapsed during the earthquake, resulting in 115 casualties (Chih-Chieh  et al., 2017). The general geology of the area includes alluvial deposits of the Holocene Era. The groundwater table is very shallow, ranging from 0.55-0.95m below ground level.

Tainan City has large residential areas reclaimed from old fish farm ponds. During reclamation many years ago, little to no compaction was carried out. During the earthquake, most of the large buildings in

20

the area experienced settlement due to the foundation bearing capacity being reached once the surrounding looser soils liquefied (Chih-Chieh et al., 2017). The peak ground acceleration range was estimated to be between 0.15 to 0.25g during the earthquake. Geologists believe that the value can be much higher, up to 1.5 times more, due to the PGA's that were amplified in very loose backfill material (Chih-Chieh et al., 2017). Analysis of the liquefied soils in the area indicated silty sands with fines ranging from 9 to 40%. SPT testing in the area indicated that most of the areas had very low SPT-N values, of 2 to 11 (Chih-Chieh et al., 2017).

Figure 2.11 shows three buildings in the City of Tainan that experienced large differential settlements due to the soil below their foundations being liquefied.



*Figure 2.11: Building Settlement in Meinong (Chih-Chieh et al., 2017)*

### 2.3.4   History of Liquefaction in South Africa

Liquefaction was observed in Cape Town on the 4th of December 1809. Eyewitnesses reportedly saw volcanoes of sand and muddy water spurting out of fountains. The term liquefaction was not used during that time, but by analysing witness accounts it could most probably be that of sand boils due to soil liquefaction (Hartnady, 2003). This was the only account of soil liquefaction being documented near the City of Cape Town or on the Cape Flats. Liquefaction in mine tailings and dumps is however a well-documented risk for the mining industry in South Africa.

Mining is a major part of the South African economy. Mine tailings are the material that is left after the mineral or ore has been extracted from the source rock. The tailings from gold mines have a grading size of approximately 0.075mm, while the tailings from coal mines have a grain size of about 0.05mm. The behaviour of these grain sizes is similar to the behaviour of clean sand under seismic loading (Puri & Kostecki, 2013). In the absence of a major earthquake, liquefaction within mine tailings can also occur due to cyclic loading, continuous saturation of the soil or static loading (Seed et al., 2003). In

South Africa, a gold tailings dam failed near the town of Virginia in the Free State in 1994. A large thunderstorm deposited 50mm of rain within 30minutes. The result was the failure of the dam and 600 000 cubic meters of mine tailings flowed in a liquid state into the town. Unfortunately, on that day, 17 people lost their lives (Chamber of Mines, 1994). After the accident, investigators realised that the tailings were in a very loose saturated state in-situ. The loose state of the tailings itself was not to blame, but rather the poor construction and maintenance of the dam itself. The outer layer of the dam wall became eroded overtime causing the dam wall to weaken and deteriorate. This deterioration was not picked up soon enough and the dam wall continued to weaken with time (Chamber of Mines, 1994).



*Figure 2.12: Tailings dam failure in South Africa (Chamber of Mines, 1994)*

In addition, the thunderstorm that deposited large amounts of water within a short time weakened the dam wall even further, until it failed. The result was a flow failure that took place due to static liquefaction within the tailings. The heavy downpour caused the tailings to become saturated in a very short time, and with insufficient drainage within the tailings, the pore water pressure increased, and the effective shear became less (Puri & Kostecki, 2013).

The failure of the tailings dam lead to amendments being made to the current Code of Practice for Mine Residue Deposits. The Council for Scientific and Industrial Research (CSIR) developed a code for the operation and closure of tailings dams. One of the key changes was that all dam walls should be fitted with drainage systems to carry excess water away to a return-water dam system. In addition, houses are not allowed to be constructed within one kilometre of a tailing dam and also not downslope of the dam (Chamber of Mines, 1994).

Some of the other mines where flow failures were observed in tailings in South Africa include Arcturus (1978) and Saaiplaas (1992) gold mines, the Bafokeng (1974) platinum mine and the Stava (1985) fluorite mine.

## 2.4    Determining Soil Susceptibility to Liquefaction

Liquefaction caused considerable damage to buildings and underground services during the large earthquake that struck Niigata in Japan in 1964. Japanese engineers decided to empirically correlate the data of hundreds of in-situ soil tests with areas that had undergone liquefaction compared to areas that had not. This lead to empirical formulas being derived for this purpose and these formulas are now used worldwide to quickly determine with large amounts of data if soils are susceptible to liquefaction (Terzaghi  et al., 1996; Idriss & Boulanger, 2010).

Several testing methods are used in the field and laboratory, when the primary goal is to identify soils likelihood to undergo soil liquefaction. Various references indicate that there are numerous methods. This section will briefly outline two of these testing methods, namely:

1.   The Standard Penetration Test (SPT).
2.   The Piezocone Penetrometer Test (CPT).

The use of the data obtained from Standard Penetration Tests (SPT) and Piezocone Tests (CPTu) according to a certain empirical method will be discussed. The use of these two methods will also be used in this project to determine if a soil is susceptible to liquefaction.

Throughout the chapter, reference will be made to the cyclic stress ratio (CSR) and the cyclic resistance ratio (CRR). The CSR can briefly be described as the force or input within the soil that would initiate liquefaction, whereas the CRR is the force or resistance that would resist liquefaction from occurring. These two factors allow one to calculate a factor of safety for the soil body being investigated. These two factors will be further explained in this chapter.

Simply put, if the factor of safety  $F_s < 1.0$ , then liquefaction is likely to occur.

$$F_s = \frac{CRR}{CSR}$$

*Equation 2.3: Factor of safety for liquefaction resistance*

Determining whether a soil is potentially dilatant or contractive during shear is another way of establishing if a soil is potentially liquefiable during shear. This was used with the CPT testing, and relates closely to the use of critical state soil mechanics in establishing soil properties.

### 2.4.1   Soil properties

Over many years of research, engineers have realised that, for a soil to be susceptible to liquefaction, certain criteria should be met. One of the primary components is that of the grain size and density (Seed et al., 2003). Atterberg Limits, created by Albert Atterberg, is the foundation for defining the engineering properties of a soil. The Atterberg Limits define the plasticity, liquid limit and shrinkage

limit. Soil can be in one of four states, either solid, semi-solid, plastic or in a liquid state. Within each of these states the soil will behave differently (Craig, 2010).

The first step in any assessment is to determine if the soil has a potential to liquefy by looking at the basic soil properties. Chinese engineers in 1979 used data from liquefied soil samples and plotted the natural water content of the soil to that of its liquid limit (LL) (Seed et al., 2003).
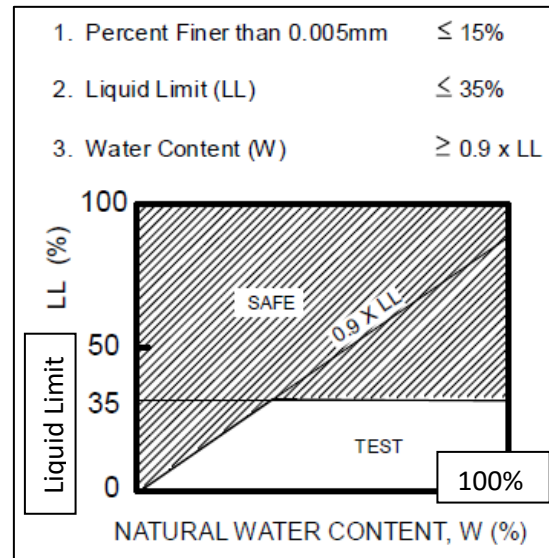


*Figure 2.13: Chinese Criteria (Seed et al., 2003)*

The Chinese Criteria graph also includes a criterion for fines content. For a soil to undergo liquefaction, according to the Chinese Criteria, a soil should have less than 15% clay (smaller than 0.005mm). The LL should be equal to or less than 35% and the current in-situ water content should be greater than or equal to 90% of the LL (Seed et al., 2003). However, these criteria were found to be too broad and a more refined criterion was needed. Furthermore, most cohesionless sandy soils have a liquid limit so low that it will plot near zero on the graph. Andrews and Martin (2000) formed a graph that distinguishes between higher and lower clay contents, as well as liquid limits, as shown in Figure 2.14.

Andres and Martin (2000) indicated that one problem within the research circles is that most of the emphasis and studies are done on relatively clean sands. Little research has been done on soils with various grain sizes and soils with high clay or silt content. The fact is that these are the most common types of soils encountered daily in engineering practice. Engineers need to know which types of commonly found soils are more susceptible to liquefaction in order to design for earthquakes.

24

|  | Liquid Limit[1] < 32 | Liquid Limit ≥ 32 |
|---|---|---|
| Clay Content[2] < 10% | Susceptible | Further Studies Required <br><br> *(Considering plastic non-clay sized grains – such as Mica)* |
| Clay Content[2] ≥ 10% | Further Studies Required <br><br> *(Considering non-plastic clay sized grains – such as mine and quarry tailings)* | Not Susceptible |

Notes:
1. Liquid limit determined by Casagrande-type percussion apparatus.
2. Clay defined as grains finer than 0.002 mm.

*Figure 2.14: Liquefaction susceptibility of silty sands (Andrews & Martin, 2000)*

Silts can be described as very fine sands. The boundary for the grain size between sands and silts is 0.074(5) mm. Silt has a very small grain size, so small that it can barely be seen by the naked eye. This, however, does not make it less prone to liquefaction. Silt has many of the same criteria as sands, for instance both are derived from rock-forming minerals and they have the same structural shape. They also have similar attraction forces such as hydrogen bonds and Van Der Waals bonds (Andrews & Martin, 2000). Clay however is much smaller at 0.002 mm (depending on which classification system is used). Clay minerals also differ in shape from silt, being plate-like, potentially expansive and having a plastic nature (Andrews & Martin, 2000). It can thus be said that silts and sands will have similar liquefaction potential properties, and very different properties to those of clays.

Figure 2.15 indicates case studies of liquefaction events plotted on a triangular graph or tertiary plot with the amount of clay, silt and sand indicated. The graph shows that most of the liquefaction events occurred in soils with sand content above 70% and clay and silt content less than 20% (Andrews & Martin, 2000). The graph was also analysed and plotted on a box diagram for easier interpretation (Figure 3.12).

25
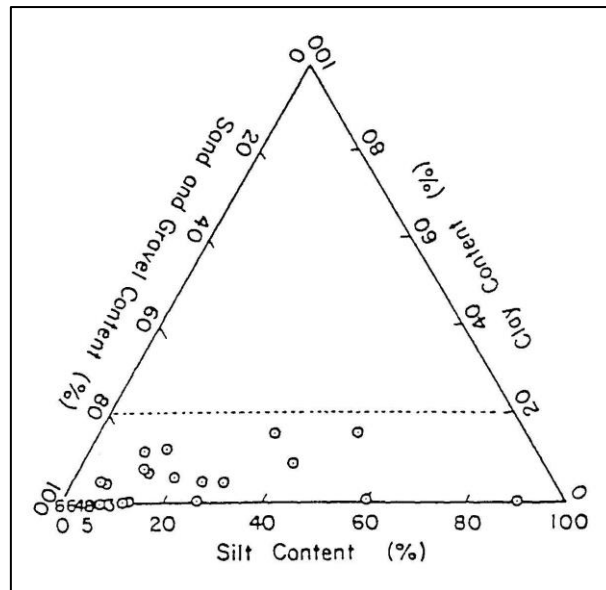
*Figure 2.15: Grain sizes of liquefied soils (Andrews & Martin, 2000)*

Furthermore, coarse grained sand can be graded to rank sandy soils according to their particle size. Soil gradation is important in geotechnical engineering and soil mechanics because it is used in other properties such as shear strength, compressibility and hydraulic conductivity. Sandy soils are generally graded according to two standards, one being the Unified Soil Classification System or the other being the AASHTO Soil Classification System. The graded soils can be defined according to certain categories and are plotted on a gradation curve diagram to visually represent gradings (Craig, 2010). Figure 2.16 indicates these graded categories, each with its related pattern.
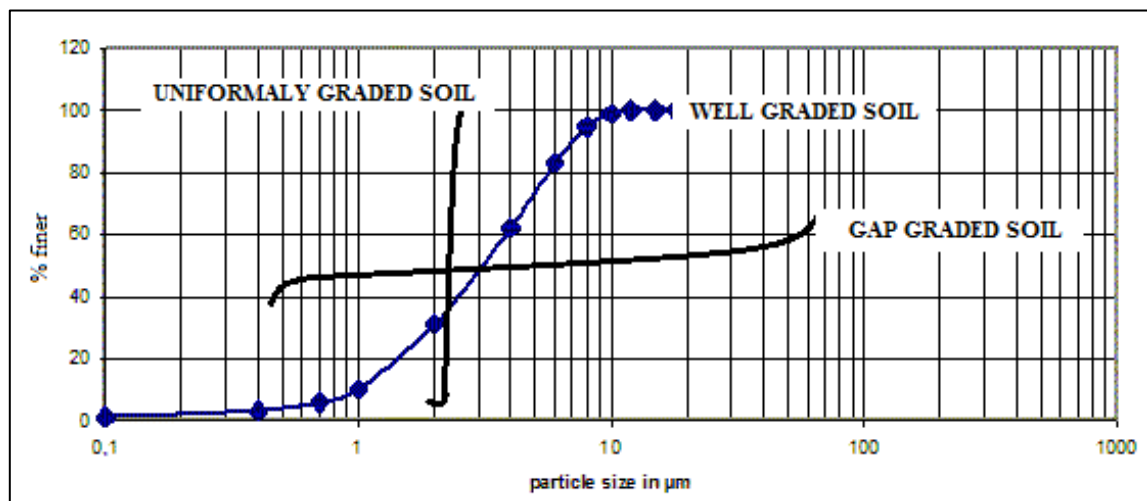


*Figure 2.16: Example of various grading curves (Fabbrocino et al., 2017)*

Uniformly graded soils (in the sand size range) are known to liquefy more easily compared to gap-graded or well-graded soils (Fabbrocino et al., 2017).

26

A large earthquake struck Nepal on the 25th of April 2015. The earthquake had a moment magnitude of 7.8 and a PGA value of 0.18. Liquefaction occurred over large areas across Barpak Village and scientist took samples of these liquefied soils. Grading analysis and grading curves were created for each sample and is presented on the Asian grading chart in Figure 2.17 (Fabbrocino et al., 2017).
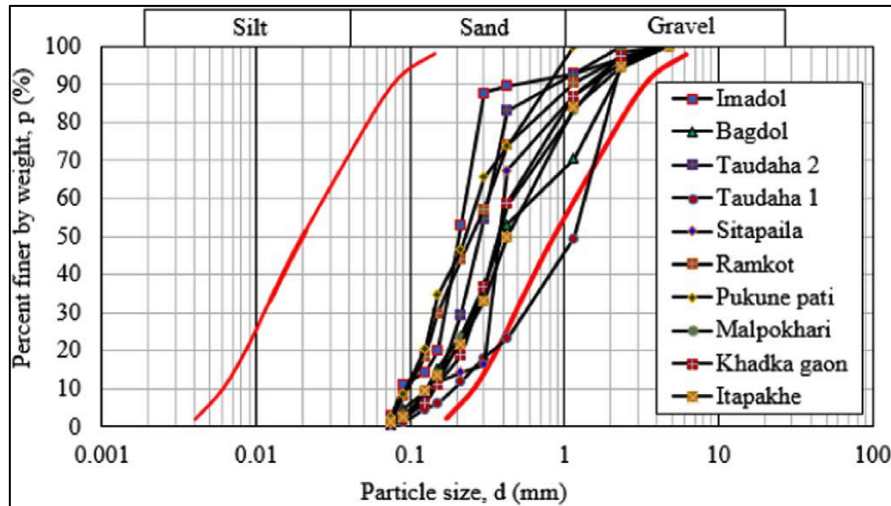


*Figure 2.17: Grading curves of liquefied soil in 2015 Nepal earthquake (Fabbrocino et al., 2017).*

The red lines to the left and right of the grading curves are the limit curves for potential liquefiable sands. These are suggested by the International Navigation Association for seismic design for port structures (Fabbrocino et al., 2017). The grading curves obtained from liquefied soil samples are an important addition to the physical characteristics of soils that are susceptible to liquefaction. These grading curves can be used to pre-screen certain soils and their likelihood to experience liquefaction. Figure 2.18 is an example of the British soil classification chart, indicating the soil gradation types and sieve sizes (Atkinson, 2000).
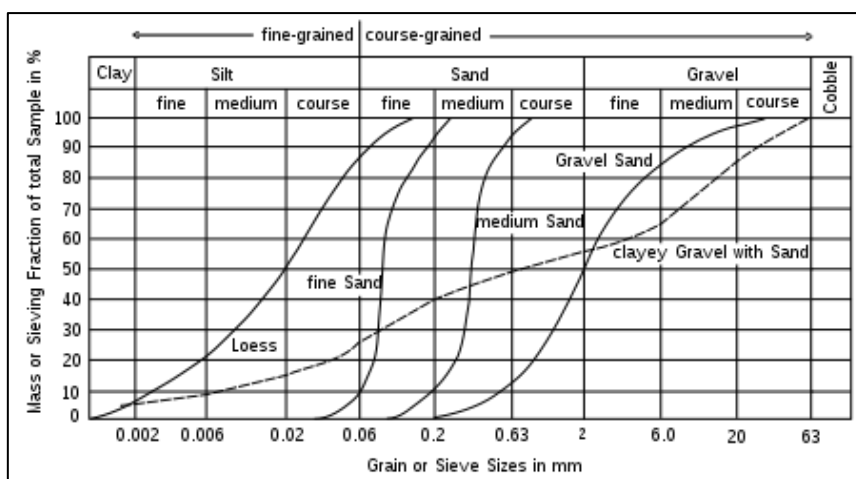


*Figure 2.18: Soil classification graph (Atkinson, 2000)*

The water table is another important aspect, as it is one of the main factors that causes a soil to liquefy. By knowing the depth of the water table and the unit weight of all the soil layers involved, the total

27

vertical stress and effective stress can be calculated, at a certain depth within the soil. The total vertical stress is the weight of all materials, the soil and water, above a certain depth. For a soil with a water table at surface, the total vertical stress $\sigma_v$ is:

$$\sigma_v = y_{sat}z$$

*Equation 2.4: Vertical stress*

Where $y_{sat}$ is the saturated unit weight of the soil multiplied by the depth ($z$) in question. The unit weight of water ($y_w$) is $9.81kN/m^3$ and this allows one to determine the pore water pressure (u) at any depth (z):

$$u = y_w z$$

*Equation 2.5: Pore water pressure*

Knowing the pore water pressure allows one to determine the effective vertical stress $\sigma'_v$ at any depth:

$$\sigma'_v = \sigma_v - u$$

$$\sigma'_v = (y_{sat-}y_w)z$$

*Equation 2.6: Effective vertical stress*
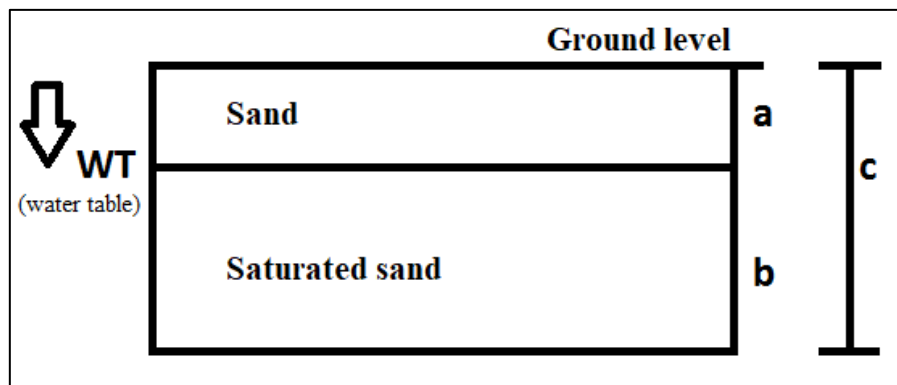


*Figure 2.19: Calculation of effective stress example*

The illustration in Figure 2.19 will be used when calculating the total effective vertical stress in the example below. If the depth of the water table (in this case, "$a$") is known, as well as the unit weights of all the layers above the depth in question, then the vertical stress (at depth "c") can be calculated. For example, if the depth to the water table (a) is 3m,  the depth in question ($a + b = c$) is 5m, the unit weight of sand above the water table is $17\ kN/m^3$, and the unit weight of saturated sand, below the water table, is $20\ kN/m^3$, then the total effective vertical stress will be as follow:

$$\sigma_v = (3 * 17) + (2 * 20) = 91\ kPa$$

$$u = (2 * 9.81) = 19.6\ kPa$$

$$\sigma'_v = \sigma_v - u \text{ , thus } 71\ kPa$$

So, the effective stress at a depth of 5m below ground level for the above example is 71 kPa.

The value of the effective stress, amount of fines and other properties such as the Atterberg Limits can now be used together with empirical correlations to determine if a certain soil body is susceptible to liquefaction.

### 2.4.2    Standard Penetration Test

This section will discuss the use of the SPT test, using SPT-N values to empirically correlate susceptibility of a soil to liquify. Although there are numerous empirical testing procedures, it was decided to use the updated *SPT-based liquefaction triggering procedures* by Idriss and Boulanger (2010:1-136). This method is used by several authors and has been proven to correlate to that of liquefied soil samples.

#### 2.4.2.1    Testing Procedure

The Standard Penetration Test (SPT) is an in-situ test that dynamically penetrates a sample tube, or a thick-walled sample tube, into the ground to determine the penetration resistance and hence the geotechnical engineering properties of the soil. Normally, the sample tube has an outer diameter of 50.8 mm, an inner diameter of 35 mm, and a length of 650 mm (Byrne  et al., 2008).

SPT sampling goes hand in hand with core drilling. The SPT test is done at set intervals of depth, determined by either the engineering geologist or the engineer overseeing the operation. Tests are carried out to determine density and strength with depth. In addition, a disturbed sample is retrieved with the sample tube for analysis and laboratory testing. The driller can decide to continuously do SPT testing and not only at set intervals when the recovered core samples, obtained during drilling, becomes unsatisfactory, or not enough of the sample is obtained. This is because SPT testing provides more and better-quality ground samples, but at a slower rate. These samples are, however, also disturbed.

During testing, the sample tube is hammered into the ground (Figure 2.20). The hammer, with a mass of 63.5 kg, falls through a distance of 760 mm along a sliding rod. The sampling tube is driven to a depth of 450 mm, and then the number of blows from the hammer to penetrate each successive 75 mm is counted. The sum of the last four readings (last 300mm) is the SPT-N value. This value can then be used by the engineer to aid in the design of foundations, for example, or be used in empirical correlations with many geotechnical parameters.

*Figure 2.20: SPT-Drill rig*

The SPT-N value provides an indication of the relative density (Figure 2.21) within granular deposits (Byrne et al., 2008). It is very difficult to obtain an undisturbed sample from deposits such as gravels and sand. It is also not always possible to obtain borehole samples within granular deposits. In these cases, continuous SPT sampling can provide more samples compared to conventional core drilling.

Some limitations do exist. Soils that became cemented or calcretized can give an unusually high SPT reading, such as calcrete that forms in lenses. These lenses, or the presence of gravel, can give the driller an indication that he might be in hard rock or that very dense soils are being encountered, and that the operation should stop accordingly. However, unknowingly, looser sediments can still possibly be encountered below the cemented layers. Another limitation is the SPT rig itself. The weight and height of the drop hammer, as well as the condition of the sample tube must all be correct to provide accurate readings. The counting and determining of the SPT-N values can also be done incorrectly, due to field conditions and operational errors. These limitations, and several others more, can be managed by appointing skilled and trained drillers and field personnel. A trained driller can identify calcrete or other pedogenic lenses from samples obtained during drilling and adjust accordingly. Trained operators will also ensure that all equipment is in good working condition and readings are corrected accordingly. Figure 2.22 depicts a general cross section of a SPT sampler.
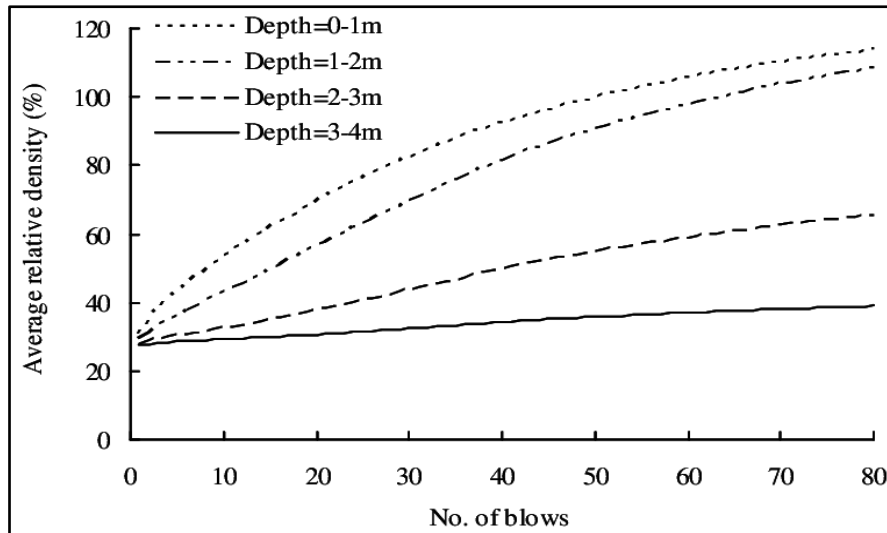
*Figure 2.21: Relative density compared to SPT-N value (Seed  et al., 2003)*
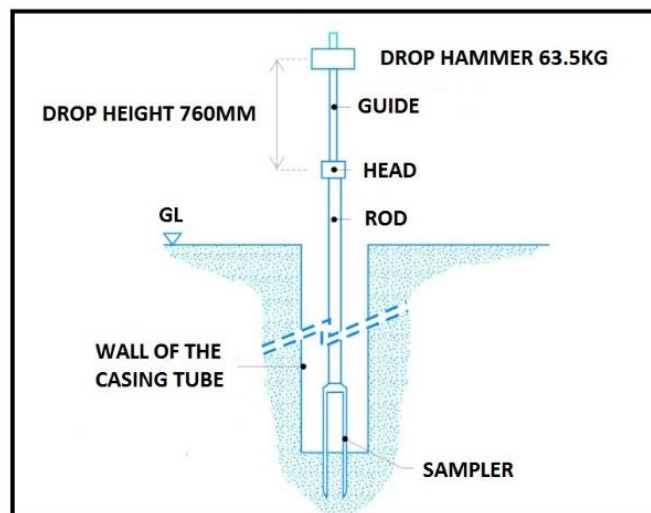


*Figure 2.22: Cross section of SPT sampling (Seed  et al., 2003)*

### 2.4.2.2    Results analysis and correction

The standard penetration test, or SPT, can be used in the evaluation of a soil's susceptibility to liquefaction using the method from Idriss and Boulanger (2010:1-136). Empirical correlation of this kind became more researched after the Niigata earthquake in Japan in 1964, where the need for empirical correlations instead of time consuming laboratory tests was realised. The primary goal of the method discussed is to compare the cyclic stress ratio (CSR), as result of an earthquake, to that of the cyclic resistance ratio (CRR) of the soil. The stiffness or the shear strength of a soil body needs to be determined before comparing it to liquefiable soil types and before attempting an empirical correlation. A layer of soil near ground surface is assumed to move as one intact body in the horizonal direction.

31

The shear strength at a depth $z$ is equal to the acceleration at the ground surface times the mass of soil lying above (Terzaghi et al., 1996).

$$\tau_{max} = \frac{a_{max}}{g} \sigma_{vo} \qquad \textit{Equation 2.7: Earthquake induced shear strength}$$

Where:

$\tau_{max}$        = Maximum earthquake induced shear strength.

$a_{max}$        = Peak ground surface (horizontal) acceleration/PGA.

$g$        = Acceleration of gravity.

$\sigma_v$        = Total overburden stress at depth of investigation

However, because the soil body is variable with depth, the shear value or stress (varying with depth) is less than what is calculated above. Therefore, a reduction factor $r_d$ is multiplied to the previous equation. The value ranges from 1.0 at ground surface, to 0.9 at a depth of 10m below ground level. The value for $r_d$ is calculated as follows: $\qquad r_d = exp\big[(\alpha(z) + \beta(z))M\big]$

Where:

$$\alpha(z) = -1.012 - 1.126sin(\frac{z}{11.73} + 5.133)$$

$$\beta(z) = 0.106 - 0.118sin(\frac{z}{11.28} + 5.142)$$

*Equation 2.8: Reduction factor*

$$\tau_{max} = \frac{a_{max}}{g} \sigma_{vo\,r_d}$$

*Equation 2.9: Maximum shear strength*

The reduction factor can also be obtained from Figure 2.23.
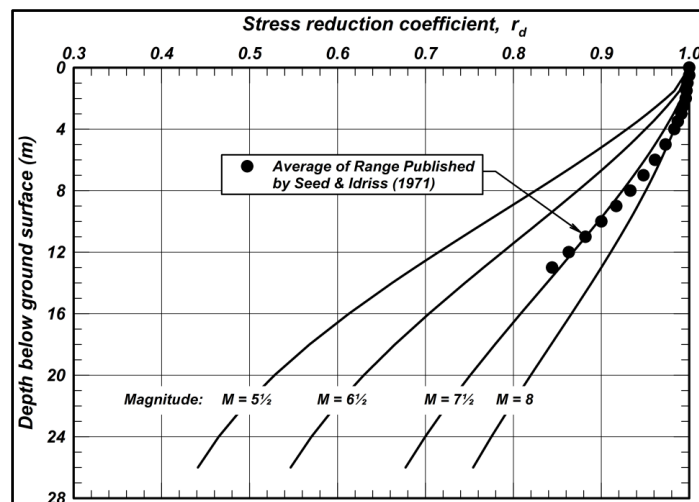


*Figure 2.23: Stress reduction factor $r_d$ (Idriss & Boulanger, 2010)*

Earthquakes have proven to be inconsistent in terms of shearing stress, and laboratory tests require a constant value for cyclic shear stress with a constant amplitude and frequency. The shear stress pulses are therefore converted to a uniform value having an amplitude 65% of the maximum shear stress (Idriss & Boulanger, 2010; Terzaghi et al., 1996; Seed et al., 2003).

The ability of a soil to resist liquefaction, or liquefaction resistance, is characterised by an equivalent uniform cyclic stress required to produce liquefaction in the same number of cycles. The capacity of soil to resist liquefaction is called the cyclic resistance ratio or CRR. The relationship of CRR to that of in-situ field tests has been formed to aid the empirical correlation of in-situ tests to that of laboratory tests. During an earthquake or seismic event, the seismic demand on the soil due to the vibration is called the cyclic stress ratio or CSR (Andrus & Stokoe, 2000; Idriss & Boulanger, 2010). The correlation of the cyclic stress ratio required to cause liquefaction will be designated as CRR to distinguish it from the cyclic stress ratio CSR induced by the earthquake ground motions (Idriss & Boulanger, 2010). The CSR in this study will be discussed as if it is from a seismic event such as an earthquake. The CSR at a depth of $z$ within the soil being investigated is expressed as 65% of maximum cycle shear stress ratio within the soil profile. The subscripts of CSR are for a certain Magnitude, M and in-situ vertical effective stress, $\sigma'_v$, calculated at a depth $z$. The maximum earthquake induced shear stress, $\tau_{max}$, can be determined from dynamic response analysis and site analysis that includes acceleration time series characterisation. The maximum induced shear stress can also be calculated with the following equation:

$$CSR_{M,\sigma'_v} = 0.65 \frac{\sigma_v}{\sigma'_v} \frac{a_{max}}{g} r_d$$

*Equation 2.10: Cyclic Stress Ratio*

Where:

$a_{max}$            = Peak ground surface (horizontal) acceleration

$g$            = Acceleration of gravity

$\sigma'_v$            = Initial effective overburden stress (vertical) at depth of investigation

$\sigma_v$            = Total overburden stress at depth of investigation

$r_d$            = shear stress reduction coefficient to adjust for the flexibility of the soil

The CRR of a soil can be correlated to the in-situ value of SPT-N blow count. Various factors influence the SPT-N value, as briefly discussed before, and these need to be corrected to a standard form. Some of these factors are the length of the rods, energy input to the hammer, borehole size and effective overburden stress. SPT-N values are therefore corrected for use in CRR correlations as follows:

$$(N_1)_{60} = C_N C_E C_R C_B C_S N_m$$

*Equation 2.11: Normalised penetration resistance*

33

Where:

| | | |
|---|---|---|
| 1. | $C_N$ | = Overburden correction factor |
| 2. | $C_E$ | = Hammer energy correction |
| 3. | $C_R$ | = Rod correction factor |
| 4. | $C_B$ | = Correction factor for non-standard borehole diameter |
| 5. | $C_S$ | = Correction factor for the use of split spoons (samplers) with no liner |
| 6. | $N_m$ | = Measured SPT blow count value |

## 1.  Overburden correction factor for penetration resistance $C_N$

With depth, stress increases within a soil profile. This is due to the increase in weight of the overlying soil horizon. A correction factor is therefore needed to normalise the resulting effect of the additional weight and friction on the SPT-N value. To correct for additional load and effective stress, the overburden correction factor is implemented, as follows:

$$C_N = (\frac{P_a}{\sigma'_V})^m \leq 1$$

*Equation 2.12: Overburden Correction Factor*

Where $m = 0.784 - 0.0768\sqrt{(N_1)_{60cs}}$ (Idriss & Boulanger, 2010) and $P_a$ is the atmospheric pressure.

The calculation of the overburden correction factor requires the normalised SPT-N value, whereas the calculation of the normalised SPT-N value requires the overburden correction factor. This means that iteration is required. Idriss and Boulanger (2010:1-136) plotted calculated overburden correction factor values to that of vertical effective stress (Figure 2.24). These graphs can be used to conveniently determine an overburden correction factor at a known effective stress and $(N_1)_{60cs}$ value. Iteration will be discussed and used in the piezometer section. Figure 2.24 will be used in this section to determine the overburden correction factor.
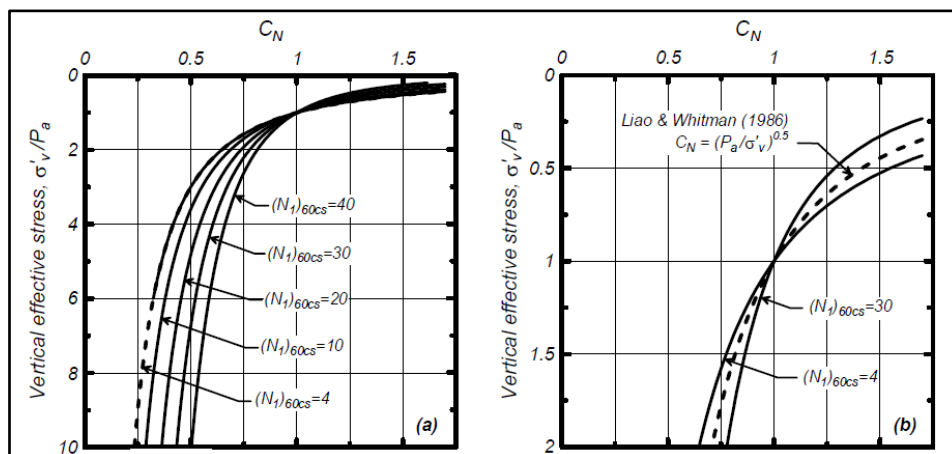


*Figure 2.24: Overburden correction factor plotted to effective stress (Idriss & Boulanger, 2010)*

### 2.    Hammer energy correction $C_E$

The hammer energy correction factor is used to normalise excessive or too little input from the sliding hammer. This requires that the energy input should be measured for each blow and an average value from the rig should be used in the calculation. The ideal value should be equal to one and is calculated by comparing what the theoretical energy from the drop hammer should be compared to what is delivered. Some loss can be expected, for example from friction.

From examining case studies, it was clear that in some cases a value higher than one was used, with values in examined case studies ranging between 0.88 – 1.28 (Seed, et al., 2003). A gain in hammer energy is therefore also possible, possibly as a result from the releasing mechanism.

### 3.    Short rod correction factor $C_R$

Not all SPT drilling rigs are the same, and various rod lengths are used, depending on the rig type and site conditions that might restrict high rod lengths. The rod length is also increased as the borehole increases with depth. The rod length is the length between the SPT testing cone head and the upper part below the dropping hammer. Different rod lengths can have a varying effect on the blow or penetration force. Research done by Idriss and Boulanger (2010:1-136), lead to the short rod correction factor being implemented. Idriss and Boulanger made a simple table with values to use in the $(N_1)_{60}$ equation.

*Table 2.3: Short rod correction factor (Idriss & Boulanger, 2010)*

| Rod Length (m) | <3 | 3 - 4 | 4 -6 | 6 - 10 | 10 - 30 |
|---|---|---|---|---|---|
| $C_R$ | 0.75 | 0.80 | 0.85 | 0.95 | 1.00 |

The use of this correction factor is debated in the literature, as some see the margin of error so small that it can be ignored.

### 4.    Correction factor for non-standard borehole diameter

The correction factor for non-standard borehole diameter ($C_B$) is generally equal to one if the standard diameter is used. The literature is very vague on how this should be corrected if non-standard diameters are used and it appears that authors tend to use only information with the standard diameter.

### 5.    Correction factor for use of split spoon samplers with no liners

The correction factor for the use of split spoons samplers with no liner ($C_S$) are set equal to the value of one, if the standard penetration procedures are followed.

### 6.    Measured blow count from SPT

Finally, the measured blow count from the SPT sampling is used for $N_m$ . Normalised SPT-N values $(N_1)_{60}$ can now be determined.

**Magnitude scaling factor *MSF***

The cyclic stress ratio (CSR) behaves differently at various earthquake magnitudes. The CSR increases with an increase in magnitude (Idriss & Boulanger, 2010). This makes it difficult to find a relationship between CSR and SPT-N value when more than one case study of different magnitudes is compared to each other.

Various authors have suggested that corrections need to be made to normalise the earthquake magnitude to one common magnitude (Andrus & Stokoe, 2000; Idriss & Boulanger, 2010). The magnitude scaling factor is to account for the amount and duration of loading cycles (earthquake), which ultimately lead to liquefaction. The MSF is used with the calculated CSR value to determine a common magnitude M value. This is normally taken as M = 7.5. The CSR is divided by the calculated MSF to obtain a CSR value that is representative to that of the measured earthquake.

Idriss and Boulanger (2010) formulated an equation (Equation 2.13) for the MSF:

$$MSF = 6.9 \, . \, exp\left(\frac{-M}{4}\right) - 0.058 \, \leq 1.8$$

*Equation 2.13: Magnitude scaling factor*

The relationship between an earthquake with magnitude M and the resulting MSF is illustrated in Figure 2.25 and can be used for easy and fast reference.
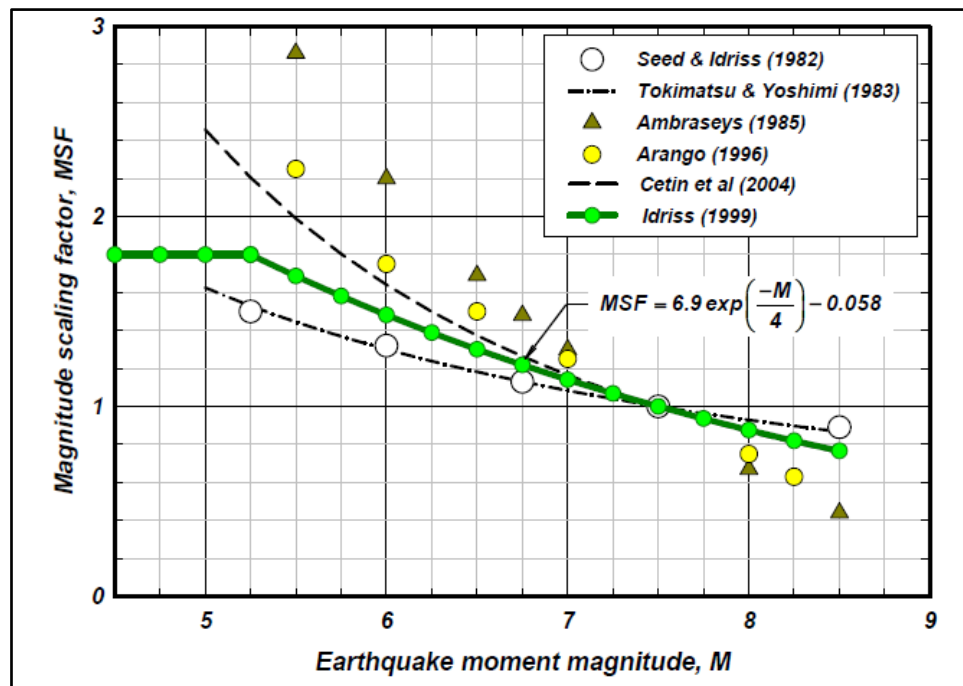


*Figure 2.25: Magnitude scaling factor (MSF) (Idriss & Boulanger, 2010)*

36

**Cyclic Resistance Ratio *CRR***

The CRR must be calculated to establish a boundary line for soils susceptible to liquefaction, compared to those that are not. The resulting CRR value, determined from corresponding SPT-N values, can be used to establish a factor of safety by relating the CRR to that of the CSR. The CRR can be calculated (using the Idriss and Boulanger (2004) method) from corrected $(N_1)_{60cs}$ values as follows:

$$CRR = exp\{ \frac{(N_1)_{60cs}}{14.1} + \frac{((N_1)_{60cs})^2}{126} - \frac{((N_1)_{60cs})^3}{23.6} + \frac{((N_1)_{60cs})^4}{25.4} - 2.8\}$$

*Equation 2.14: Cyclic Resistance Ratio*

The results for $(N_1)_{60cs}$ of three testing procedures (established by three authors) are plotted against CRR in Figure 2.26. It should also be noted that these data have been normalised to a magnitude of M=7.5 and an effective overburden stress of 1 atm (Idriss & Boulanger, 2010).
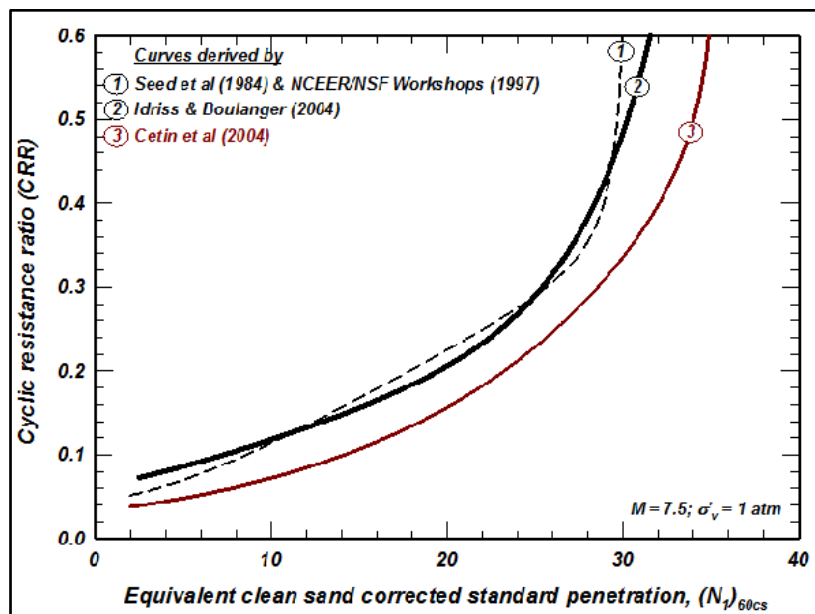


*Figure 2.26:$(N_1)_{60cs}$ plotted to the CRR for three authors (Idriss & Boulanger, 2010)*

### 2.4.2.3   Empirically correlating data

Results obtained can now be compared to that of areas that had undergone liquefaction during a seismic event, and to those that had not experience liquefaction. Values for $(N_1)_{60}$ can be compared to various factors, such as the CSR. The addition of the clean sand $(N_1)_{60cs}$ values can further increase the accuracy of work done by Idriss and Boulanger (2004).

37
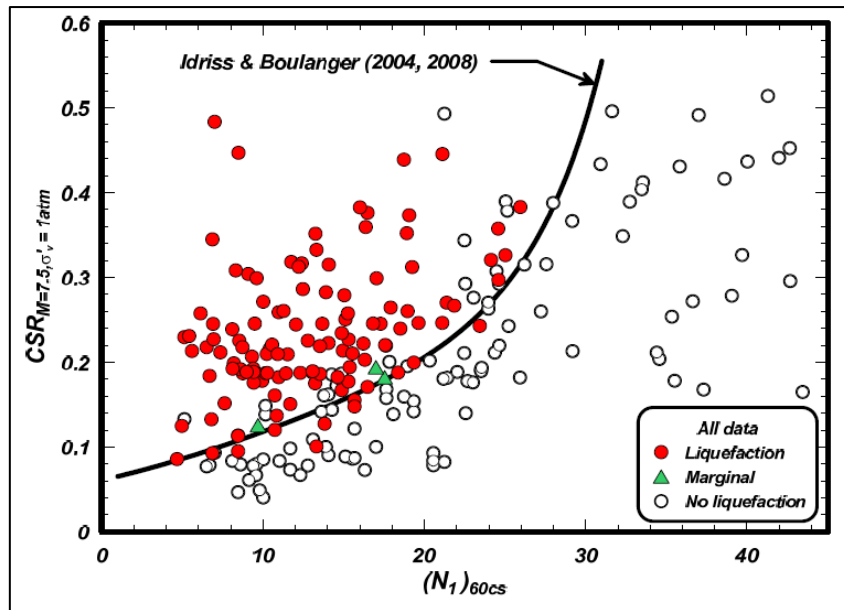
*Figure 2.27: SPT case history data (Idriss & Boulanger, 2010)*

Idriss and Boulanger (2010) combined the results from numerous earthquakes around the world. They normalised all data to one or more criteria and compared results with the same criteria. The process was simple, and charts were created displaying the results of $(N_1)_{60cs}$ to the CSR value. The boundary curve was determined from CRR calculations. Evident from Figure 2.27, areas that had undergone liquefaction separates almost perfectly compared to areas that had not undergone liquefaction. This allows a boundary to be drawn between areas of liquefaction and non-liquefaction. Areas near the boundary line can be said to partially undergo liquefaction and might require further testing to determine the susceptibility to liquefaction (Idriss & Boulanger, 2010).

Idriss and Boulanger (2010) took the data from the same case studies and plotted them on the same graph (Figure 2.28) and included their fines content (FC). The almost random spreading of the different FC tends to show that there is no relation between the number of fines and the susceptibility to liquefaction. However, further investigation proved that the peak ground acceleration (PGA) for the sites that did not liquefy were almost all lower than for soils with the same FC that did experience liquefaction. The magnitude of the earthquake that occurred within these soils was thus lower. Another aspect is the duration of the seismic activity. In most case studies, the duration was not recorded and could be the reason that liquefaction did not initiate within these specific soil types. This reasoning is to be expected, considering that pore water pressure will increase with continuous or long enough shearing. If the shearing stops before peak pressures are reached, groundwater will simply dissipate, restoring some of the original ground strength (Idriss & Boulanger, 2010).

38
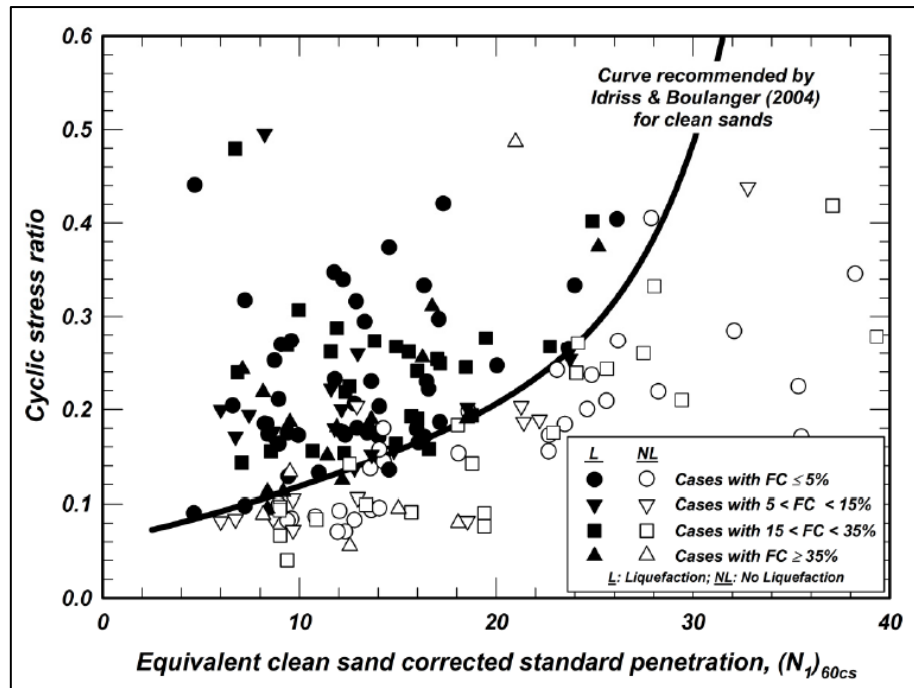
*Figure 2.28: SPT case history data with fines content (Idriss & Boulanger, 2010)*

### 2.4.2.4   Dynamic Probe Super Heavy Test

The Dynamic Probe Super Heavy Test, or DPSH (Figure 2.29), was developed as an infill test to the Standard Penetration Test (SPT). Benefits of the DPSH are that they are much more cost effective, and mobile compared to the SPT (MacRobert & Beales, 2011). The DPSH rig is an alternative to the more expensive SPT test. It can be used to determine the general density and depth to various dense soil layers. The idea is generally to use the DPSH test to infill and extrapolate findings from a SPT test (Byrne  et al., 2008; MacRobert & Beales, 2011). Much in the same way as the SPT, the DPSH uses a dropping weight of 63.5kg to fall through a height of 760mm. The main difference is that the DPSH uses a solid cone to penetrate the soil, compared to the split spoon sampler of the SPT. The other difference is that a SPT test is done in a borehole (often cased) which reduces rod friction, whereas rod friction can be considerable with DPSH. Soil samples are therefore not brought back to the surface when using the DPSH, but instead a continuous record of penetration is recorded without interference from moving the sampler in and out of the test hole (MacRobert & Beales, 2011).

The penetrating cone has a diameter of 50.5mm and an apex angle of 60º. A guide to practical geotechnical engineering, The Franki Blue Book (Byrne  et al., 2008), well-known in the geotechnical engineering field of South Africa, suggests that readings obtained from the SPT and DPSH be taken as similar, due to certain similarities such as having the same hammer weight and being dropped from the same height. However, some differences between the two techniques do occur. The SPT only needs to penetrate a depth of 450mm. The borehole is then drilled deeper, and the SPT is reinserted to penetrate another 450mm. Conversely, the DPSH must continuously be driven into the ground without being

removed from the borehole or test hole. The latter may lead to the build-up of friction, increasing the observed SPT-N value (MacRobert & Beales, 2011). With the DPSH, the number of blows it takes to penetrate 300mm is recorded to give an equivalent SPT-N value. There are however many uncertainties and variables that could affect the equivalent SPT-N value.



*Figure 2.29: DPSH rig mounted on a trailer*

Studies done on SPT and DPSH tests around Cape Town (MacRobert & Beales, 2011) indicated that in most cases the two testing methods provided similar data when testing was carried out in aeolian and alluvial sands within 5m of ground surface. However, with depth, the difference in SPT and DPSH values increased slightly. The error factor was even greater in pedogenic and cemented soils. Furthermore, soils with a high silt and clay content also indicated some deviation with regards to SPT and DPSH testing results (MacRobert & Beales, 2011).

Using the DPSH test on its own is somewhat risky and should probably be used with SPT testing methods. It makes financially sense to use both the DPSH and SPT tests when large sites are investigated. The DPSH can then be used to verify SPT results and vice versa. Many contractors and consultants prefer to use only the DPSH test due to the high cost involved with conventional SPT testing. Therefore, the DPSH test can provide relatively accurate and cost effective SPT-N value data for the purpose of this study.

### 2.4.3    Piezocone Penetrometer Test

In this section, the use of the CPTu will be discussed to determine whether a soil is susceptible to liquefaction. As with the SPT, various empirical methods exist. This study will use the paper: "*Evaluation of Flow Liquefaction and Liquefied Strength Using the Cone Penetration Test*" from Robertson (2010).

#### 2.4.3.1    Testing Procedure

The Cone Penetration Test (CPTu), with pore pressure measurement, consist of an instrumental cone that is pushed into the ground at a constant rate of 20 mm/s (Figure 2.30) (Pagani, 2017). These tests can be conducted in areas of clay and sand and can provide the user with a wide range of results. Basic results include the resistance of the soil due to penetration of the cone, resulting friction on the cone, and associated results such as the pore water pressure which can provide the depth to the water table. These tests are however very expensive, and a limited amount of CPTu testing has been carried out in the Western Cape of South Africa. The CPTu test is favourable in developed countries and is used in areas of sensitive sediments where liquefaction is of concern.

Measurements are taken at set intervals with depth. These measurements include the tip resistance of the cone ($q_c$), penetration or sleeve friction ($f_s$) and the pore water pressure (u). The measurements are then recorded on a computer at surface.
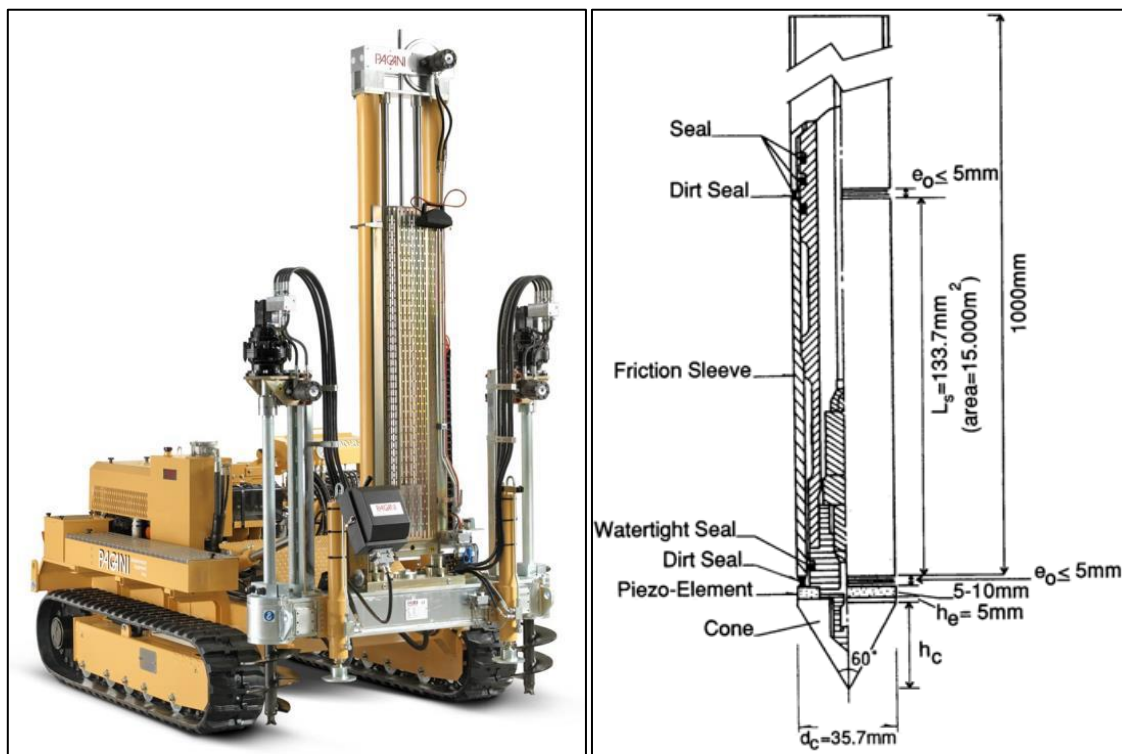


*Figure 2.30: CPT rig and cone (Pagani, 2017)*

### 2.4.3.2    Results analysis and correction

Once a selected area has been tested, the following parameters are obtained with a depth profile:

1. Tip resistance of the cone ($q_c$).
2. Penetration or sleeve friction ($f_s$).
3. Pore water pressure at the tip of the cone (u).

These values must however be corrected for certain soil conditions before they can be used in calculations. Pore water pressure, for example, is one of the properties that influences the friction reading of the cone. Due to the way in which the cone is shaped and the area of the cone, surrounding water pressures influences the actual tip resistance and sleeve friction. This is more commonly known as the unequal area effect (Robertson & Cabal, 2012). To correct the measured tip resistance ($q_c$), the corrected cone resistance ($q_t$) is determined. The value *a* is the area ratio determined from calibration and is supplied by the contractor. The value of *a* is typically 0.70 – 0.85 (Robertson & Cabal, 2012).

$$q_t = q_c + u\,(1 - a)$$

*Equation 2.15: Corrected cone resistance*

The correction for tip resistance is mostly done for soft clays and silts. Well graded, sandy soils should have a $q_t$ value equal (or very close) to that of $q_c$ (Robertson & Cabal, 2012). Generally, the corrected cone resistance ($q_t$) is high in sands, and low in clays and silts. Robertson (2010) developed a soil behaviour type (SBT) chart (Figure 2.31) based on normalised CPT parameters. These parameters are normalised by the effective overburden stress to produce the normalised cone resistance ($Q_t$) and the normalised friction ratio ($F_r$) for the use of the chart (Robertson, 2010).

$$Q_t = (q_t - \sigma_{vo})/\sigma'_{vo}$$

*Equation 2.16: Normalised cone resistance*

$$F_r = \left[\frac{f_s}{q_t - \sigma_{vo}}\right] 100\%$$

*Equation 2.17: Normalised friction ratio*

Where $q_t$ is the CPT corrected total cone resistance, $f_s$ the CPT sleeve friction, $\sigma_{vo}$ the preinsertion in-situ total vertical stress, and $\sigma'_{vo}$ the preinsertion in-situ effective vertical stress. However, overburden stress and effective stress should be established before one can determine parameters required for the SBT chart.

$$\sigma'_v = \sigma_v - u$$

*Equation 2.1: Effective stress*

The effective vertical stress, $\sigma'_v$, at a certain depth $z$ can be calculated if the depth of the water table is known, as well as the unit weight of all layers above the depth in question.



| Zone | SBT |
|------|-----|
| 1 | Sensitive, fine grained |
| 2 | Organic soils, clay |
| 3 | Clay, silty clay to clay |
| 4 | Silt mixtures, clayey silt to silty clay |
| 5 | Sand mixtures, silty sand to sandy silt |
| 6 | Sands, clean sands to silty sands |
| 7 | Gravelly sand to dense sand |
| 8 | Very stiff sand to clayey sand |
| 9 | Very stiff fine grained |
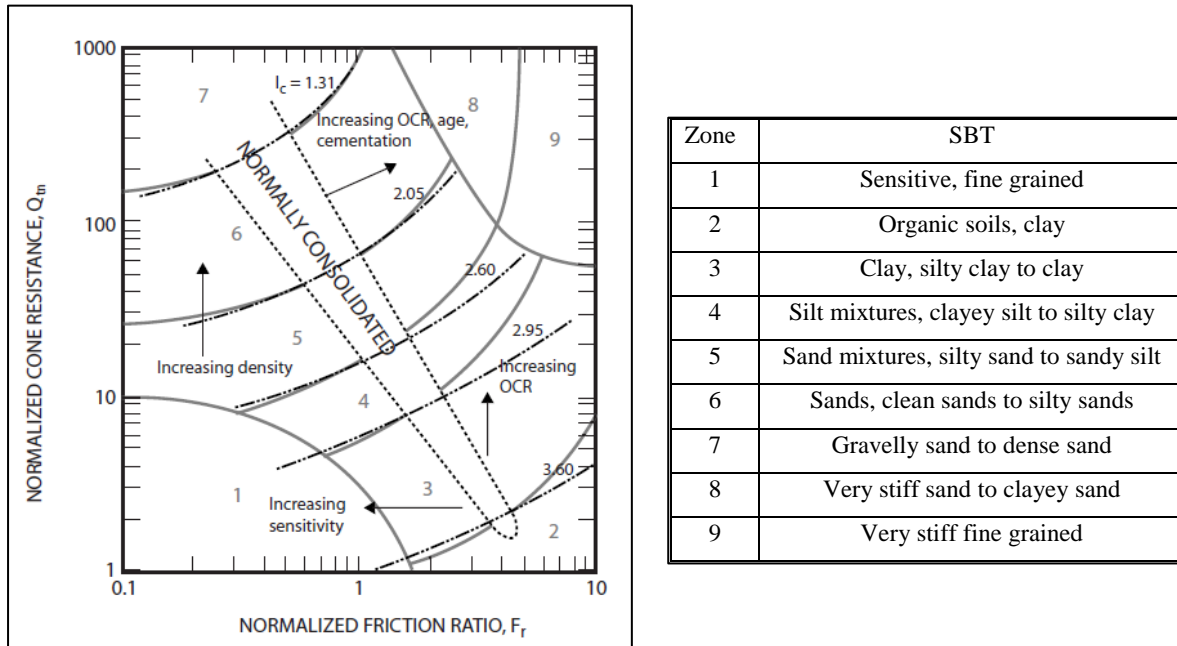
*Figure 2.31: SBT chart based on normalized CPT parameters (Robertson, 2010)*

Furthermore, the boundaries between the soil types within the SBT chart can be indicated by the soil behaviour type index (Ic). The equation for Ic is suggested by Robertson (2010) as:

$$Ic = [(3.47 - log\, Qt)^2 + (log\, Fr + 1.22)^2]^{0.5}$$

*Equation 2.18: Soil behaviour type index*

However, seeing as no two samples of soil behave the same, correction must be made for stress that varies with ground conditions and depth. To add a variable stress component, as is the case in natural soil, a normalised cone resistance ($Q_{tn}$) value with the addition of an SBT ($n$) component is needed.

$$Q_{tn} = [\frac{q_t - \sigma_{vo}}{p_a}](p_a/\sigma'_{vo})^n$$

*Equation 2.19: Normalised cone resistance with SBT component*

Where:

$[\frac{q_t - \sigma_{vo}}{p_a}]$        = Net cone resistance

$(p_a/\sigma'_{vo})^n$        = Stress normalisation factor

$n$        = Stress component that varies with SBT

$p_a$        = Atmospheric pressure

According to these equations, the clean sand region of the $Q_{tn} - F_r$ SBT chart (zone 6) should have a stress component (*n*) in the region of 0.5, and in the clay region (zone 3) the value should be close to 1.0 (Robertson, 2010). The values of $Q_{tn}$ and $F_r$ also increases as soils become denser.

$$where \ n \leq 1.0 \qquad n = 0.381 \ (I_c) + 0.05 \left(\frac{\sigma'_{vo}}{p_a}\right) - 0.15$$

*Equation 2.20: Stress component (SBT)*

Furthermore, the normalised cone resistance will decrease and the $F_r$ will increase as the soil becomes finer grained. This is because fine grained soils are more compressible compared to coarse grained soils. The soil behaviour index, $I_c$, will also increase as soils become finer grained, and when $I_c$ is more than 2.60, the soil tends to be even more fine grained containing silts and/or clays. The values for $Q_t$ and $F_r$ increases as the type of soil becomes stronger, stiffer and denser with age (Robertson & Cabal, 2012).

Flow liquefaction requires strain softening within a soil and the loss of shear strength. Robertson (2010) indicates that very loose sands as well as clays with a low PI can experience sudden strength loss that results in the loss of undrained shear strength. Robertson further states that the key in determining if a soil is susceptible to flow liquefaction is to identify very loose and coarse grained sandy soils. Whether a soil is loose or not, relates to the void ratio of a soil (Robertson, 2010).

Critical state soil mechanics recognises that the state of a soil is characterized by a combination of the effective stress and the total void ratio. A soil can strain soften in undrained shear if the soil is loose in either the steady or the critical state (Robertson, 2010). Robertson (2010) refers to Been and Jefferies (1985), who used the concepts of critical state soil mechanics to form the *state parameter* (Ψ) concept. The state parameter can be described as the difference between the void ratio at the critical state ($e_{cs}$) and the in-situ void ratio ($e_o$). A soil will be dilative and will strain harden during undrained shear if the soil is denser than the critical state Ψ < 0 (Robertson, 2010). If the soils are however looser than the critical state (Ψ > 0), it will strain soften and be contractive in undrained shear. If a soil has a state parameter of Ψ > - 0.05 then strain softening and strength loss can be expected in undrained shear.

A simplified method for determining the relationship between the state parameter and the normalised cone resistance is suggested by Robertson (2010) as:

$$\Psi = 0.56 - 0.33 \log Qtn.cs$$

*Equation 2.21: State parameter*

The proposed boundary between contractive and dilative soils is indicated in Figure 2.32. The figure also indicates that as $I_c$ increases for a specific soil, the normalised cone resistance decreases for the same soil. In addition, Robertson (2010) indicates that the figure below can only accurately be applied to clean sands where $F_r < 1\%$.
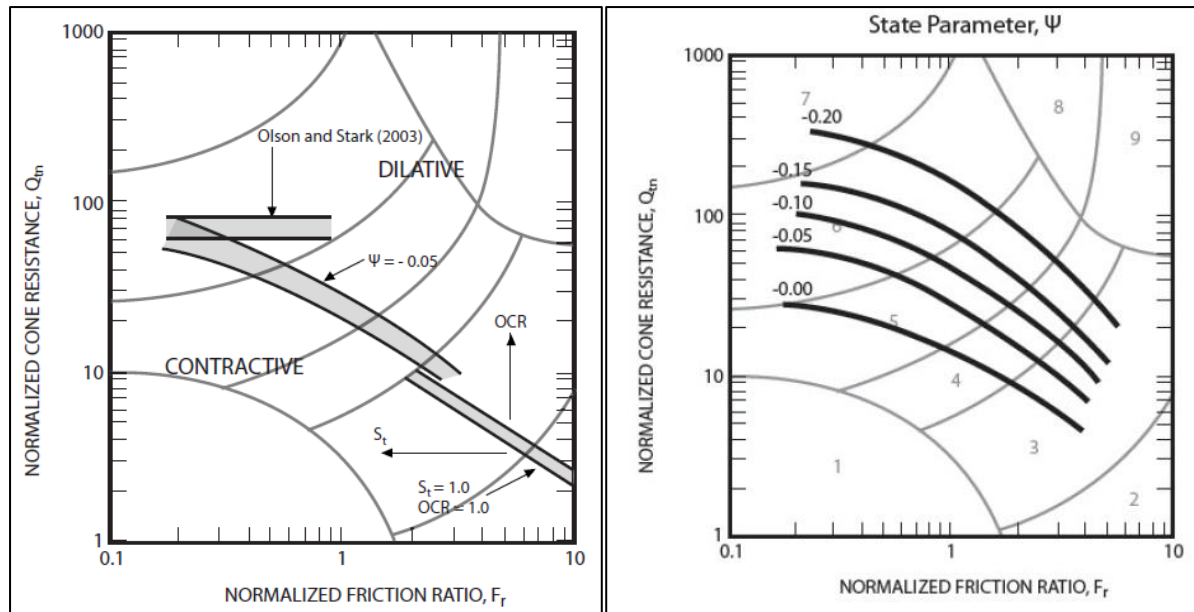
*Figure 2.32: Boundary between contractive and dilative soils (Robertson, 2010)*

A correction factor can be added to normalise cone resistance of silty sands to an equivalent clean sand value.

$$Q_{tn,cs} = K_c Q_{tn}$$

*Equation 2.22: Normalised cone resistance with SBT component and clean sand correction*

Where $K_c$ is the correction factor, which is a function from the particle size and can be determined by using $I_c$ in the following equation:

$$K_c = 1.0 \ if \ I_c \leq 1.64$$

$$K_c = 5.581 I_c{}^3 - 0.403 I_c{}^4 - 21.63 I_c{}^2 + 33.75 I_c - 18.88 \ if \ I_c > 1.64$$

*Equation 2.23: Clean sand correction factor for normalised cone resistance*

Iteration is however needed, because $K_c$ is a function of Ic, and Ic is influenced by Qtn. Figure 2.33 indicates the suggested method from Robertson and Cabal (2012) to determine the cyclic resistance ratio from corrected CPT values.
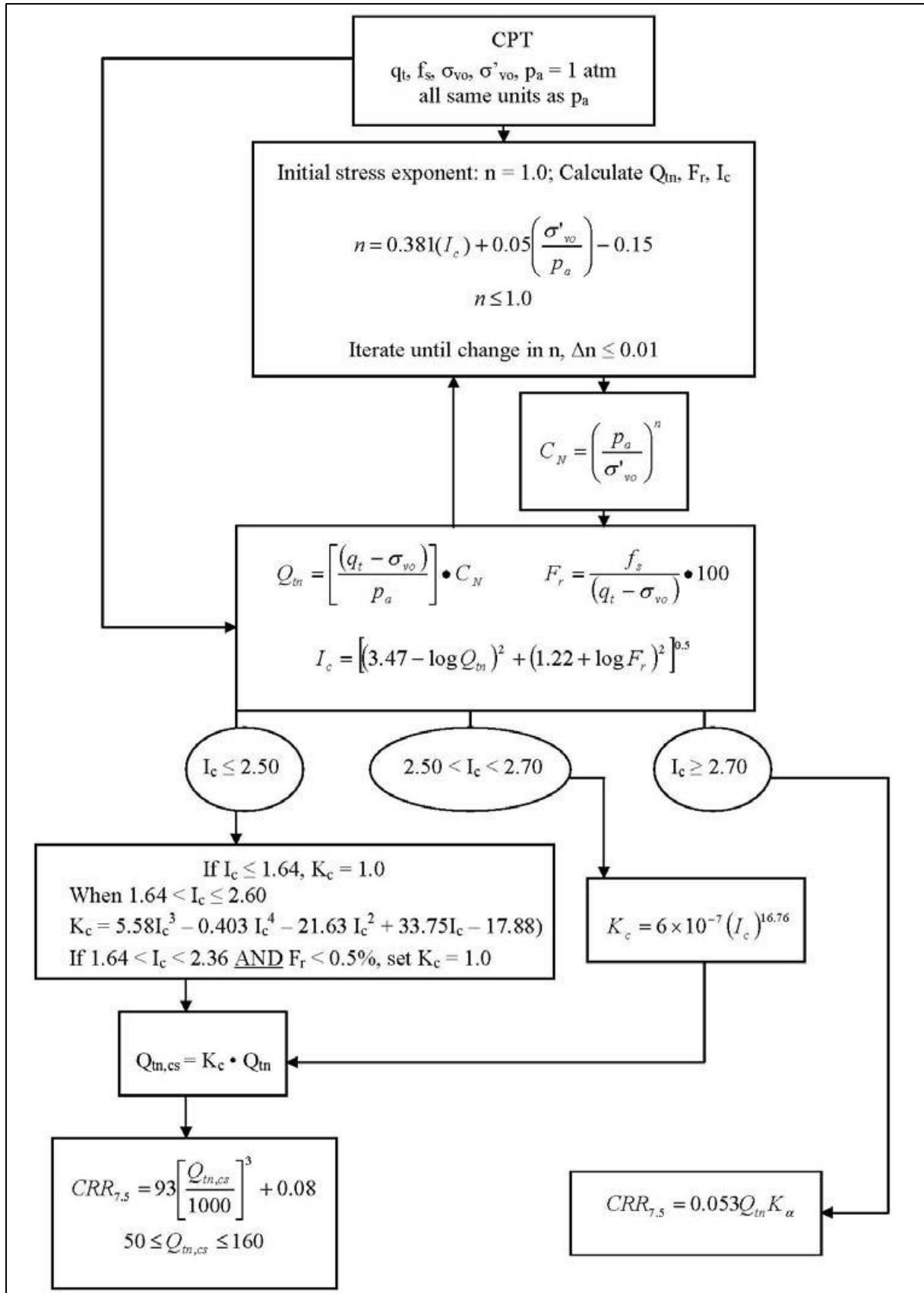
*Figure 2.33: Flow chart to evaluate cyclic resistance ratio from CPT (Robertson, 2010)*

The Figure 2.34 indicates the clean sand penetration resistance. The contours of the clean sand resistance follow a trend similar to that of the dilative and contractive boundaries. A value of between 50 and 70 most probably represents the boundary between the dilative and contractive state of soils (Robertson & Cabal, 2012). The dilative and contractive boundary (CD) can be used to determine whether a soil will dilate or contract. A value of CD = 70 is seen as conservative for sands. Samples that plot more than 70 will tend to dilate and smaller will likely contract and liquefy (Robertson, 2010).

$$CD = (Q_{tn} - 11)(1 + 0.06F_r)^{17}$$

*Equation 2.24: Contractive dilative boundary*
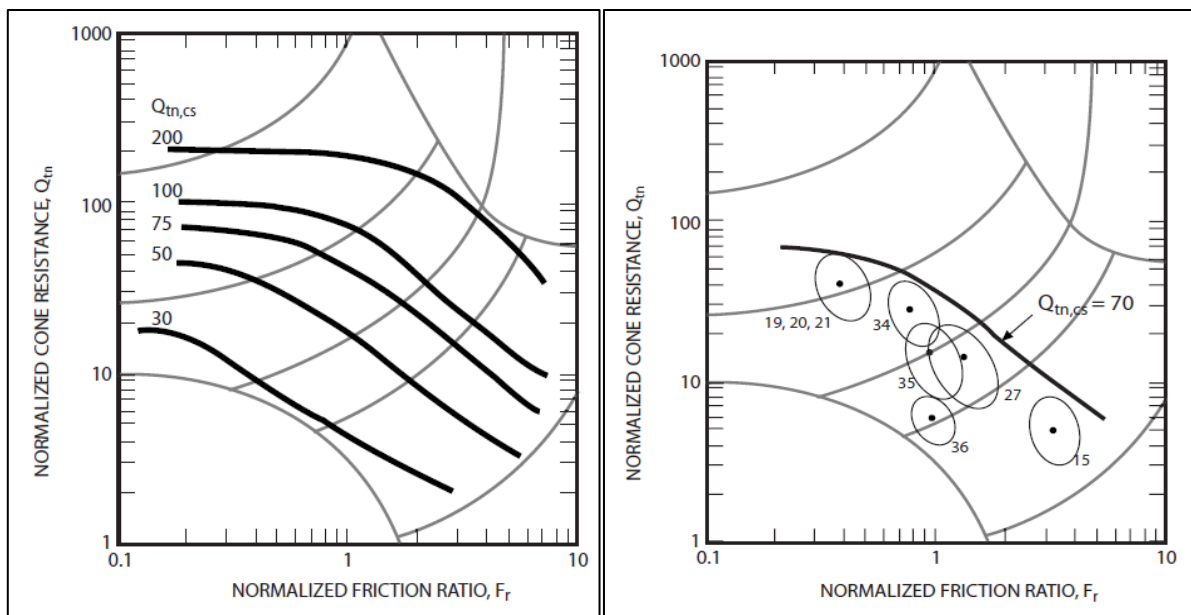


*Figure 2.34: Contours for clean sand normalised cone resistance (Robertson, 2010)*

The contour lines in the above figure have a similar profile to that of the state parameter. It can therefore be deduced that a constant value for the clean sand normalised cone resistance will have more or less the same state parameter and probably have the same response to loading (Robertson, 2010).

The second graph in Figure 2.34 indicates the same SBT graph with the addition of case studies that Robertson (2010) investigated. All these case studies experienced liquefaction and plot below the normalised clean sand penetration resistance contour. The susceptibility of a soil to liquefy can by evaluated with these parameters. Liquefaction is said to be possible if the value of CD or $Q_{tn,cs} \leq 70$ (Robertson, 2010).

47

### 2.4.3.3   Empirically correlating data

Normalised Soil Behaviour Type or SBT charts can be used to present the results of the CPT test visually. This requires the normalised friction ratio and normalised cone resistance, after Ic has been determined through the iteration process. Calculated values for Ic and CD can be added to the SBT plots to separate potential liquefiable soils. Ic and CD can also be presented individually with depth to establish if there are any particular problematic depth zones.

The criteria to be used with the SBT graphs of Robertson (2010) in predominantly sandy soils can be summarised as follows:

*Table 2.4: Criteria for liquefiable soils (Robertson & Cabal, 2012)*

| Criteria | Limit or boundary | If smaller | If larger |
|---|---|---|---|
| Contractive Dilative (CD) | 70 | Contractive and potentially liquefiable | Dilative |
| Soil Behaviour Zone (Ic) | 2.6 | Sand like and potentially liquefiable | Clay Like |

| Zone | SBT |
|---|---|
| 1 | Sensitive, fine grained |
| 2 | Organic soils, clay |
| 3 | Clay, silty clay to clay |
| 4 | Silt mixtures, clayey silt to silty clay |
| 5 | Sand mixtures, silty sand to sandy silt |
| 6 | Sands, clean sands to silty sands |
| 7 | Gravelly sand to dense sand |
| 8 | Very stiff sand to clayey sand |
| 9 | Very stiff fine grained |

| | | |
|---|---|---|
| Cohesionless soils | A1 A2 | Evaluate potential behaviour using CPT-based case-history liquefaction correlations |
| | A1 | Cyclic liquefaction possible depending on level and duration of cyclic loading |
| | A2 | Cyclic liquefaction and flow liquefaction possible depending on loading and ground geometry |
| Cohesive soils | B C | Evaluate potential behaviour based on in situ or laboratory test measurements or estimates of monotonic and cyclic undrained shear strengths |
| | B | Cyclic softening possible depending on level and duration of cyclic loading |
| | C | Cyclic softening and flow liquefaction possible depending on soil sensitivity, loading, and ground geometry |
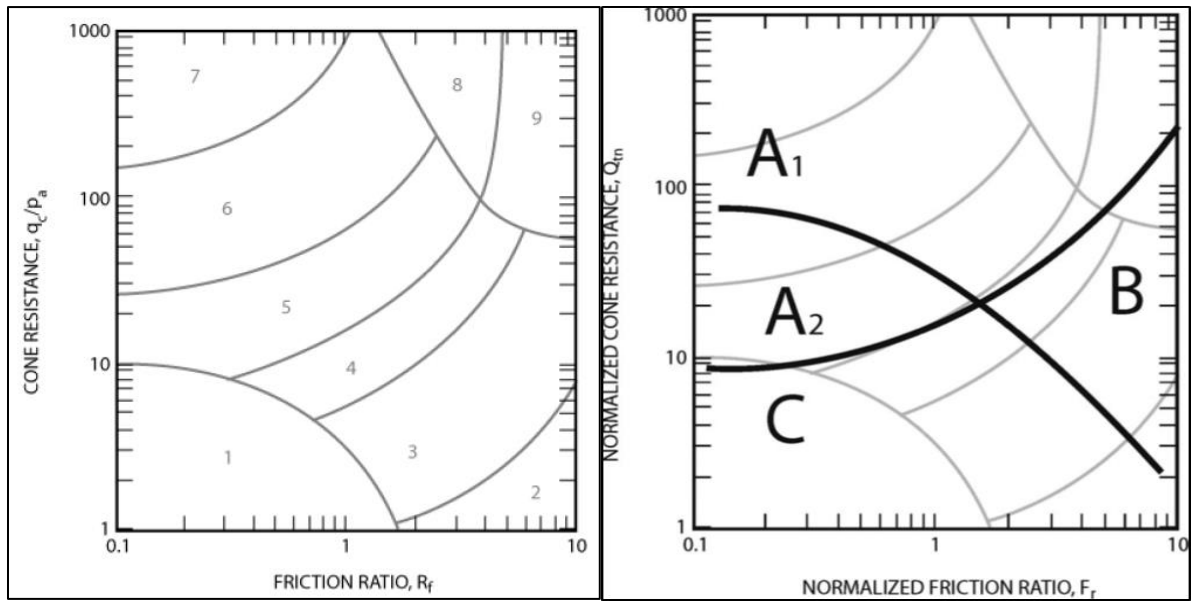
*Figure 2.35: SBT chart for soil properties (Robertson, 2010)*

Computer software also exist for use with CPT and liquefaction analysis. CPT tests can have continuous real-time readings, and professional software helps to plot and create easy to read resistance, friction and pore water pressure graphs, as well as SBT charts.
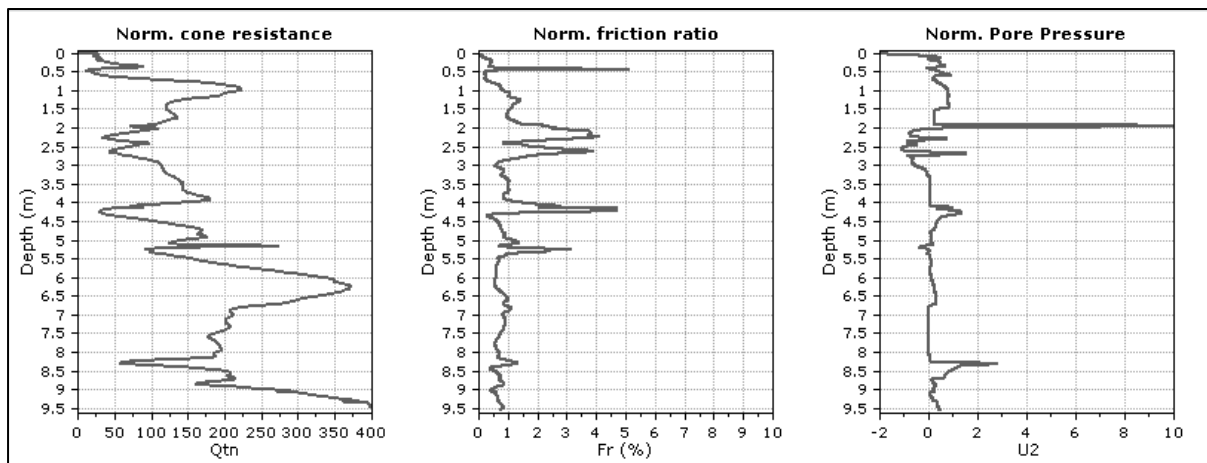


*Figure 2.36: Example of software used (Robertson & Cabal, 2012)*

## 2.5   Synthesis

The literature review summarises the term liquefaction. From the literature, we can understand how liquefaction occurs and how to determine whether a soil will liquefy during undrained shear. The literature defines the soil type and the mechanical properties of a soil that will likely liquefy during an earthquake. The literature also describes the use of two invasive testing methods, namely the SPT and CPT.

Soil properties as well as the SPT and CPT testing methods can now be used to empirically correlate samples and determine the likelihood of liquefaction. The method will be discussed in the following chapter, which also includes the use of a vibrating table to test the various types of soils and the effect of density.

# 3   Methodology

## 3.1   Introduction

This chapter will discuss the various types of testing and methods used to determine the susceptibility of Cape Flats sands to liquify.

The following flowchart roughly highlights the key points and steps during this research.
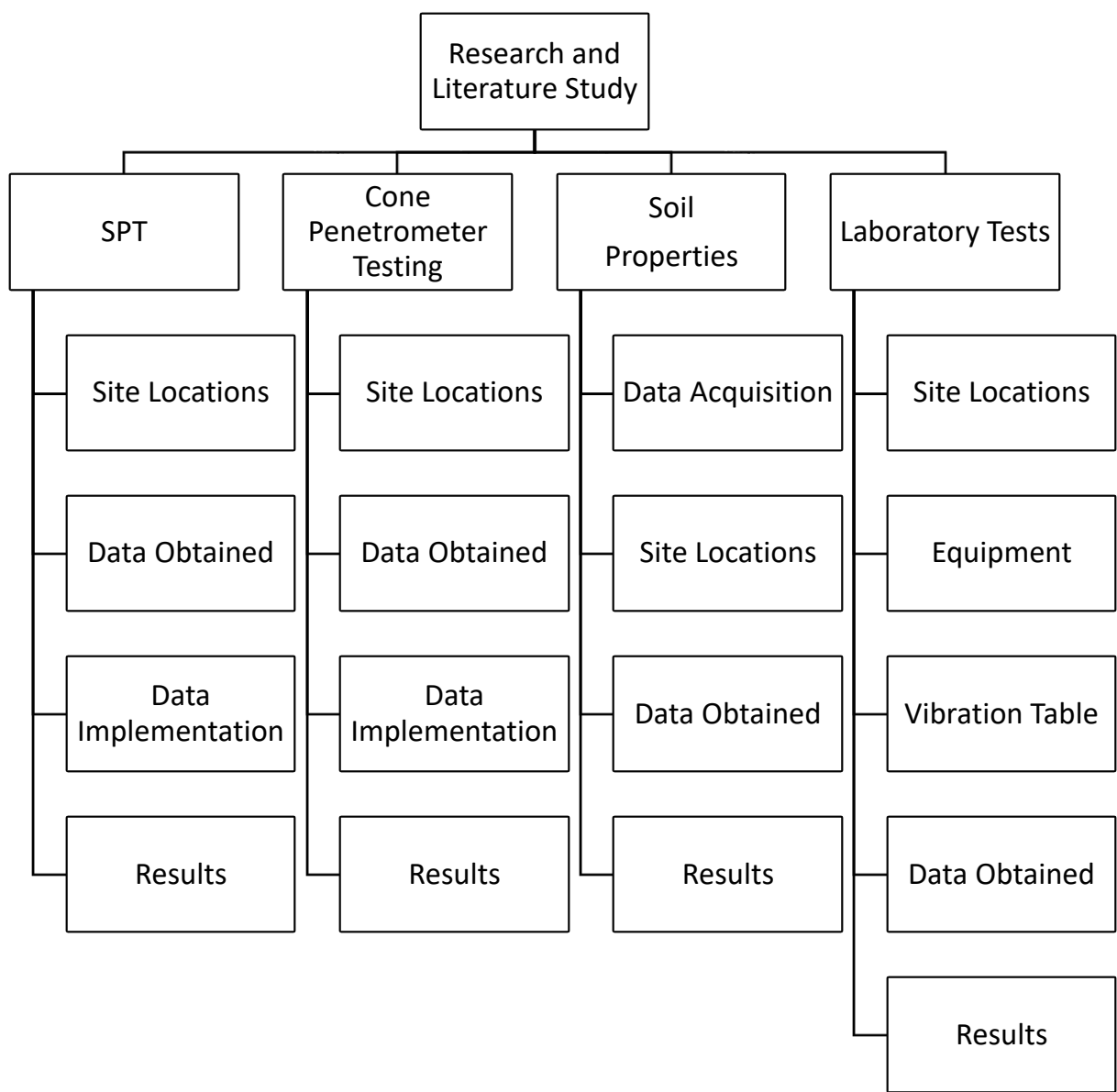
*Figure 3.1: Flowchart highlighting key points and steps followed*

## 3.2    Estimation of liquefaction potential with the Standard Penetration Test

### 3.2.1    Introduction

This section will discuss the method used to empirically correlate SPT-N values from drilling and DPSH testing. Data obtained through research and the implementation thereof will be discussed in this chapter. The final data and outcome of the research are explained in the next chapter.

### 3.2.2    Site locations

SPT testing is generally done to determine soil engineering properties and strength with depth, to aid in the construction of buildings or other large structures sensitive to subsidence or differential settlement.

Records from Fairbrother Geotechnical Engineering in Cape Town were used in this study. Fairbrother has carried out hundreds of SPT and DPSH testing across Cape Town. Unfortunately, most of these tests have been carried out in soils other than the Cape Flats. Data from DPSH testing was also incorporated into the research for this reason. Nevertheless, results were obtained, and their locations are indicated in Figure 3.1 and Figure 3.2.
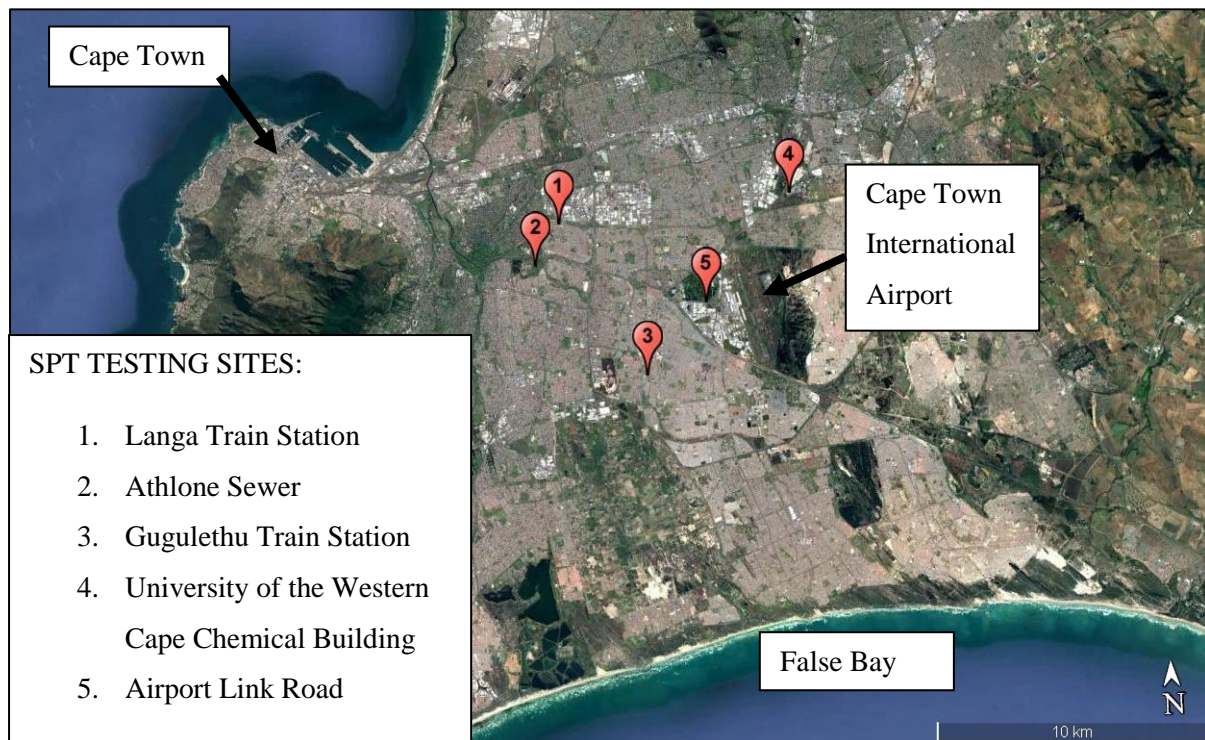


*Figure 3.1: SPT drilling site locations*

DPSH TESTING SITES:

1. Bellville CPUT
2. Airport Area
3. Bellville Weighbridge
4. Bellville WWTW
5. Gateway Office Park
6. Heideveld Station
7. Mitchells Plain Station
8. Khayelitsha
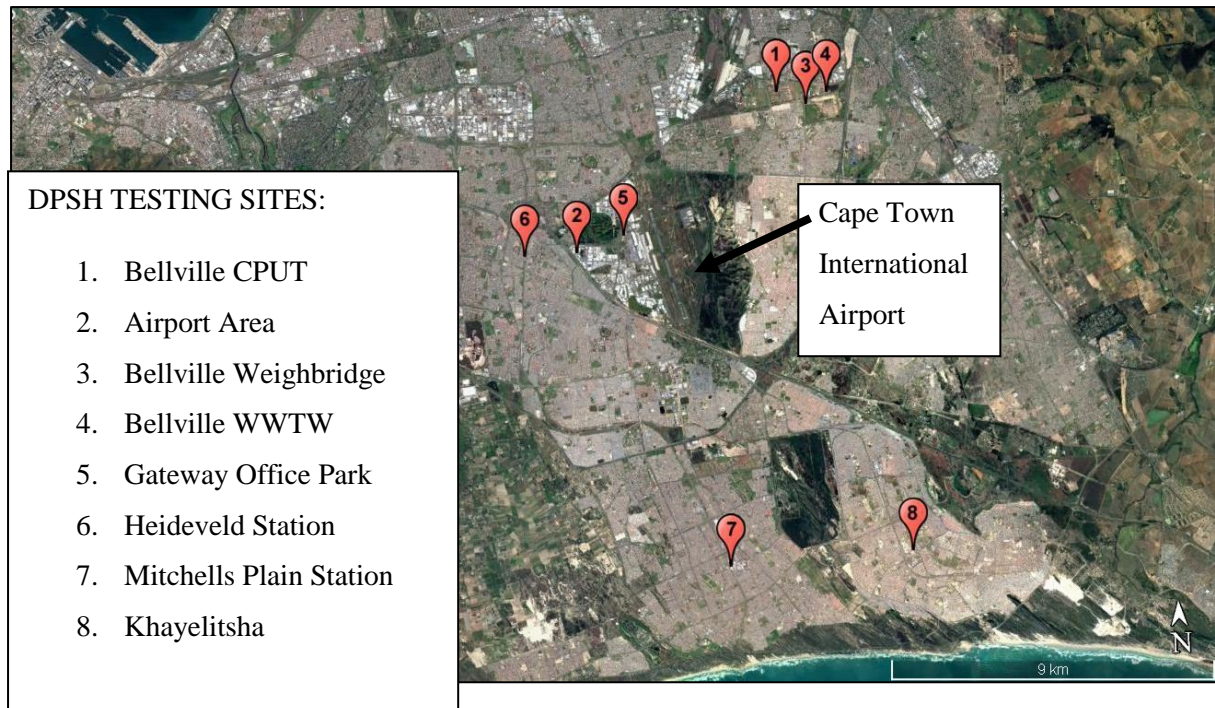
*Figure 3.2: DPSH Testing Locations*

### 3.2.3    Data obtained

A full geotechnical site investigation for the majority of the sites follow a series of tests and inspections. The type and number of tests needed depends on the project and geological concerns. An example of a geotechnical investigation needed to determine whether an area on the Cape Flats is susceptible to soil liquefaction can be as follow: The area to be investigated should be walked over, and any noticeable geological features should be noted. A series of test pits, soil profiling and soil sampling should then be carried out. Core drilling with SPT testing or other penetration tests should be spread out over the site. These cores and data obtained can then be analysed together with the soil profiles and soil sampling results.

For example, a walkover will tell one if there are any steep slopes or flat low-lying areas, both of which behave differently during seismic activity. Test pits, soil profiling and soil sampling (testing) will provide one with the geology, water table and properties of the underlying soils. Lastly penetration tests will provide the engineer/technician with the density, a crucial aspect in determining whether a soil is susceptible to liquefaction.

Most of the data in this study were obtained from historic work done by geotechnical contractors. The data was in its raw state, in the way the driller would present it. These values where processed and plotted as SPT-N (and $N1_{(60cs)}$) values to depth. This allows one to visually see relative density and soil strength increasing with depth. Figure 3.3 is an example of data received from the contractor for a SPT rig. The values indicated in the total section is the sum of the last four readings. Figure 3.4 is an example of data received from the contractor for a DPSH rig. The data is presented in one metre penetration

53

intervals. Each metre is further divided in 10 sections (each section is a 100 mm). The amount of blows it takes to penetrate each 100 mm is then recorded. Adding the values of three consecutive (300 mm) readings gives an equivalent SPT-N value.

Therefore, both the SPT and the DPSH tests use a reading equal to the sum of 300 mm.



*Figure 3.3: SPT Field data example*



*Figure 3.4: DPSH Field data example*

As discussed in Chapter Two, SPT-N values needs to be corrected for several factors before it can be used in the empirical correlations. These include the short rod correction factor and hammer energy efficiency. The data used in this study is derived from both conventional SPT and DPSH testing. In addition, each of these machines have been custom made, and in most cases, differ with each test. This gives room for error and extrapolating of the error onto the next equation.

This project did not have access to measured hammer energy data. Therefore, this project will assume that no losses or gains were experienced with regards to the hammer energy, consequently, using the value of one instead. This assumption does allow room for error and can be seen as one of the limitations. Resulting outcomes should therefore be used conservatively. Furthermore, to correct for clean sand equivalent, one needs to have gradings with each of the tests. The data required for these corrections were not available for most of the investigations. It was therefore decided to use the average fines content from laboratory test results obtained for this project. The average fines content from obtained results from the Cape Flats is 6% for all samples.

Furthermore, from the literature study we know that an earthquake with a magnitude (M) of 6 and PGA of 0.15g is possible. Other parts in South Africa can however expect a PGA of 0.25g, and possibly a magnitude (M) of 8. It was therefore decided to use these values for fines, magnitude and PGA in the calculations and corrections, for both DPSH and SPT testing. These are discussed further in the following sections.

### 3.2.4   Data implementation

To start with, the depth of the water table for the investigated site must be known. Seeing as the water table can vary considerably in the Cape Flats area, it was decided to use two water table depths for calculations; one at two metres below ground level, and the other at one metre below ground level. This seems adequate, as some areas have an even shallower water table during winter months. Furthermore, the unit weight of both drained and undrained soil samples must be determined. For the purpose of this study, the unit weight of the saturated soil layer (below the water table) was taken as $19 kN/m^3$, and the dry unit weight as $17 kN/m^3$. In addition, ground acceleration data must be obtained for the areas being investigated. Ground acceleration maps for South Africa are discussed in Chapter two and indicates that up to 0.15g's can be expected for the Cape Town area (Figure 3.5). The maximum acceleration in South Africa can however be up to $2.45 m/s^2$ or 0.25g's. Therefore, both values 0.15g and 0.25g where used in the calculations (Wium, 2010).
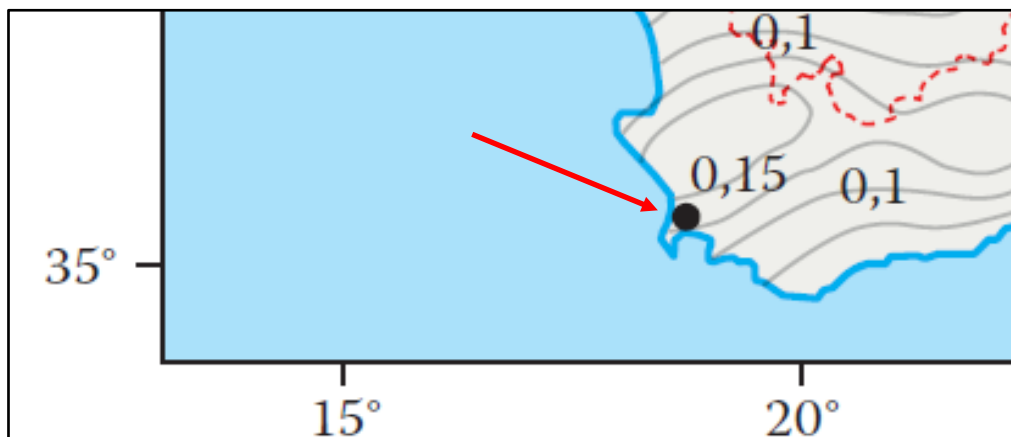


*Figure 3.5: PGA Map for the study area (Wium, 2010)*

As discussed in Chapter two, the magnitude scaling factor will have a value of one if an earthquake with a magnitude (M) of 7.5 occurs. This study will assume a magnitude for M = 6 with a PGA of 0.15g and M = 8 with a PGA of 0.25g. The reason for these two magnitudes is discussed further in the methodology section. Corrections were then also made according to the magnitude. SPT-N values were also corrected and considers a fines content of 6%. This number of fines was chosen as it is more or less the average amount of fines present in grading results obtained over the Cape Town Metropolitan Area. Subsequently, the CSR and CRR values can now be calculated for each layer tested in both the DPSH and SPT profiles. With depth, increase in shear needs to be adjusted for, and the shear stress reduction factor needs be calculated for each depth of testing. Values obtained for the CSR were plotted with each of the corrected SPT-N values. This was done for each of the DPSH and SPT sites. Each site was plotted with a PGA of 0.15g and 0.25g, at a groundwater table of 1m below ground level.

The Idriss and Boulanger (2004) calculations were used to determine a boundary line (

Figure 3.6) for areas that will be potentially susceptible to liquefaction compared to areas that should be safe against liquefaction. The Idriss and Boulanger method was chosen because it is the most recent method based on the experience of several other authors (Idriss & Boulanger, 2010). The CRR must be calculated to determine the boundary line. The CRR, cyclic resistance ratio, uses an exponential calculation and is determined from in situ SPT-N values (Equation 2.14).
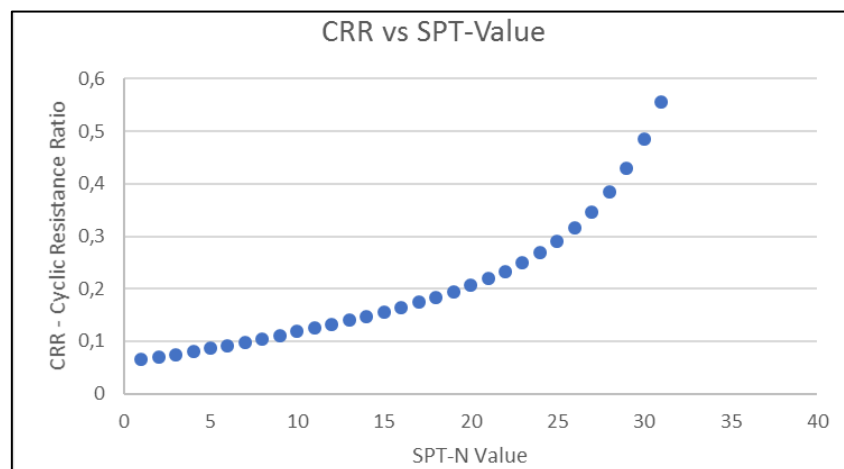


*Figure 3.6: Established boundary curve for potentially liquefiable soils*

A Microsoft Excel spreadsheet was setup for each site that underwent investigation. This made it easy to determine several other factors, one being the factor of safety based on the CRR and CSR. If the factor of safety is smaller than 1.0, liquefaction is likely to occur.

The PGA and Magnitude for each area were changed to obtain a complete new set of data for each site. By plotting the CRR against the SPT-N value, a boundary curve could be obtained and used with each set of data.

Figure 3.7 is a screenshot of the Microsoft Excel spreadsheet that was used in calculating results.

| WT | M | Fines | Unit weight of water Yw kN/m3 | Unit weight of sat sands kN/m3 | Unit weight of dry sands kN/m3 | PGA | Acceleration of gravity m/s/s | | | | | | | |
|---|---|---|---|---|---|---|---|---|---|---|---|---|---|---|
| 1 | 6 | 6 | 9,81 | 19 | 17 | 0,15 | 9,81 | | | | | | | |
| | | | | | | | | | | | | | | |
| Depth | SPT N | σ'vo (kPa) | (N1)60 | Δ(N1)60 | (N1)60cs | CRR | σvo (kPa) | a(z) | b(z) | Ln(rd) | rd | CSR | MSF | CSR7.5 |
| 1,00 | 2 | 17 | 5 | 0,027 | 5 | 0,09 | 17 | -0,027 | 0,0035 | -0,01 | 0,99 | 0,097 | 1,45 | 0,067 |
| 2,00 | 4 | 28,2 | 8 | 0,027 | 8 | 0,10 | 36 | -0,077 | 0,0091 | -0,02 | 0,98 | 0,122 | 1,45 | 0,084 |
| 3,00 | 6 | 39,4 | 10 | 0,027 | 10 | 0,12 | 55 | -0,134 | 0,0154 | -0,04 | 0,96 | 0,131 | 1,45 | 0,090 |
| 4,00 | 8 | 50,6 | 11 | 0,027 | 11 | 0,13 | 74 | -0,197 | 0,0225 | -0,06 | 0,94 | 0,134 | 1,45 | 0,092 |
| 5,00 | 10 | 61,8 | 13 | 0,027 | 13 | 0,14 | 93 | -0,266 | 0,0302 | -0,09 | 0,92 | 0,135 | 1,45 | 0,093 |
| 6,00 | 12 | 73 | 14 | 0,027 | 14 | 0,15 | 112 | -0,341 | 0,0385 | -0,11 | 0,90 | 0,134 | 1,45 | 0,092 |
| 7,00 | 14 | 84,2 | 15 | 0,027 | 15 | 0,16 | 131 | -0,420 | 0,0473 | -0,14 | 0,87 | 0,132 | 1,45 | 0,091 |
| 8,00 | 16 | 95,4 | 16 | 0,027 | 17 | 0,17 | 150 | -0,504 | 0,0566 | -0,16 | 0,85 | 0,130 | 1,45 | 0,090 |
| 9,00 | 18 | 106,6 | 18 | 0,027 | 18 | 0,18 | 169 | -0,591 | 0,0663 | -0,19 | 0,82 | 0,127 | 1,45 | 0,088 |
| 10,00 | 20 | 117,8 | 19 | 0,027 | 19 | 0,19 | 188 | -0,682 | 0,0763 | -0,22 | 0,80 | 0,124 | 1,45 | 0,086 |
| 11,00 | 22 | 129 | 19 | 0,027 | 20 | 0,20 | 207 | -0,775 | 0,0865 | -0,26 | 0,77 | 0,121 | 1,45 | 0,083 |
| 12,00 | 24 | 140,2 | 20 | 0,027 | 20 | 0,21 | 226 | -0,869 | 0,0969 | -0,29 | 0,75 | 0,118 | 1,45 | 0,081 |

*Figure 3.7: Excel Spreadsheet for data calculations*

Finally, after calculating all necessary data, the CSR value for each area were plotted against the corresponding corrected SPT-N value. The outcome of the plotted data is summarised and discussed in the results chapter.

Results were plotted using either the graph function in Microsoft Excel, or CoPlot, a software application that allows large data sets with more than one input to be plotted.

### 3.3   Empirical correlation by using the CPTu

### 3.3.1   Introduction

This section will discuss the results that were obtained after testing the ground conditions at two sites with the use of a piezocone penetrometer. Consequently, these results were empirically correlated with the method discussed in the literature review. Results will be implemented and discussed in more detail in this section. These results can be used to determine whether sands from the tested areas are susceptible to liquefaction.

### 3.3.2   Site locations

Two areas were chosen, which were situated within the study area and had safe access. The first location was at Geoscience Laboratories in Airport Industrial, Cape Town. The second location was near Muizenberg in Capricorn Park, an industrial estate north of Muizenberg.

The locations of these two sites are indicated in Figure 3.8.



*Figure 3.8: Piezocone - CPTu Testing Locations*

### 3.3.3  Piezocone - CPTu Testing Procedure

A Pagani CPTu rig was used in the testing of the two sites. The machine pushes a cone with pressure and friction sensitive sensors into the ground by means of a hydraulic driven piston. The cone, pushed into the ground at a steady rate, continuously returns readings to the surface where they can be interpreted by the operator. Naturally, pressure and friction forms around the cone as it is pushed into the ground. When the cone is pushed through saturated soils, pore water pressure starts to increase around the cone and pressure sensors. The operator can decide at any time if he or she wants to measure actual pore water pressure at a specific depth, or when pressure reaches a point that the unit starts to lose sensitivity.

The phreatic surface or water table is known as the depth below ground level where pore water pressures are the same as that of the atmospheric pressure. This is the point below ground level were the soil is 100% saturated. This is useful, as determining the water level in fine grained soils can be difficult due to the natural effect of capillary rise. Capillary tension attracts and pulls groundwater upwards, causing negative pore water pressure to develop.

Furthermore, the rate or time for dissipation can provide the operator with the permeability or hydraulic conductivity of the soil. If the pore pressure dissipates quickly, it can indicate the existence of highly permeable soils where groundwater flows easily. However, if the pore pressure dissipates slowly, an aquitard or impermeable layer can be present, restricting groundwater flow. Determining soil properties and accurate hydrological features can be improved if more than one CPT test is carried out in the area. This could also provide the user with a three-dimensional groundwater map, indicating information such as depth and direction of groundwater flow.

### 3.3.4  Data obtained

Two tests were carried out at each of the two sites. This gave four data sets in a Microsoft Excel Spreadsheet format, each including the tip resistance of the cone ($q_c$), penetration or sleeve friction ($f_s$) and the pore water pressure at the tip of the cone (u). Figure 3.9 shows the actual CPT rig used and an example of the raw and unprocessed results obtained from it.

These results are however in their raw state and no corrections are made for pore water pressure or type of soils encountered. To correct the measured tip resistance ($q_c$), the value $q_t$ is determined, the corrected cone resistance. The value *a* is the area ratio determined from calibration and is supplied by the contractor. A value of 0.80 was used for *a* in this study.

$$q_t = q_c + u\,(1-a)$$

*Equation 3.1: Corrected cone resistance*
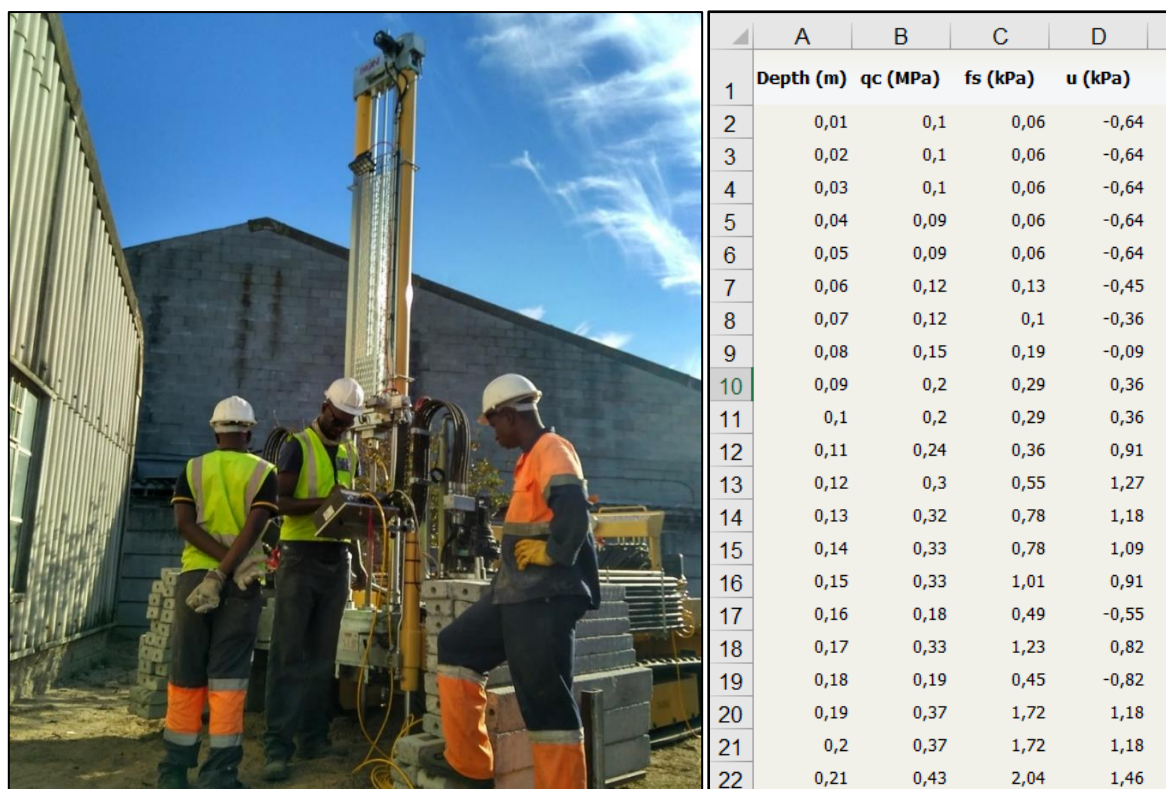
*Figure 3.9: CPTu rig used during testing and sample of results obtained*

Where $q_c$ and $u$ are measured by the CPT rig at a constant rate with depth, $q_t$ is determined for each CPT tip reading or every 10 mm. The effective overburden stress within the soil is then used to determine the normalised cone resistance ($Q_t$) and the normalised friction ratio ($F_r$). The water table can also be determined by using the dissipation results obtained from the operator. Figure 3.10 is an example of the dissipation test performed by the operator. The image indicates that a test was carried out at a depth of 5.98 m below ground level. The measured pore water pressure as the probe is inserted ($u_0$) is measured as 58.66 kPa and the pressure of penetration ($u_2$) achieved an equilibrium pressure at approximately 34.00 kPa. The steady state pore water pressure of penetration along with the unit weight of water ($\gamma_w$), which is 9.81 kN/m³, can then be used to determine the depth of the water table:

$$Water\ table\ depth = Test\ depth - \frac{u_0}{\gamma_w}$$

*Equation 3.2: Depth of the water table using CPTu*

60
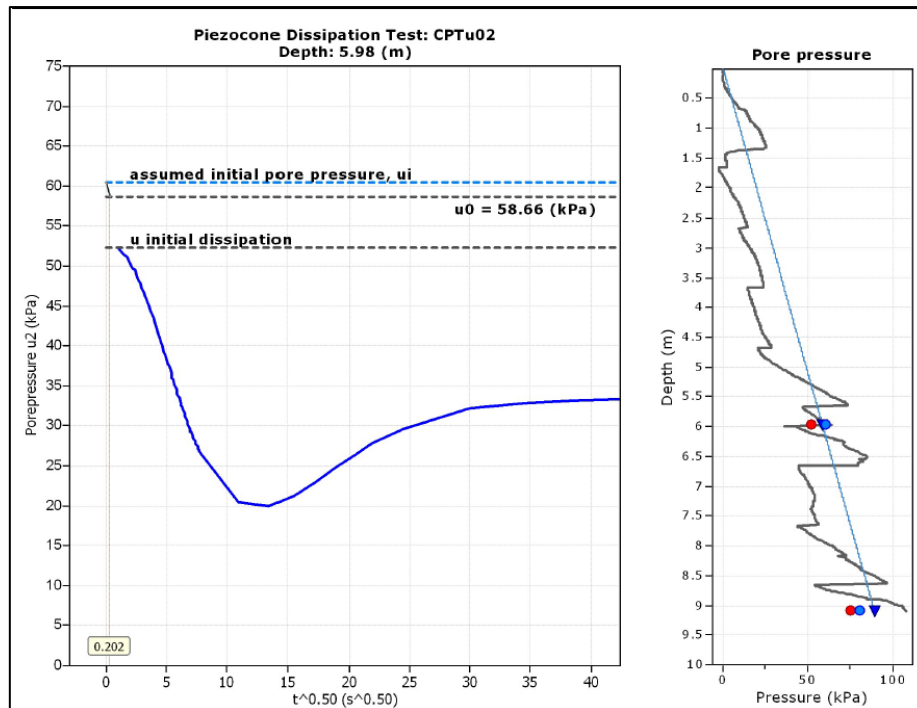
*Figure 3.10: Dissipation test*

The depth to the water table is required to determine the liquefaction resistance of the soil during an earthquake. Areas with a deeper water table are more resistant to liquefaction compared to areas with a shallow groundwater table.

### 3.3.5  Data implementation

The data obtained from the CPT test (that of the tip resistance of the cone ($q_c$), penetration or sleeve friction ($f_s$) and the pore water pressure at the tip of the cone (u)) is used with the known depth of the water table in empirical correlations. A Microsoft Excel spreadsheet was made for each of the four CPT tests. Figure 3.11 is a screenshot of one of the calculation sheets. The screenshot shows two calculated water table depths, as two dissipations tests were carried out. The average of the two levels was used as the groundwater table. The unit weight of saturated sands and dry sands was taken as 19 and 17 kN/m$^3$ respectively, as these values are relatively standard for similar soil types. Not all of the columns seen in the screenshot were used in this section.

The normalised friction and cone resistance parameters (Equation 2.16 and Equation 2.17) were calculated as suggested by Robertson (2010), followed by the total and effective overburden stresses. The value of  the area ratio, a, as discussed earlier, is taken as 0.80. The study area lies close to sea level and the atmospheric pressure is therefore assumed to be a value of 101.3 kPa.

| test depth (m) | kpa at test | kpa at dissipation | kpa at dissipation / unit weight of water | water table depth | Ave WT | unit weigt of water | Unit weight of sat sands kN/m3 | Unit weight of dry sands kN/m3 | | | | | | | | | | | |
|---|---|---|---|---|---|---|---|---|---|---|---|---|---|---|---|---|---|---|---|
| 4,27 | 41,89 | 17,00 | 1,73 | 2,54 | 2,64 | 9,81 | 19 | 17 | | | | | | | | | | | |
| 9,68 | 94,96 | 68,00 | 6,93 | 2,75 | | | | | | | | | | | | | | | |

| Depth (m) | qc (MPa) | fs (kPa) | u (kPa) | qc (kPa) | u (kPa) Abs | Total effective stress kPa | Depth below water table | Vertical Stress or overburden Pressure kPa | a | Pa | qt | Qt | Fr | Qtn | CN | n | Ic | Ic | n | Qtn |
|---|---|---|---|---|---|---|---|---|---|---|---|---|---|---|---|---|---|---|---|---|
| 0,01 | 0,12 | 0,13 | 0 | 120,00 | 0,00 | 0,17 | -2,633 | 0,17 | 0,8 | 101,3 | 120,00 | 704,88 | 0,11 | 3,08 | 2,61 | -0,15 | 0,00 | 0,672277274 | 0,106221551 | 2,332050592 |
| 0,02 | 0,12 | 0,13 | 0 | 120,00 | 0,00 | 0,34 | -2,623 | 0,34 | 0,8 | 101,3 | 120,00 | 351,94 | 0,11 | 2,77 | 2,35 | -0,15 | 0,00 | 0,958353077 | 0,215300341 | 4,027362283 |
| 0,03 | 0,12 | 0,16 | 0,09 | 120,00 | 0,09 | 0,42 | -2,613 | 0,51 | 0,8 | 101,3 | 120,02 | 284,54 | 0,13 | 2,68 | 2,27 | -0,15 | 0,00 | 1,073393107 | 0,259170079 | 4,889044631 |
| 0,04 | 0,12 | 0,13 | 0,09 | 120,00 | 0,09 | 0,59 | -2,603 | 0,68 | 0,8 | 101,3 | 120,02 | 202,27 | 0,11 | 2,55 | 2,16 | -0,15 | 0,00 | 1,192141005 | 0,304496937 | 5,644768087 |
| 0,05 | 0,11 | 0,13 | 0 | 110,00 | 0,00 | 0,85 | -2,593 | 0,85 | 0,8 | 101,3 | 110,00 | 128,41 | 0,12 | 2,20 | 2,04 | -0,15 | 0,00 | 1,393185296 | 0,381223144 | 6,666627222 |
| 0,06 | 0,12 | 0,13 | 0 | 120,00 | 0,00 | 1,02 | -2,583 | 1,02 | 0,8 | 101,3 | 120,00 | 116,65 | 0,11 | 2,34 | 1,99 | -0,15 | 0,00 | 1,426733885 | 0,394089065 | 7,192237779 |
| 0,07 | 0,12 | 0,13 | 0 | 120,00 | 0,00 | 1,19 | -2,573 | 1,19 | 0,8 | 101,3 | 120,00 | 99,84 | 0,11 | 2,28 | 1,94 | -0,15 | 0,00 | 1,493341405 | 0,41955044 | 7,568365796 |
| 0,08 | 0,14 | 0,16 | 0,09 | 140,00 | 0,09 | 1,27 | -2,563 | 1,36 | 0,8 | 101,3 | 140,02 | 109,18 | 0,12 | 2,63 | 1,92 | -0,15 | 0,00 | 1,459397942 | 0,406657467 | 8,123047341 |

*Figure 3.11: Screenshot from CPT Data Calculation in MS Excel*

Visual Basics Applications (VBA) were used in Excel to write an iteration code for the calculating of n and Ic. The new written formula can then simply be used in the same way as with any other formula in Excel.

The input starts with an initial stress component setting n = 1, calculating the following:

$$n \rightarrow C_N \rightarrow Q_{tn} \rightarrow I_c \rightarrow n$$

The value of n, set as = 1 initially, is used to determine $C_N = (\frac{Pa}{\sigma'_{vo}})^n)$ which in turn is used to calculate

the normalized cone resistance $Q_{tn} = \left[\frac{(q_t - v_o)}{Pa}\right] . C_N$. The normalized friction ratio is calculated from

corrected CPT data as $F_r = \left[\frac{f_s}{(q_t - \sigma_{vo})}\right] . 100$

The normalised friction ratio and the normalised cone resistance values can then be used to calculate the soil behaviour type index:

$$I_c = [(3.47 - log\ Q_{tn})^2 + (log\ Fr + 1.22)^2]^{0.5}. \qquad \textit{Equation 3.3: SBT Index}$$

The Ic value should replace the initial value of (n), followed by a re-calculation. This iteration should continue until the difference between n and Ic is less than 0.01. The iteration was completed and the Ic for each layer was determined. With the corrected cone resistance being calculated from the final Ic value, the value of CD (Contractive Dilative value) was determined:

$$CD = (Q_{tn} - 11)(1 + 0.06F_r)^{17} \qquad \textit{Equation 3.4: Contractive Dilative Boundary}$$

The soil behaviour type index and Contractive Dilative boundary value can be used together with the normalised friction ratio and normalised cone resistance as suggested by Robertson (2010) to determine if the soil will be susceptible to liquefaction. Soils that have an *Ic* of less than 2.6 will have sand-like properties, and soils with a CD less than 70 will be potentially contractive and liquefiable. Data was presented or plotted using either the Microsoft Excel graph function, or graphs made from the Gregg CPT software tool.

### 3.4    Empirical correlation by using soil properties

### 3.4.1    Introduction

This section will discuss the use of soil gradings obtained from sites all over the study area. The literature indicates various soil properties, or different gradings of soil more prone to liquefaction compared to other gradings.

### 3.4.2    Data acquisition

Figure 2.15, from the literature, indicates the gradings of liquefied soil on a tertiary graph (Andrews & Martin, 2000). The gradings on the tertiary graph were used to plot the data onto a bar diagram for easier comparison with data obtained during this research and is displayed in Figure 3.12.
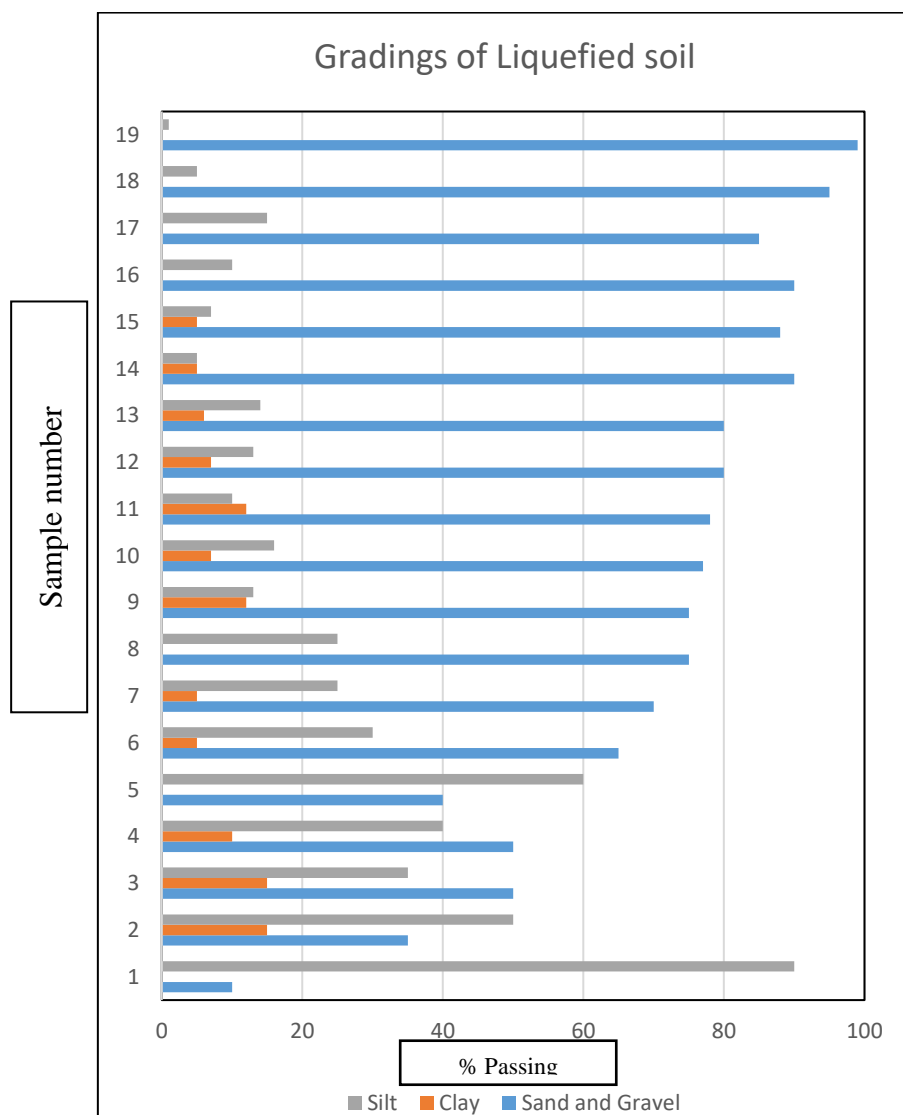


*Figure 3.12: Gradings of Liquefied soils*

Figure 3.12 shows data obtained by Andrews and Martin (2000) from liquefied soil from 10 earthquakes in Japan. The data is divided into three categories, namely:

- Sand and gravel
- Silt
- Clay

From the bar diagram, Figure 3.12, it is evident that soils with a large sand content, experienced liquefaction. In only two cases, the liquefied soil had a silt content of more than 50%, however, all the samples had a clay content of less than 20%. The aim of this section in the study was to see how samples from the Cape Flats compare to the data gathered by Andrews and Martin (2000) and ultimately determine whether samples from the Cape Flats might experience liquefaction.

### 3.4.3   Site Locations

Consultants in Cape Town provided soil laboratory results such as gradings, Atterberg limits and moisture content for numerous sites across the Cape Flats. The sites range from the west in Philippi to Khayelitsha and Blackheath in the east. Bellville south is the furthest point north in the study area.
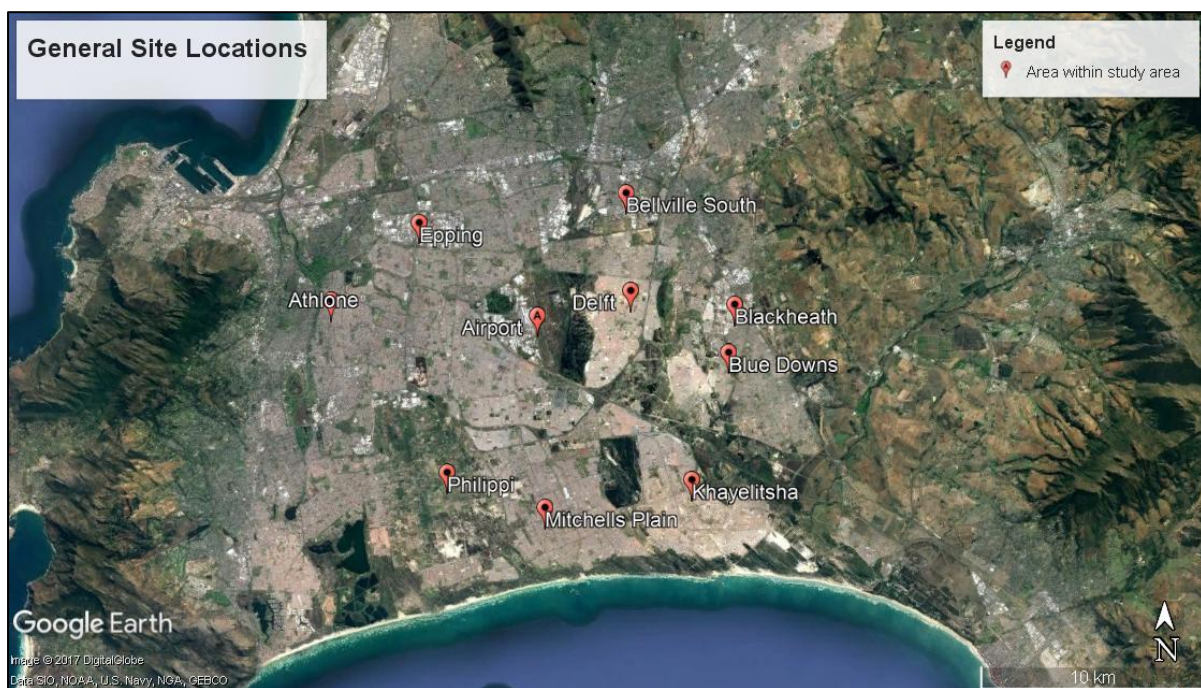


*Figure 3.13: Site locations for soil gradings*

Atlantis falls outside the scope of the study area and is not part of the Cape Flats. Atlantis lies 50km north of Cape Town. Nevertheless, it was decided to add the data sets for Atlantis, due to the area being characterised by aeolian sands from the Witzand Formation, which is also present in certain areas of the Cape Flats.

## 3.5   Laboratory Tests

### 3.5.1   Introduction

This section will discuss the various testing carried out within the laboratory. A custom method was developed to test liquefaction in the laboratory. Practical knowledge led to the design and building of a shaker, or vibration table that can simulate an earthquake. The primary goal of this test is to simulate vibration that would naturally occur from an earthquake and initiate liquefaction. The laboratory testing was performed, and will be discussed, as two sections. The first section includes the initial samples obtained and testing performed. Results from the first phase of testing, led to the second section. The second section is essentially an improvement and follow-up from the first section.

### 3.5.2   Site locations (for first phase of testing)

Bulk samples from five sites have been chosen for use in the laboratory, due to safety and ease of access. It was then easy to obtain additional samples for use in the laboratory. Figure 3.14 shows the location of these five sites on the Cape Flats.
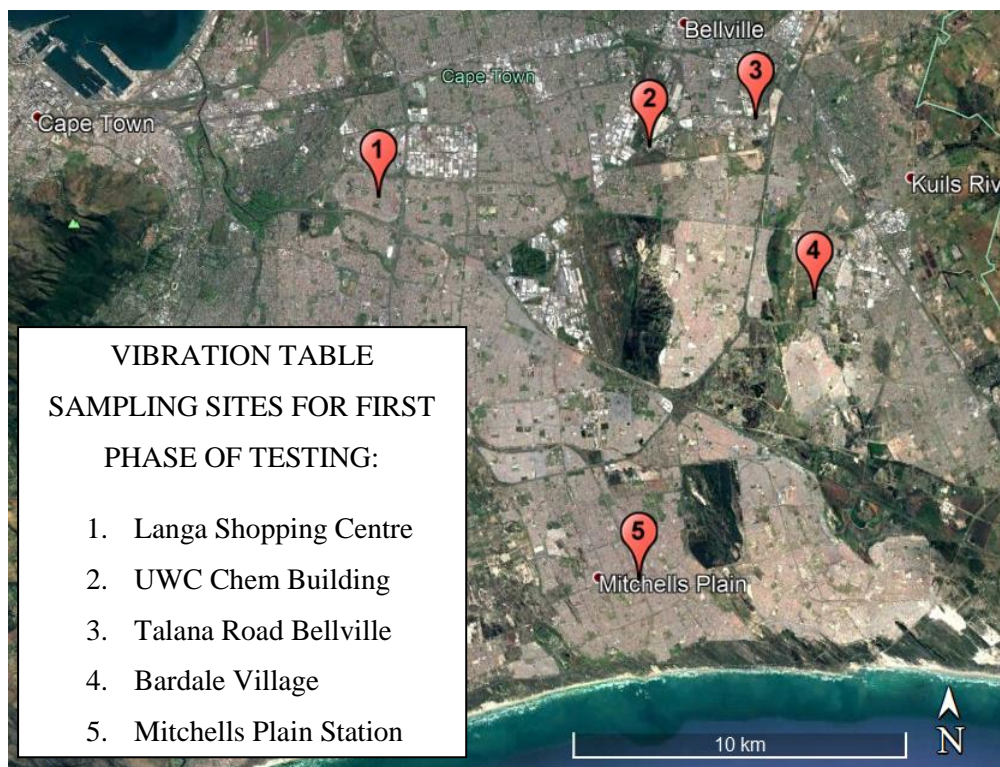


*Figure 3.14: Site chosen for sampling and testing with vibration table.*

The University of The Western Cape (UWC) was also chosen as a testing site, as it allows for safe controlled access. The UWC also has permanent water boreholes within the study area to supply much needed water table data. Samples obtained from the five sites were all uniformly-graded. It was therefore decided to manually mix more samples that vary in grading, namely well-graded, uniformly-

65

graded and gap-graded. These manually graded samples formed the second part (or second phase) of testing. The method used in grading these soils is discussed in this section. The results of the gradings are discussed in the following, results section.

### 3.5.3   Equipment

As described earlier, a vibration table was designed and built for this study. Plastic containers filled with sample sand can then be placed on the table and vibrated at various accelerations for observation purposes.

This section used the following equipment and software:

- Mechanical shaker or soil grader for sieve analysis and manual mixing
- Vibration Table 1.0 x 0.5m
- Two 40 litre plastic containers for sand
- Accelerometer with data computer
- Guralp data acquisition software
- Scream data viewer and analysis software
- Mobile phone with built in accelerometer
- VibSensor Mobile Phone Application
- 50 x 100 x 200mm stone block to be used as building model
- Troxler density tester

The custom-built vibration table has the capability to move (vibrate) in all three axes, namely X, Y and Z. The frequency can be controlled by a variable speed electric AC motor installed below the table. The table has an axis mounted below the bed with an adjustable off-centre weight which can be adjusted to obtain larger or lesser horizontal and vertical movements.

Figure 3.15 shows the two plastic containers on the vibration table. The second image is the mobile phone and VibSensor application. A professional accelerometer (see Figure 3.16) was obtained with the help of the Hartebeesthoek Radio Astronomy Observatory. It was however decided to use a simple, easy-to-use and, most importantly, repeatable mobile phone application. Furthermore, a wireless-enabled mobile phone was found to work well for the required application.

In contrast, the accelerometer is big and requires continuous power from an AC source. It also needs to be connected to the internet by means of a local area network. Data retrieving, and analysis is also very time consuming, considering that the laboratory test involves many short-run tests.

*Figure 3.15: Vibration table and mobile measuring device with application*
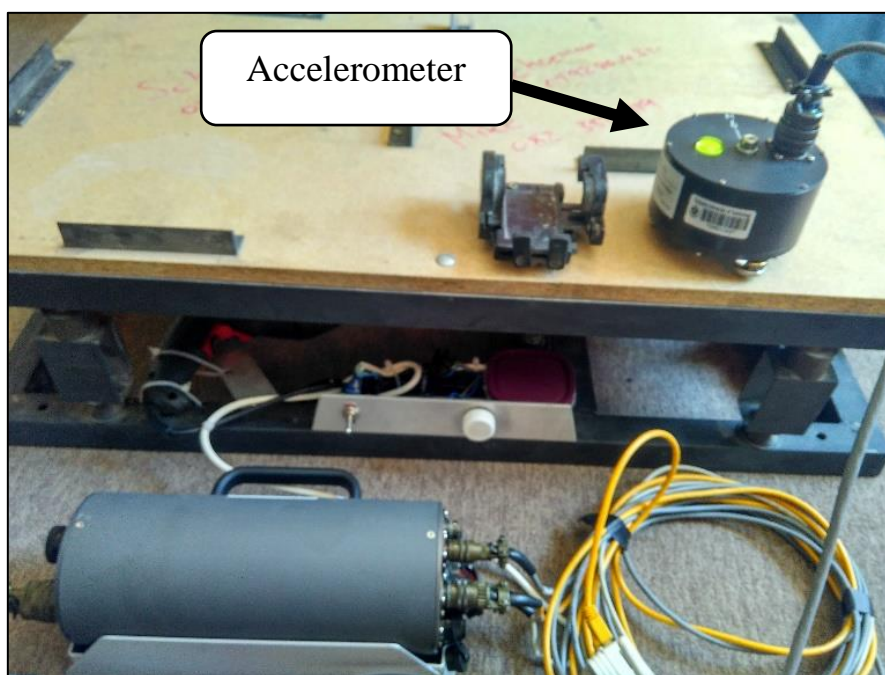


*Figure 3.16: Accelerometer and data capturing computer*

Trusting an unknown mobile phone application is however somewhat debatable. It was therefore decided to conduct a few tests to determine whether the mobile phone is accurate enough compared to the accelerometer.

Results from tests indicated that in most cases the variation error was less than 8-10% with low acceleration (0.1 $m/s^2$) and less than 8-12% with high acceleration (5.0 $m/s^2$). This is regarded as acceptable for the purpose of this study.

### 3.5.4    Vibration table testing

A method for testing samples was developed after a reliable measuring system was set in place. Various methods exist for the measuring of density and placing of soil samples. Some of these methods were however somewhat difficult to achieve in the project due to soils being placed in unconventional plastic containers for the purpose of this study.

Factors that were variable with each sample before any testing or placement, were soil grading and the initial moisture content of each sample.

The following method was then set in place and carried out with the testing of each sample.

1.  Each new sample was graded.
2.  Initial moisture content determined.
3.  Adding of the soil sample into the testing containers by means of a large funnel.
4.  Compaction of sample.
5.  Density of the placed samples was determined.
6.  The void ratio and degree of saturation were established.
7.  Concrete bricks were placed on the sample to imitate a foundation
8.  Testing was then carried out on the soil sample at various accelerations and the resulting effect on the brick was observed.

### 3.5.4.1    Initial laboratory testing

Several tests were carried out prior to vibration table testing being carried out. The moisture content of each sample was determined as well as a sieve analysis to determine the grading and grading curve of the sample. Bulk samples were tested by a laboratory and provided the optimum moisture content for compaction, maximum dry density as well as Atterberg limits.

The grading analysis for each sample was obtained by sieving the soil sample through a set of sieves, varying in sieve sizes (ASTM method 6913). After sieving, the amount of soil retained by each sieve is determined by weighing it. The weight retained from each sieve is then compared to the total weight of the soil sample, which provides one with the soil grading. The set of sieves used in this study is indicated in Table 3.1

*Table 3.1: Sieve sizes used for gradings*

| Sieve Size (mm) | 4.750 | 2.360 | 2.000 | 1.180 | 0.600 | 0.425 | 0.300 | 0.150 | 0.075 |
|---|---|---|---|---|---|---|---|---|---|
| Percentage retained | - | - | - | - | - | - | - | - | - |

The gradings for each sample will also be used to make valuable assumptions and comparisons after each vibration test.

The initial water or moisture content of the soil is needed when the degree of saturation is calculated. This allows one to determine the exact amount of water to be added to the sample in order to saturate it. The water content is determined by weighing a soil sample and then drying the sample in an oven at 110º degrees Celsius for 24 hours. The resulting change in weight is due to the water evaporating and only 100% dry soil remaining. This allows one to determine the initial amount of water as a percentage of total weight. Another method that was also used was to take the moisture content reading from the Troxler density tester.

### 3.5.4.2    Placing and compacting of soil sample into the container

A method was needed to add soil samples in the containers, in a controlled way. Sand raining is a technique of placing soil so that each batch is added in the same way, reducing areas of varying density in the soil after placing. Traditional sand raining involves a hopper with known volume, that releases sand through a certain diameter opening, which falls into the container at a fixed height.

This study used a large funnel, filled with 5kg of soil sample, rained into the container, while moving the funnel around the entire container opening. The lowest part of the funnel was kept at a fixed height, level with the container opening. This ensured that each sample was prepared in the same way. Layers were added until 20kg of sample was in the container.

Compaction was carried out after the adding of each 5kg soil layer. Each soil sample preferably needs a different density, as a varying factor for testing purposes rather than performing all tests on sand with the same density. Instead, the duration and method of compaction was kept constant for each layer of one specific sample. The unconventional containers used also made traditional compaction methods difficult. It was therefore decided to use two pieces of hardboard, glued together and cut to the same size as the container opening. A compacting hammer drill was then used to compact the entire surface of the hardboard for a certain amount of time, ensuring that the following layers are compacted for the same amount of time. Some samples were also not compacted at all, to represent a loose area of soil. They were however also placed with the same sand raining technique.

The first phase of testing where all tested at different densities. The second phase of testing were however tested in sets of two each, and the density was kept more or less the same for each set, thus ensuring some degree of reliability and uniformity.

### 3.5.4.3    Determining density

The earlier mentioned Troxler density tester that provided a moisture content, also provides the dry density of the soil sample. Figure 3.17 shows the Troxler density tester on the compacted soil sample. The unit has a measuring probe that uses a radioactive source to determine the amount of absorption in the surrounding material. The ratio of the amount reflected and absorbed allows the unit to determine the density. The measuring probe is situated below the unit. Two tests were carried out on each sample,

one in the left side of the container and the other in the right side of the container. The average of the two readings was taken as the dry density.

Another method of density testing can also be used if the volume and weight of the soil sample is known. This was used to verify the finding from the Troxler density tester. Food colouring was used with water that was added in 1 litre batches. This made it possible to easily mark the containers in one litre increments prior to testing and indicate an approximate volume.



*Figure 3.17: Troxler density tester*

### 3.5.4.4    Degree of saturation

The degree of saturation or saturation ratio (Sᵣ) is the ratio of the volume of water to the total volume of the void spaces in the sample.

The first step in determining the degree of saturation of a given soil body is to obtain the void ratio ($e$) of the compacted soil sample. The specific gravity of the soil particles ($G_s$) is needed with the density of water ($\rho_w$) which is known as 1000kg/m$^3$. The specific gravity of the soil particles can be taken as 2.67 which is a good estimate of quartz rich soils.

The dry density of the sample ($\rho_d$) to be tested is then used in determining the void ratio for the specific soil sample.

$$\rho_d = \frac{G_s}{1 + e} \rho_w$$

*Equation 3.5: Dry density*

$$e = \frac{G_s \, \rho_w}{\rho_d} - 1$$

*Equation 3.6: Void ratio*

A soil sample that is 100% saturated has a $S_r = 1$. The degree of saturation is:

$$S_r = \frac{w(G_s)}{e}$$

*Equation 3.7: Degree of saturation*

The equation for degree of saturation can then be rewritten in terms of the percentage water content needed to reach the desired degree of saturation.

$$w = \frac{(S_r)e}{G_s}$$

*Equation 3.8: Percentage water need with Sr*

The equations for sample density and degree of saturation can ultimately be rewritten in terms of water percentage needed at a desired degree of saturation and known sample density.

$$w = S_r(\frac{\rho_w}{\rho_d} - \frac{1}{G_s})$$

*Equation 3.9: Percentage water needed with Sr and known density*

The initial water content of a soil can be subtracted from the total water content needed to saturate the soil. An example will be a soil sample that weighs 20kg and have an initial moisture content of 5%. The sample has a dry density of 1650kg/m$^3$ after compaction. A total of 23% water is needed to achieve the desired saturation ratio ($S_r = 1$), according to the combined equation for water content. Only 18% water content is however needed to obtain the desired ratio, after subtracting the initial water content. The amount of water needed in litres can then be calculated from the initial weight of the soil. This gives a final answer of 3.63 litres of water needed to saturate the soil. The adding of the water to the soil sample will be discussed in the next section.

### 3.5.4.5    Placing of concrete bricks and adding water

Concrete bricks were placed on the prepared soil sample. The use of the bricks represents a foundation, with the resulting effect on the bricks being measured. The height from the top of the brick to the top

of the container was also measured for each test, allowing one to determine the amount of settlement after each test.

Each brick has a weight of 2.1 kg, and is 50 mm high, 100mm wide and 200 mm long. From these values, the applied pressure can be determined as follows.

$$pressure = \frac{force}{area}$$

*Equation 3.10: Pressure*

Where the pressure is in pascal (Pa), force in Newton (N) and the area in square metres. From this equation, the total pressure exerted by the brick onto the underlying soil is 980 Pa, or approximately 1 kPa.

The amount of water needed for the desired degree of saturation was poured onto the bricks at a steady rate. This ensured that no erosion or weaknesses formed while adding the water to the sample.

### 3.5.4.6   Testing with vibration table

As mentioned before, two phases of vibration testing have been carried out. In the first phase, each bulk soil sample was vibrated at two primary accelerations and also at a compacted and uncompacted state, totalling four results per bulk sample. The first test was done at an acceleration of 0.15g which can be expected for the Cape Town area, according to seismic and gravity acceleration maps. The second test was done at an acceleration of 0.25g, which is a worst-case scenario for southern Africa.

Each bulk sample were divided into four sets. Table 3.2 is an example of how the testing procedure was set out. The full testing sheet with results are summarised in the results section.

*Table 3.2: Example of testing procedure (first phase of testing)*

|  | Site A | | | |
|---|---|---|---|---|
| Test # | 1 | 2 | 3 | 4 |
| Compacted? | No | Yes | No | Yes |
| Density | In kg/m$^3$ | In kg/m$^3$ | In kg/m$^3$ | In kg/m$^3$ |
| At 'g' | 0.15 | 0.15 | 0.25 | 0.25 |

With each test, the time until liquefaction occurred was recorded. The time frame for testing is set at 60 seconds, and if no noticeable results are obtained the acceleration is increased. Maximum testing time was 120 seconds, as very few earthquakes last this long (Seed, et al., 2003). Any observations and results will be recorded and discussed in the results section.

The second phase of testing was however approached differently. It was decided to test eleven bulk samples. Each bulk sample was tested four times, two of which samples were deposited in a loose state and two of which were compacted. The two compacted samples were prepared in such a way as to try and keep their densities more or less similar. All of the samples in the second phase of testing were tested at a consistent acceleration or vibration at a PGA of approximately 0.15g.

The first stage of testing included only uniformly graded samples. The second phase of testing included uniformly graded, well graded and gap graded soils.

*Table 3.3: Example of testing procedure (second phase of testing)*

|  | Sample 1 | | | |
|---|---|---|---|---|
| Test # | 1 | 2 | 3 | 4 |
| Compacted? | No | No | Yes | Yes |
| Dry density | In kg/m$^3$ | In kg/m$^3$ | In kg/m$^3$ | In kg/m$^3$ |
|  | Loose | Loose | More or less similar | |
| At 'g' | 0.15 | 0.15 | 0.15 | 0.15 |

# 4    Results and Discussions

## 4.1    Introduction

This section will present and discuss results obtained during empirical correlations from using SPT/DPSH and CPT data as well as soil properties from obtained samples. This section will also include results obtained after testing the samples in the laboratory at various gradings and densities using the vibration table.

## 4.2    SPT Results

This section will discuss the data obtained with both conventional SPT testing as well as SPT-N values derived from DPSH testing. The factor of safety will also be discussed and is presented with varying SPT-N values and depth. SPT and DPSH data appeared to be reliable and trustworthy. Correction was made for the fines content, taken as 6% for all samples, as well as the magnitude scaling factor (MSF) and variable PGA values to provide more reliable CSR values.

The factor of safety was calculated at two different PGA's (0.15 and 0.25) and earthquake magnitude (M = 6 and M = 8) for varying SPT-N values. Figure 4.1 indicates the factor of safety calculated with a water table depth of 1m below ground level. The indicated SPT-N value is the actual value as obtained from the testing apparatus. The values for the factor of safety have however been calculated after corrections (as mentioned earlier) at a fines content of 6%. This allows one to take actual measured SPT-N values and establish a safety factor. The results indicate a higher initial safety factor compared to deeper below ground at the same SPT-N value. From the graph, it is evident that the factor of safety reduced considerably with an increase in PGA and associated magnitude. Both factor of safety graphs display a sharp decline in the factor of safety within the first three to four metres below ground level. This could probably be explained by the increase of overburden pressure as depth increases. The results also indicate that for the two scenarios a (actual) SPT-N value of between 6 and 30 is needed, respectively, to resist liquefaction for up to twelve metres below ground level.

SPT-N values were derived from conventional SPT testing (with core drilling) and from DPSH results. The resulting SPT-N value was corrected in the same way, for magnitude and fines content, and used to determine a $(N1)_{60cs}$ value to plot with the CSR. The water table was taken as being at 1m below ground level for all calculations. It should also be noted that no data above the water table has been presented, as liquefaction can only occur in saturated soils.

Figure 4.2 presents actual SPT-N values (with core drilling) corrected to $(N1)_{60cs}$ and plotted against the CSR. Figure 4.3 and Figure 4.4 indicate the same but for the DPSH derived samples. The curve (or boundary line) in each diagram is derived from the Idriss and Boulanger (2004) calculation for Cyclic Resistance Ratio (CRR) vs SPT-N value. All data above the boundary line have a safety factor of less

than one and has the possibility to undergo liquefaction during a seismic event, if the same ground conditions are present.
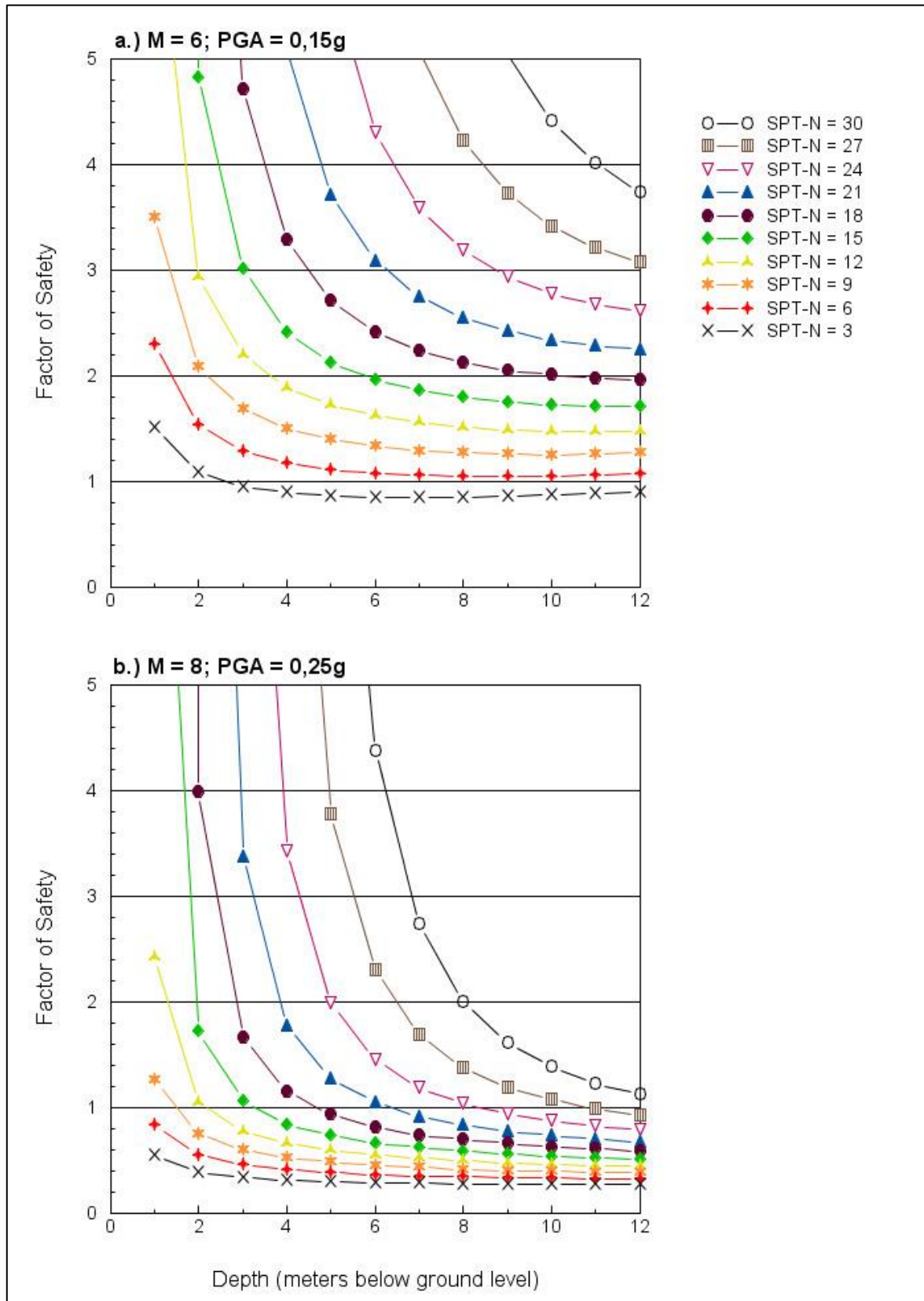


*Figure 4.1: Factor of Safety vs Depth for varying PGA at a water table of 1.0 m below ground level*
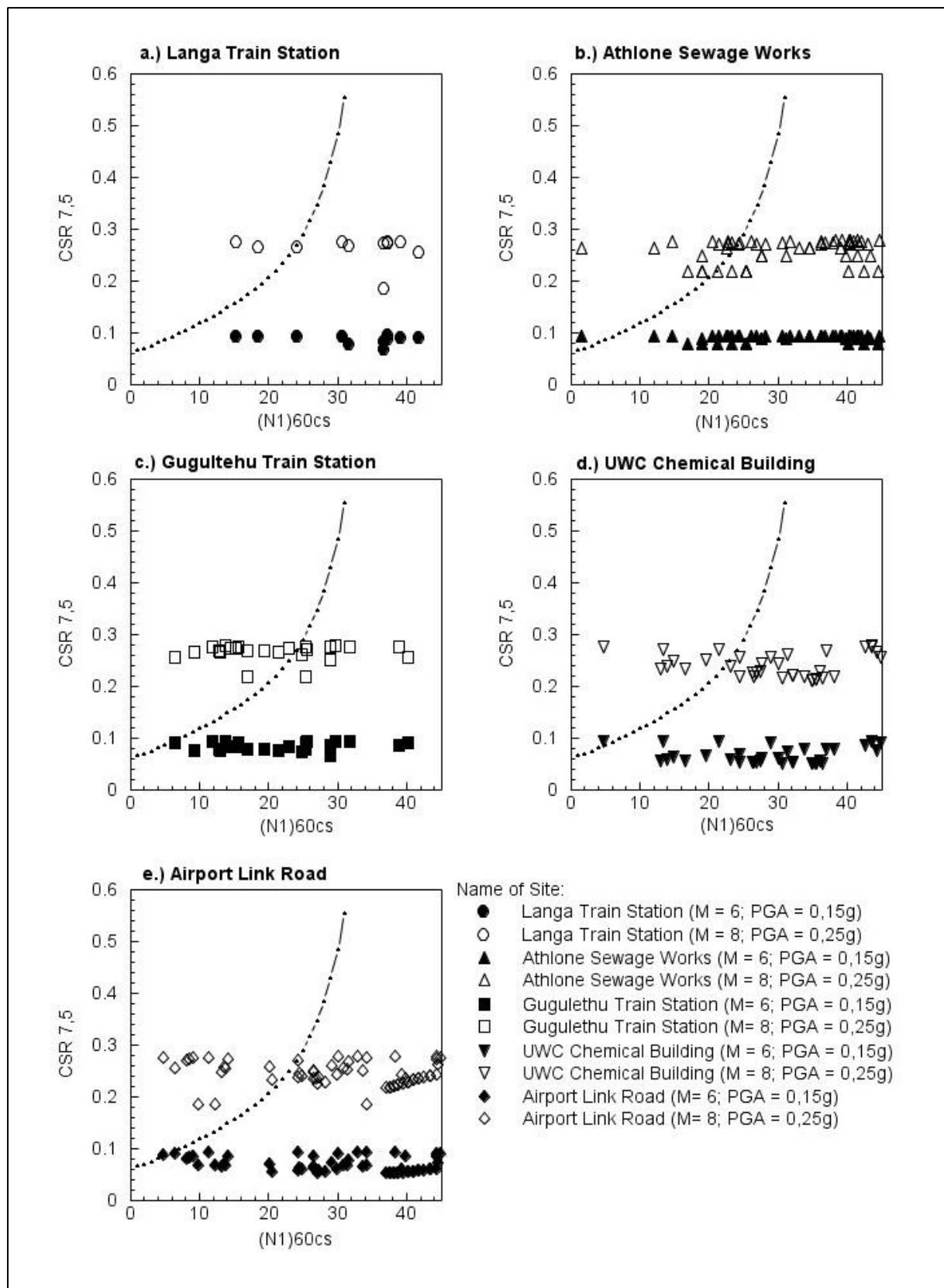
*Figure 4.2:CSR vs (N1)$_{60cs}$ for all actual SPT derived samples at varying PGA and magnitude*
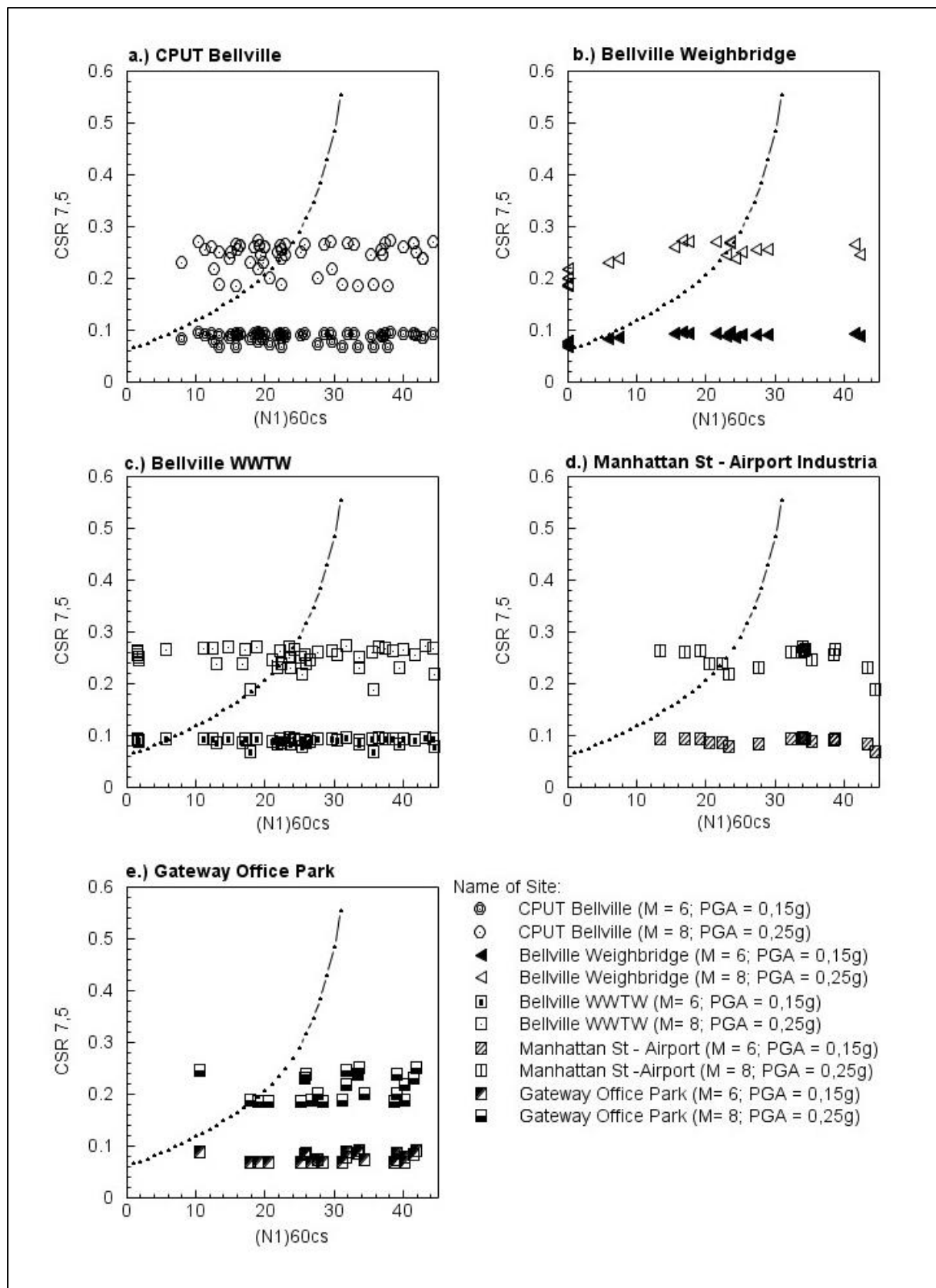
*Figure 4.3: CSR vs (N1)$_{60cs}$ for 5 of 7 DPSH-SPT derived samples (1)*
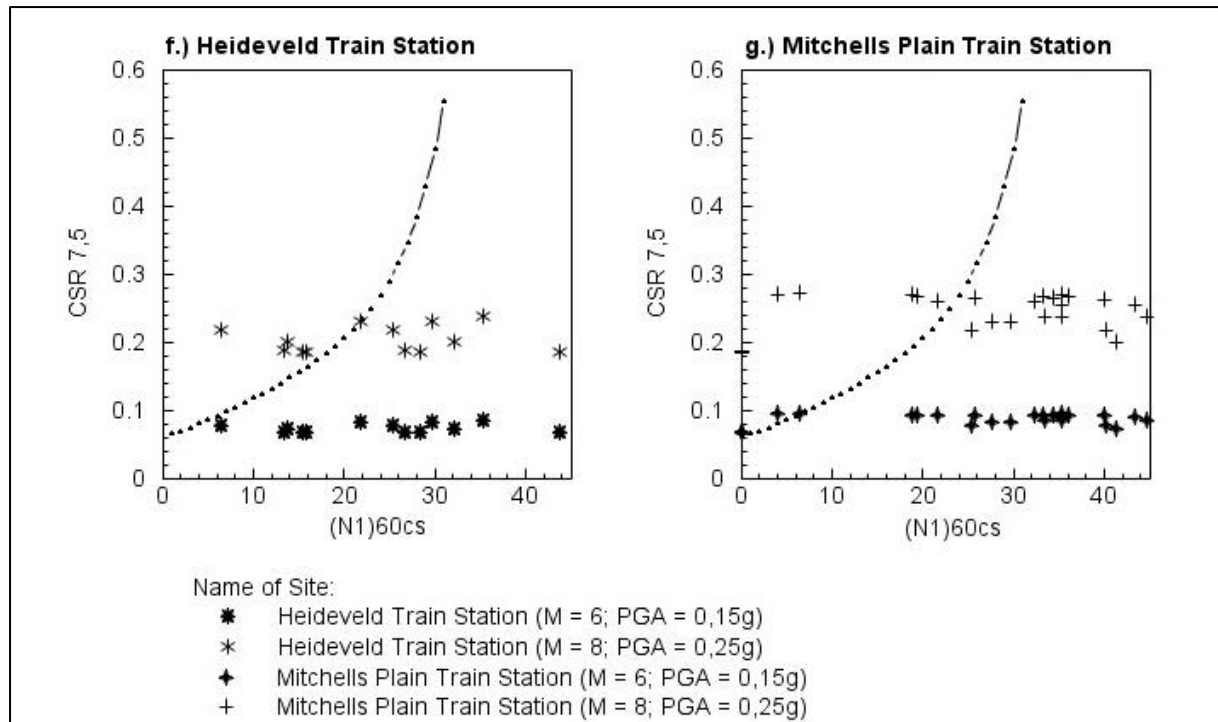
*Figure 4.4: CSR vs (N1)$_{60cs}$ for 2 of 7 DPSH-SPT derived samples (2)*

Figure 4.1 toFigure 4.4 indicate that obtained results for this study processed at a PGA of 0.15g and an earthquake magnitude of M = 6 should resist liquefaction. Only samples with a corrected SPT-N value of less than N = 6 experienced liquefaction. For the results processed at a stronger PGA of 0.25g and accompanying magnitude of M = 8 all samples experienced liquefaction. Samples with a corrected SPT-N value of more than N = 22-26 appeared to have resisted liquefaction. It can also be noted that all values appear to plot near-horizontal, for both the SPT testing sites and the DPSH sites. This is in contrast with the graph of Idriss and Boulanger (2004) that is scattered and randomly placed. This horizontal placement can however be explained. The data in this study are all obtained from one area, and the water table, magnitude and PGA's are kept at a constant for ease of calculations. The graph from Idriss and Boulanger (2004) consists of various locations, each with a different PGA and water table.

This section clearly indicates that there is at least one horizon, sometimes more, for each investigated area, susceptible to liquefaction, both for the DPSH and SPT testing sites. This should be seen as problematic, as shallow foundations are usually founded within the first metre below ground, and almost all of the case studies indicated liquefaction within the first few meters. The observed data will further be discussed in the analysis and discussion section where it will also be compared to other case study data.

Using the water table at 1.0m and 2.0m below ground level provides information of liquefaction only at these two levels. The confirmative outcome is however the fact that soils are susceptible to liquefaction at these magnitudes and similar water tables.

78

## 4.3    Piezocone Penetrometer Results

### 4.3.1    Introduction

Results for the piezocone penetrometer tests will be presented as suggested by Robertson (2010), and essentially comprises the plotting of normalised cone resistance to that of the normalised friction ratio on a logarithmic scale. The calculation of Ic and CD can further be used to define the boundaries of soil types within the SBT chart (Robertson, 2010). As discussed in the methodology, two sites were tested. The first test was at an industrial complex in Capricorn Park. The second test area was located close to the Cape Town International Airport, at Geoscience Laboratories.

Two tests were carried out at each of the two sites. The CPT penetration data as well as the dissipation results for each test were received in a raw format from the contractor. The first step was to use the obtained CPT data and determine the level of the water table at each site (Table 4.1).

*Table 4.1: Water table levels at test locations*

| Calculated depth of water table at each test location | | Capricorn Park | | Geoscience Laboratories | |
|---|---|---|---|---|---|
| | | Meters below ground | Average | Meters below ground | Average |
| CPT Test 1 | Reading 1 | 3.25 | 3.06 | 2.38 | 2.46 |
| | Reading 2 | 2.87 | | 2.54 | |
| CPT Test 2 | Reading 1 | 2.51 | 2.55 | 2.54 | 2.64 |
| | Reading 2 | 2.58 | | 2.75 | |

Table 4.2 was used in the following section to determine properties from the obtained results.

*Table 4.2: SBT Zones Properties*

| Zone | SBT |
|---|---|
| 1 | Sensitive, fine grained |
| 2 | Organic soils, clay |
| 3 | Clay, silty clay to clay |
| 4 | Silt mixtures, clayey silt to silty clay |
| 5 | Sand mixtures, silty sand to sandy silt |
| 6 | Sands, clean sands to silty sands |
| 7 | Gravelly sand to dense sand |
| 8 | Very stiff sand to clayey sand |
| 9 | Very stiff fine grained |

### 4.3.2   Results of Robertson's normalised SBT Plots

The obtained normalised SBT results were plotted with depth to interpret the SBT Plots. The graphs indicate at what depth the average SBT value deviated from the mean. Furthermore, it can be used to visually interpret various soil layers and the depth at which it is encountered. The SBT value can be compared to the SBT description table from Robertson (2010) to make valuable comparisons and establish ground conditions. Figure 4.5 and Figure 4.6 indicate the depths of SBT values for Capricorn Park and Geoscience Laboratories respectively.
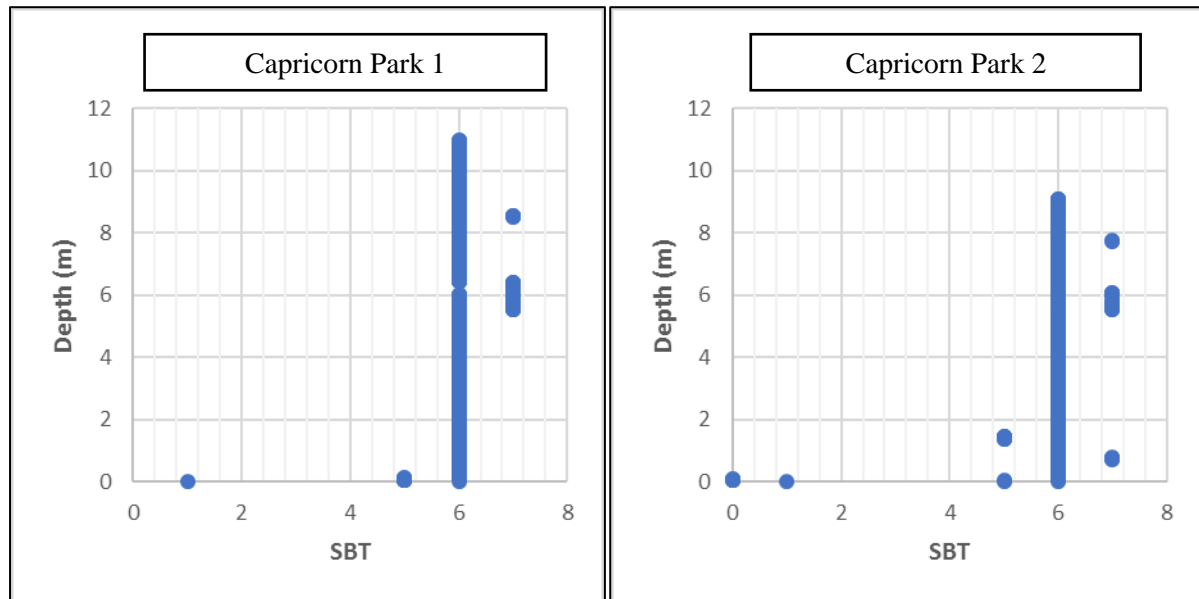


*Figure 4.5: SBT with depth for Capricorn Park CPT Tests*
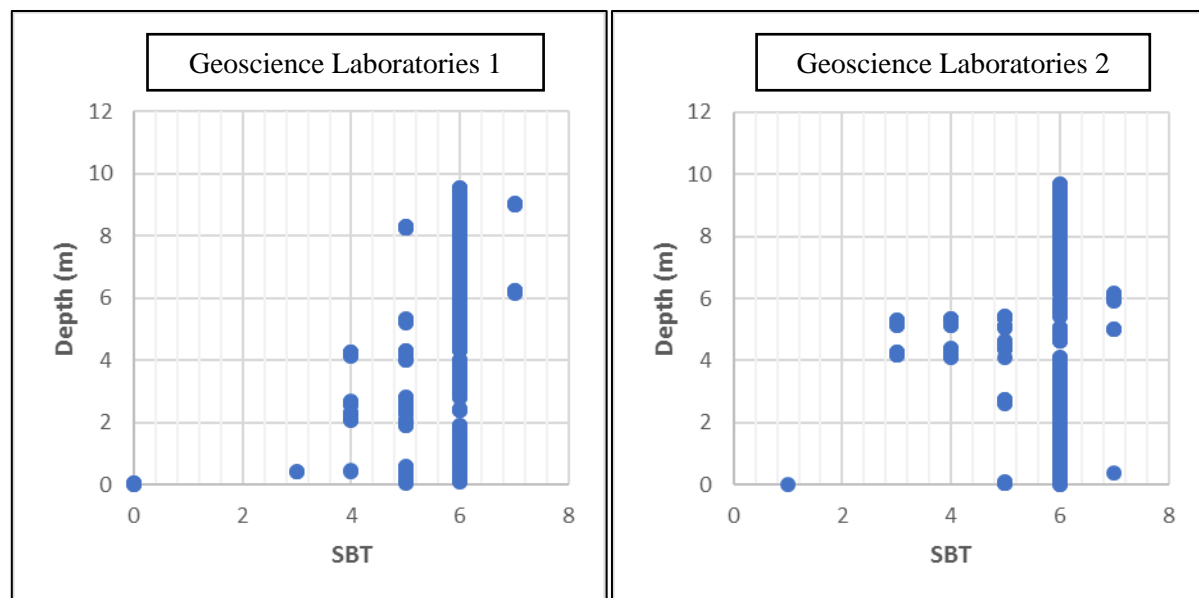


*Figure 4.6: SBT with depth for Geoscience Laboratories CPT Tests*

SBT Plot for Capricorn Park - 1Figure 4.7 to Figure 4.10 plots the Fr and Qtn for all CPT results, in both an uncorrected state as well as on the SBT chart. Most of the results plot within the zone 6 (being clean sands and silty sands), with only minor points in the more clayey and silty regions.
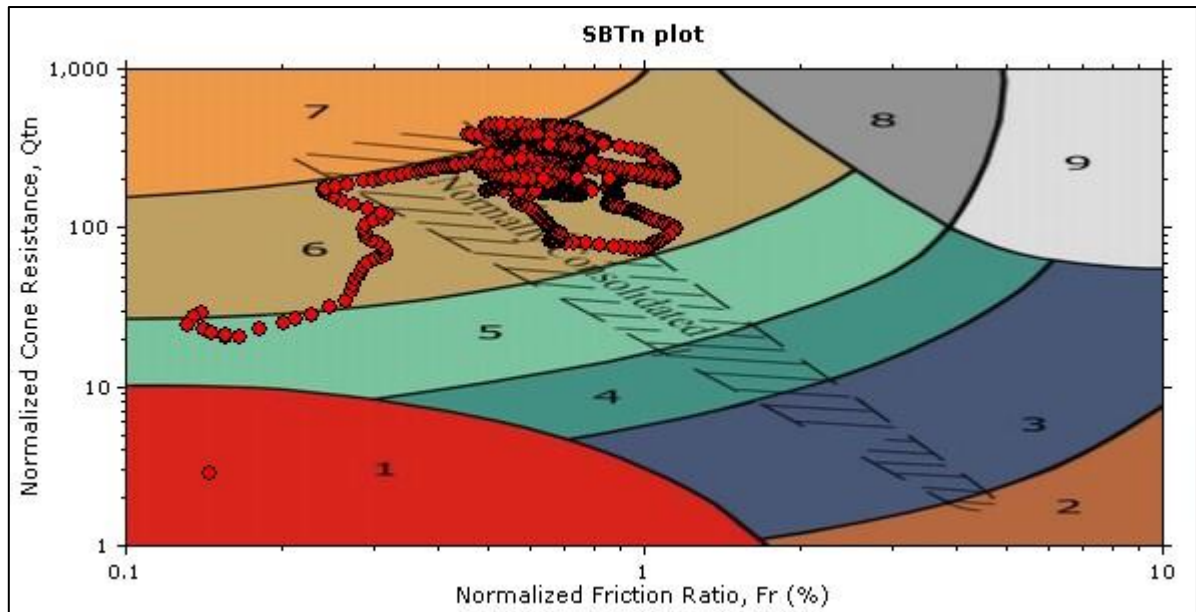


*Figure 4.7: SBT Plot for Capricorn Park - 1*
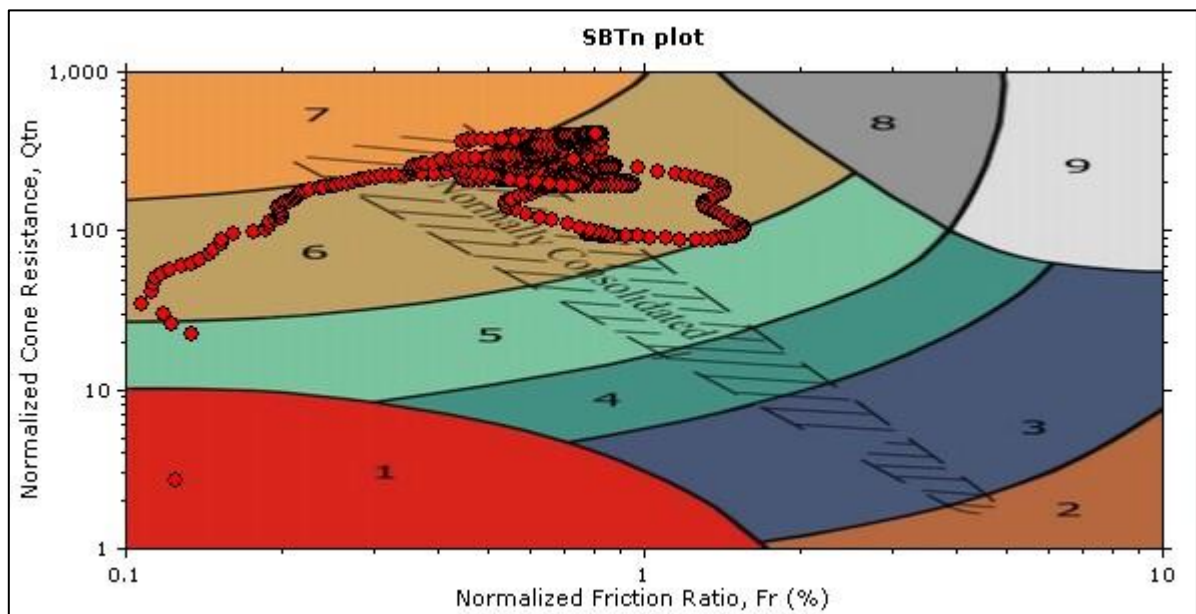


*Figure 4.8: SBT Plot for Capricorn Park - 2*
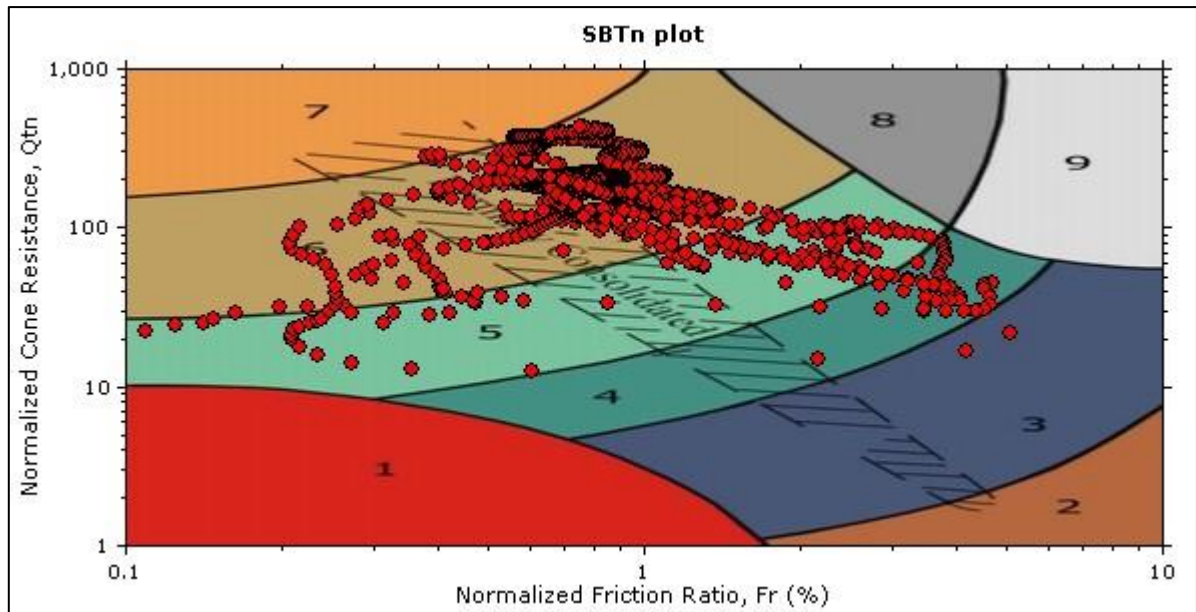
*Figure 4.9: SBT Plot for Geoscience Laboratories - 1*
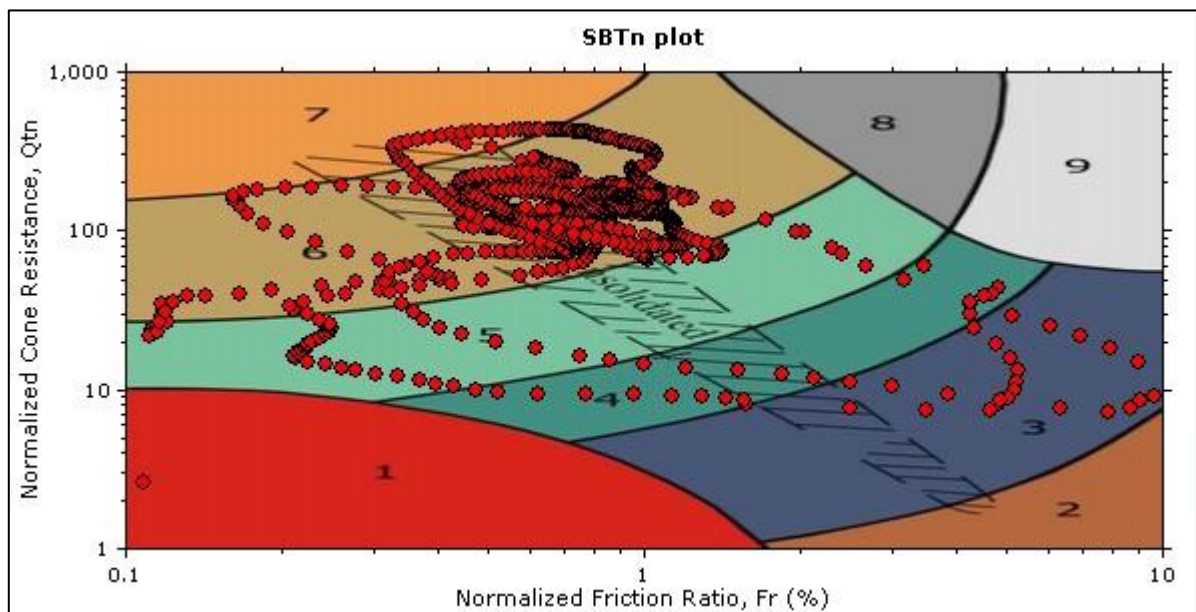


*Figure 4.10: SBT Plot for Geoscience Laboratories - 2*

### 4.3.3   Results of Soil Behaviour Zones (Ic) with depth

The soil behaviour type index or Ic have been plotted with depth in Figure 4.11. These results indicate the Ic at a specific depth. The soil exhibits sand-like and potentially liquefiable properties if the Ic is smaller than 2.6 (red line) or clay-like and not likely to liquefy if the Ic is larger than 2.6.

82
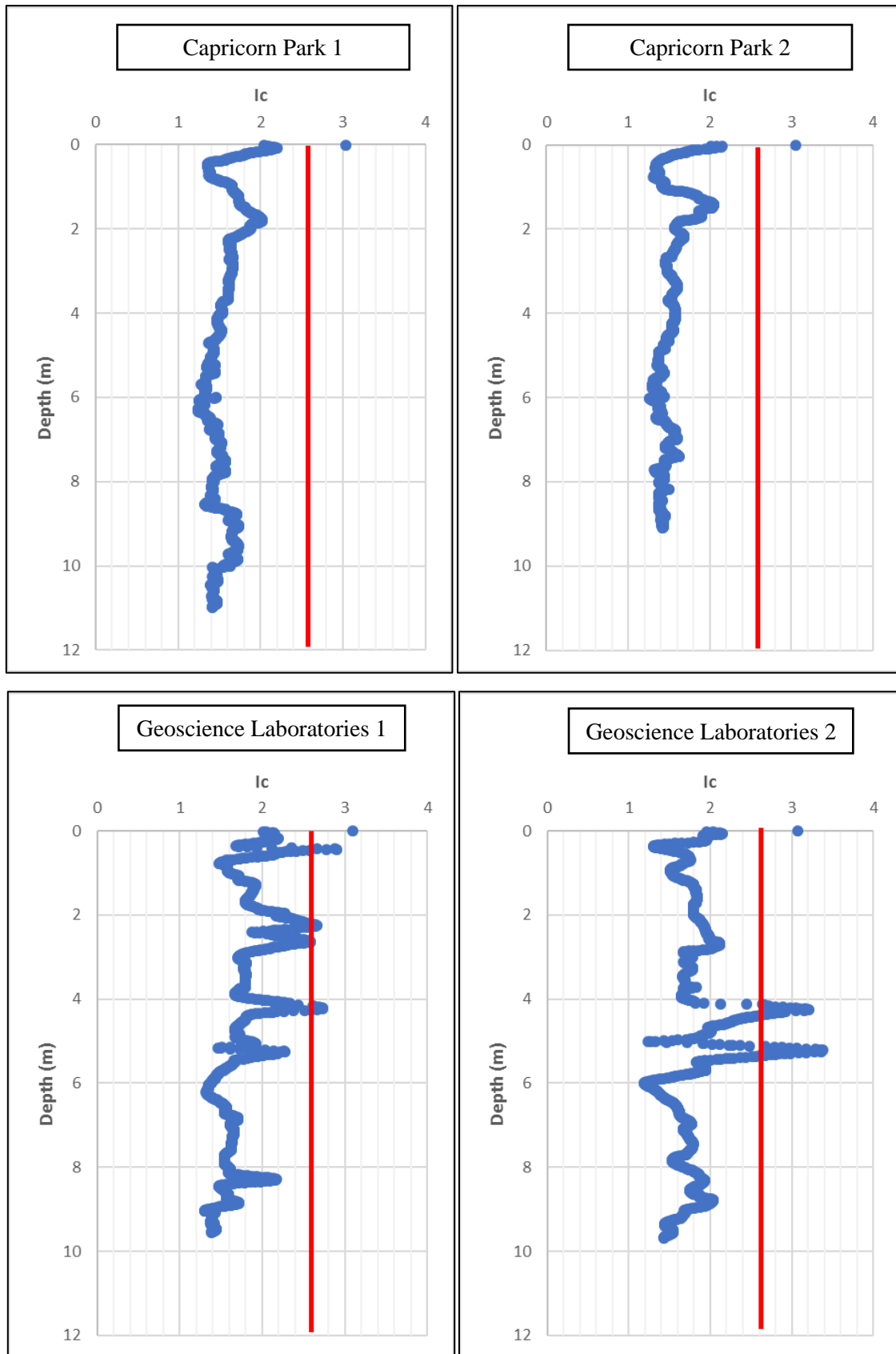
*Figure 4.11: Soil Behaviour Zones for al CPT Tests*

### 4.3.4 Results of Contractive Dilative (CD) zones with depth

Figure 4.12 indicates the contractive and dilative zones (to depth) on a logarithmic graph. A CD value of less than 70 indicates a potentially contractive and liquefiable soil, and a CD value of more than 70 indicates a dilative and strain hardening soil.
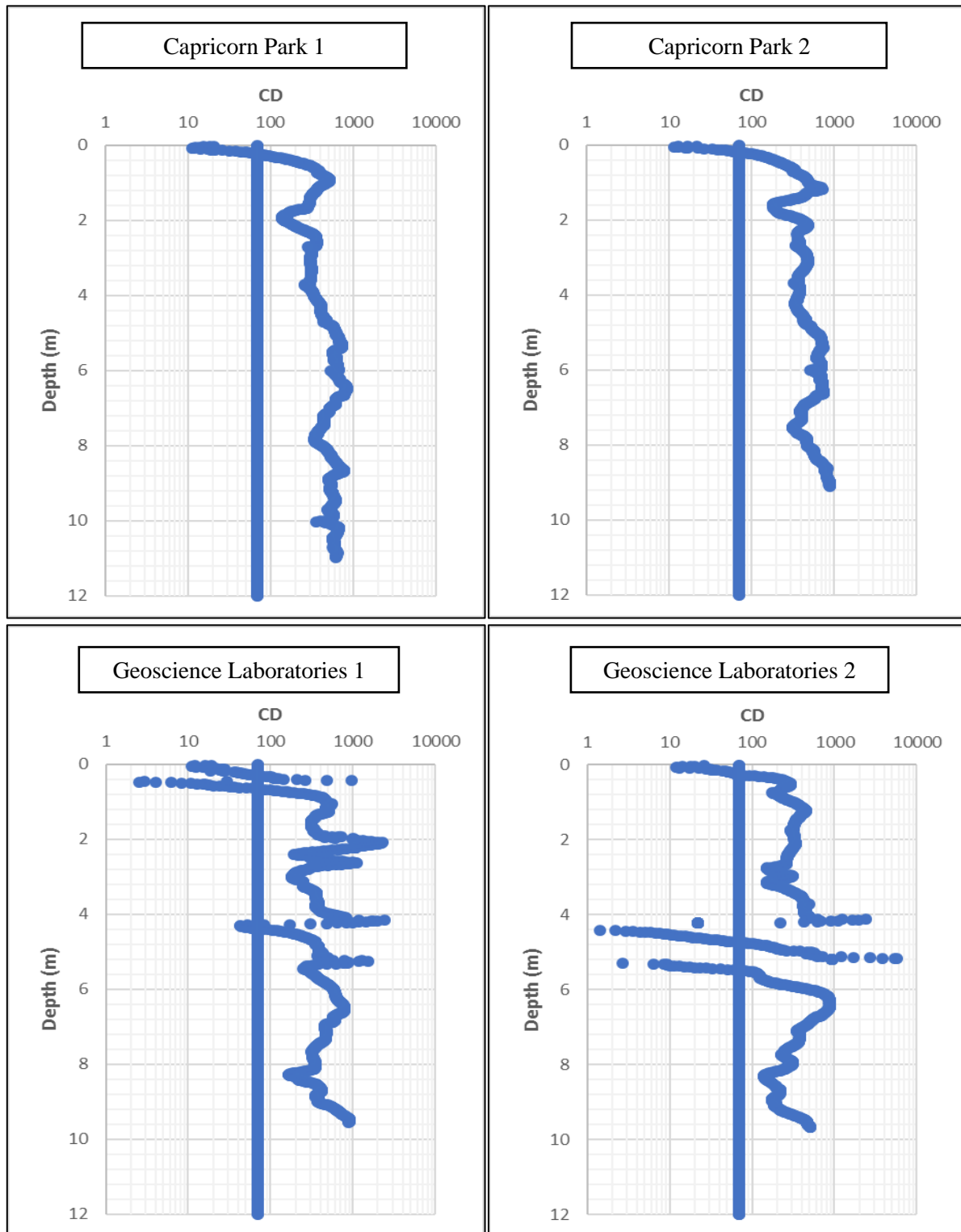


*Figure 4.12: Contractive Dilative zones for all CPT tests with depth*

84

### 4.3.5    Gregg Software tool relative SPT values

The same software that allows one to plot the SBT data onto a SBT chart, has the option to graphically provide relative SPT densities with depth for each CPT test. This gives one the opportunity to compare potentially liquefiable zones to that of the SPT testing and establish a density at which soils can be considered safe against liquefaction.
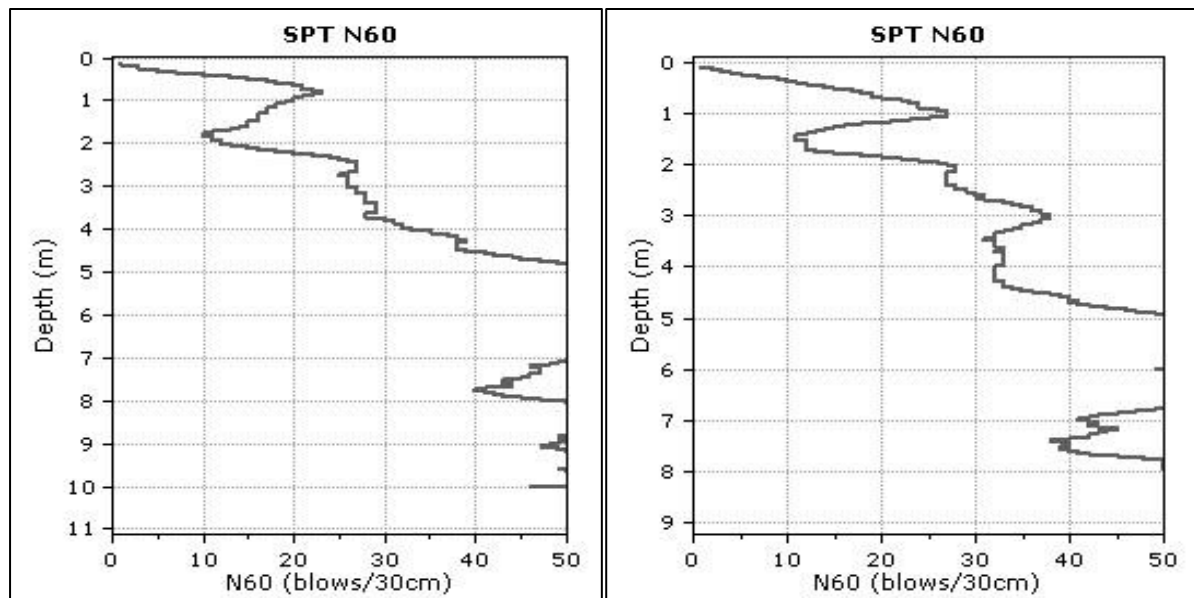


*Figure 4.13: CPT to SPT comparison for Capricorn Park 1 and 2*
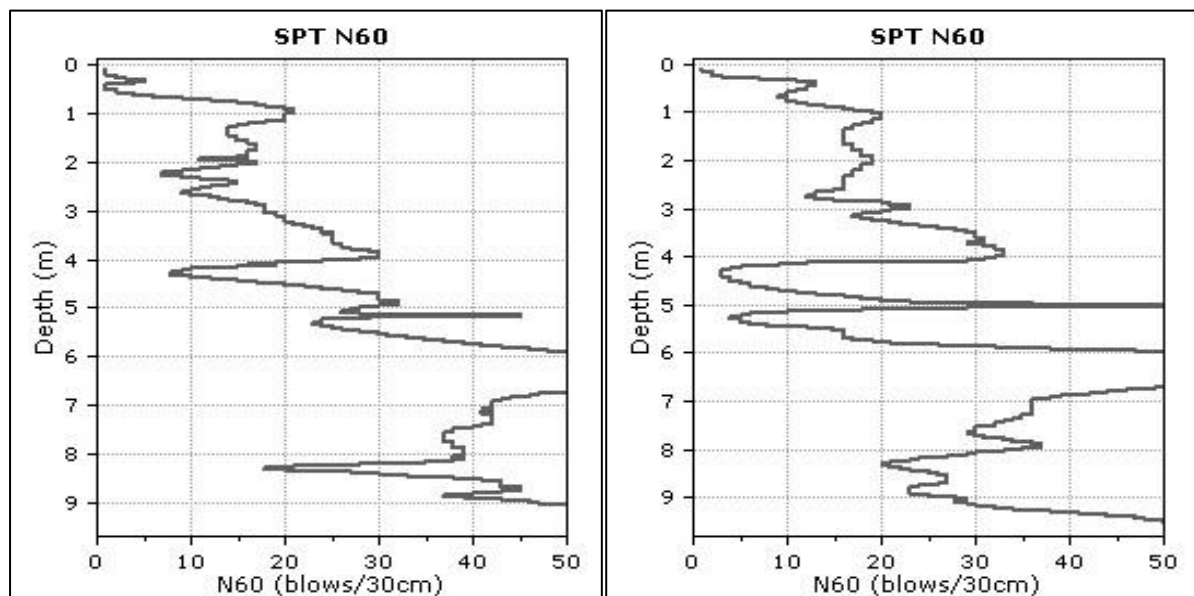


*Figure 4.14: CPT to SPT comparison for Geoscience Laboratories 1 and 2*

### 4.3.6    Analysis

Results from the cone penetrometer can be used to determine the likelihood of soil liquefaction occurring, to a reasonable extent. The results from the SBT, Ic and DC graphs all indicate sand-like soils that is potentially liquefiable and contractive. SPT derived results (Figure 4.13 and Figure 4.14)

85

indicate that the soils are relatively dense, with some loose zones. A PGA of approximately 0.25g at a magnitude of M=8 will be required to initiate liquefaction, if compared to the previous SPT section. In addition, the zones must be saturated for liquefaction to occur.

#### 4.3.6.1    Capricorn Park

SBT graphs for the Capricorn Park site indicate that majority of the points plot within the SBT zone-6. This zone is classified as sands, clean sands to silty sands. Ic for the Capricorn Park site also plots below 2.6, indicating a sand-like soil that has the potential to liquefy. The Robertson cyclic Liquefaction potential chart indicates that soils in this area, plotting in zone A1, have the potential to experience cyclic liquefaction, depending on the level and duration of cyclic loading. This means that if the soil were to experience a small magnitude earthquake for a short period of time that it could likely not liquefy. The testing method only provides the user with the likelihood of liquefaction and not the magnitude required to initiate liquefaction. The contractive dilative boundary (CD) indicates that the soils are dilative, with only the first 0.5m approximately displaying contractive properties. This is confirmed from the SPT comparison graphs which indicate that these soils are relatively dense. Both test 1 and 2 indicate a looser area at a depth of 1.0-2.0m below ground. Soils at Capricorn Park appear to be dense, dilatant and should resist liquefaction at shear of short duration.

#### 4.3.6.2    Geoscience Laboratories

The SBT graph for the Geoscience Laboratories site plots mostly in zone 6 and A1 with the same properties as Capricorn Park. There is however deviation towards zones 5 and 4 on the SBT graph, and zone B on the cyclic potential chart. This indicates predominantly sands and sandy mixtures of silty sands and sandy silt. The cyclic potential chart indicates a cohesive soil material such as clay, and that liquefaction potential should be further evaluated, perhaps with other testing methods. The SBT with depth graph indicates that this clayey cohesive material, which plots in zones 5 and 4, are mostly at depths of between 4 and 6m below ground. The Ic graph confirms this, as test two indicates an Ic of more than 2.6 at a depth of 4-6m approximately, meaning clay-like properties.

The CD graph indicates that, for test two, dilative and contractive soils are encountered at depths of between 4 and 6m. The comparison SPT graph shows that very loose to very dense soils are layered on one another. The fact that both tests 1 and 2 indicate more or less the same profile can confirm that this is not an anomaly. Instead, it is possible that very loose sands lie within layers of very stiff clay and clayey sands between depths of 4 and 6 metres. The Geoscience Laboratories site can therefore be said to be potentially liquefiable within the first 0.5m below ground, and also at a depth of 4-6m below ground. A liquefaction event in this area could lead to flow liquefaction, sand boils, from deeper lying soils, and settlement of shallow founded foundations on poorly compacted sands. Previous SPT results also indicate that even a small earthquake could result in liquefaction occurring in this area as the water table was determined to be at approximately 2.5m below ground level.

### 4.4    Soil Properties

### 4.4.1    Introduction

This chapter and the following laboratory testing chapter has three main sections. The first section includes results obtained through research, which are the grading results for 46 sites across the Cape Flats. The need to know soil properties is highly important for all stages of the investigation. One cannot interpret penetration tests such as SPT and DPSH profiles accurately without knowing the nature of the underlying soil layers. Silts and sands can be either cemented or unconsolidated and clays can be soft to very stiff. Pedogenic layers such as ferricrete and calcrete can be very dense, and they can form in thick bands or very thin lenses.

### 4.4.2    Liquefaction susceptibility from gravel, sand, silt and clay content

Knowing the underlying soil layers, their depositional history and soil properties allows one to better interpret invasive tests, such as SPT's, as well as non-invasive tests such as the shear wave velocity test. A total of 46 gradings were obtained for sites all over the study area. The results of these gradings are plotted on a box diagram in Figure 4.15. As mentioned earlier, Atlantis was also added to the data set for grain size comparison. The area is however not believed to be in danger of liquefaction as the water table here is considerably deeper.

Data obtained from the study area indicates the percentage of sand and gravel, silt and clay. Only seven sites have a sand content lower than 90%. The same seven sites have a clay content of more than 10% and one more than 20%. The location of these sites is in no way different to the other areas. One exception is that of Blue Downs. The Blue Downs grading indicates a clay content of more than 20%, and a sand content of approximately 65%. This area of Blue Downs will probably resist liquefaction if comparing it to the bar diagram (Figure 3.12) from Andrews and Martin (2000).

Liquefaction can be a high risk over the entire Cape Flats region if considering the gradings of the remaining 39 sites that all have a sand content above 90%. The literature (Idriss & Boulanger, 2010) indicates that sands with a fines content (smaller than 0.0750 mm) of less than 5 % are the most at risk for liquefaction. From the box diagram for gradings it can be seen that almost half of the graded sites have a fines content of less than 10 %. The majority of these sites are in Khayelitsha and Mitchells Plain. These areas are essentially aeolian, windblown, sands. The box diagram does however not indicate the density or soil structure of these sands. Khayelitsha have large areas of very dense, cemented sands near surface. Very dense, cemented sands have a very high resistance to liquefaction. Mitchells Plain is also known for aeolian and alluvial (water deposited) sands. These sands can be either very dense and cemented, or very loose. From the limited SPT data it is however clear that these sands are loose only in the first metre approximately.

87
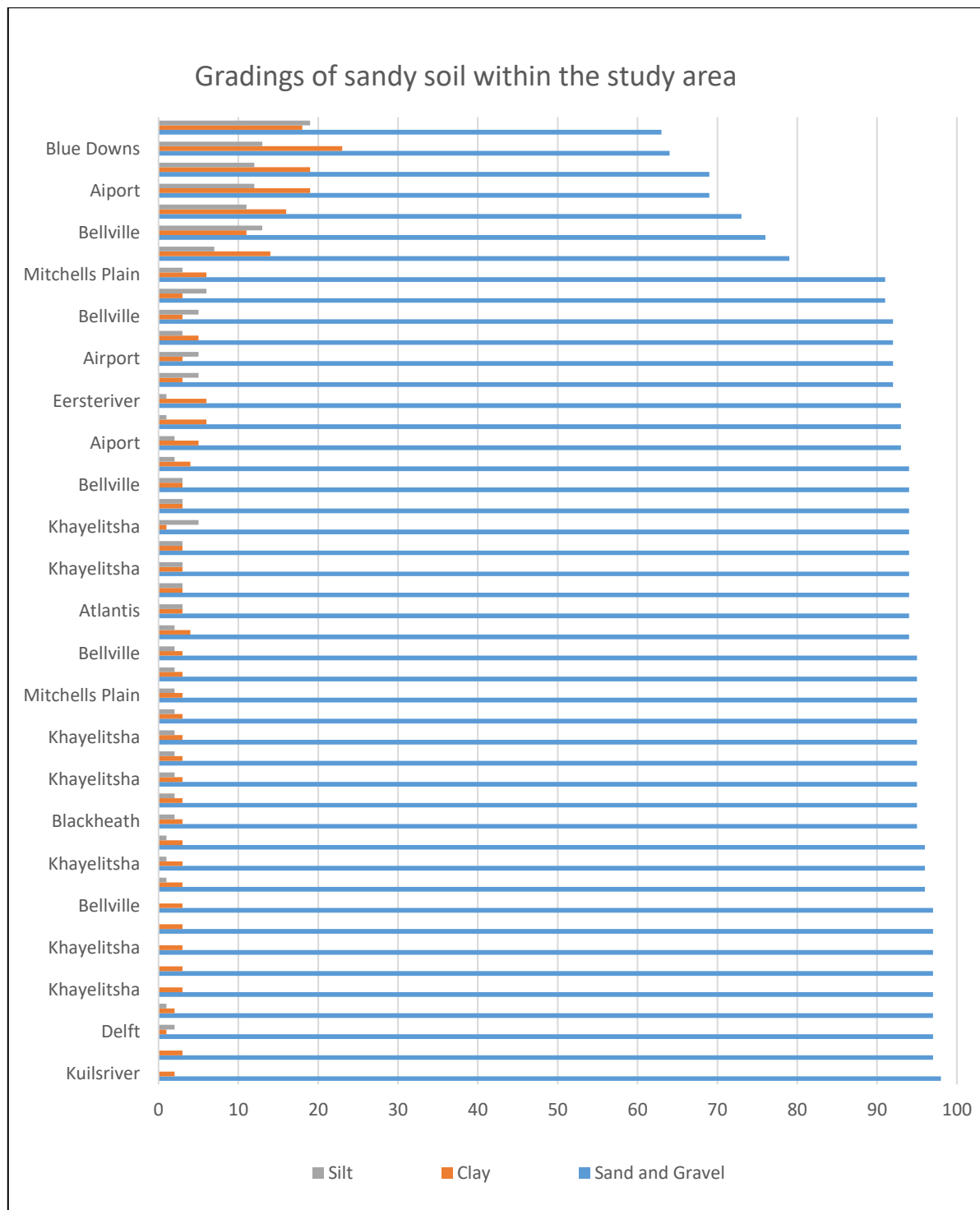
*Figure 4.15: Gradings of soils obtained within the study area*

Houses and buildings founded slightly deeper onto the more dense soils are therefore not susceptible to liquefaction. Services such sewage and storm water lines are founded just below ground level, and within sands that have been disturbed by excavation. The compaction of the pipe bedding and backfill is therefore essential, as a liquefaction event can easily force these less dense soils and pipes to float to the surface during an earthquake. The depth at which these soil samples were taken is also unknown. Soil profiles are not uniform and layers of other soil mixtures can be present throughout, varying in

thickness. Certain layers can therefore be susceptible to liquefaction and appear as sand boils on the surface. Other sand layers can resist liquefaction and be stable during an earthquake. Nevertheless, the majority of the gradings obtained are susceptible to liquefaction, although gradings are not enough to establish liquefaction potential. A better risk assessment can therefore be made if the relative density and the depth to the water table are also known. The literature (Idriss & Boulanger, 2010; Gandomi, et al., 2013) also tells us that younger soils, especially those from the Holocene, are most at risk when considering liquefaction. Soils on the Cape Flats are almost all within the Holocene age, some even younger.

### 4.4.3    Grading results from samples obtained for this study

Testing has been carried out in two phases, as mentioned before. The first part, or phase one, includes the areas labelled as UWC, Langa, Talana Road (Sacks Circle), Bardale Village, Mitchells Plain and two pre-graded samples labelled as 0.150 and 0.425. These samples were then tested on the vibrating table. Results obtained from the first phase lead to the manual grading of nine more samples, or the second phase. The second phase includes grading samples that are uniformly-graded, well-graded and gap-graded. These samples were then also tested on the vibrating table. Vibration table results are discussed in the next section. Grading curves were created for all samples. The grading curves were compared to the liquefied soils in Figure 2.17. Limit lines, in red, for potentially liquefiable soils were also added to each grading curve. Figure 4.16 - Figure 4.22 indicates the grading curves for the first phase of samples. Figure 4.23 - Figure 4.31 indicates the grading curves for the second phase of samples. Grading curves that fall between the red limit lines indicate soils that are potentially liquefiable.

If comparing Figure 4.15 and the following grading results with that of the results in Figure 2.17, then one can argue that almost all of the samples are vulnerable to liquefaction. Samples that could potentially resist liquefaction are those with a sand content less than 80% and ones that fall outside of the red boundary lines. These are however only an indication and are not based on water table, density, earthquake magnitude or PGA.



| Sieve size (mm) | Percentage passing |
|---|---|
| 4,750 | 100 |
| 2,360 | 100 |
| 2,000 | 100 |
| 1,180 | 98 |
| 0,600 | 90 |
| 0,425 | 82 |
| 0,300 | 65 |
| 0,150 | 15 |
| 0,075 | 5 |
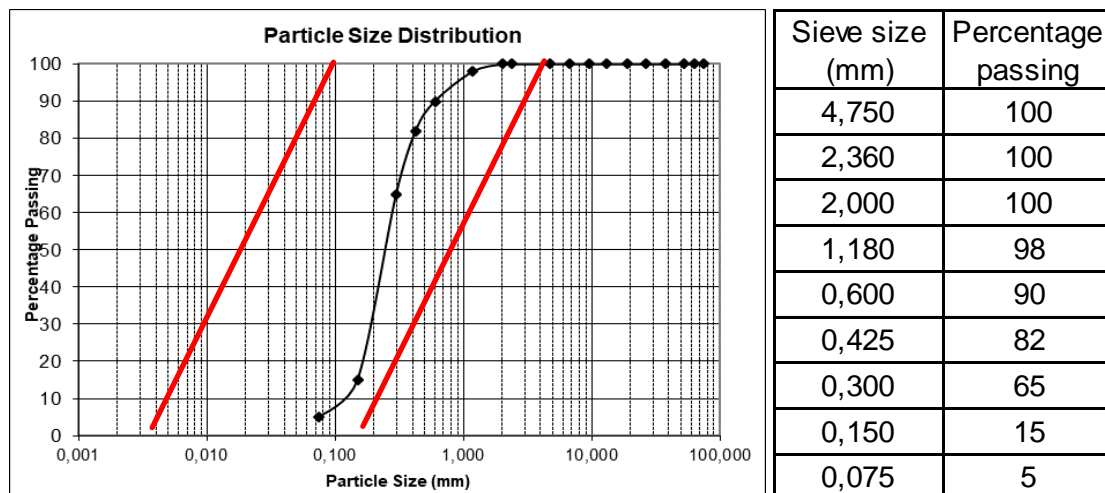
*Figure 4.16: Grading curve and sieve analysis for UWC site – Uniform graded*



| Sieve size (mm) | Percentage passing |
|---|---|
| 4,750 | 100 |
| 2,360 | 100 |
| 2,000 | 100 |
| 1,180 | 100 |
| 0,600 | 80 |
| 0,425 | 67 |
| 0,300 | 52 |
| 0,150 | 15 |
| 0,075 | 3 |
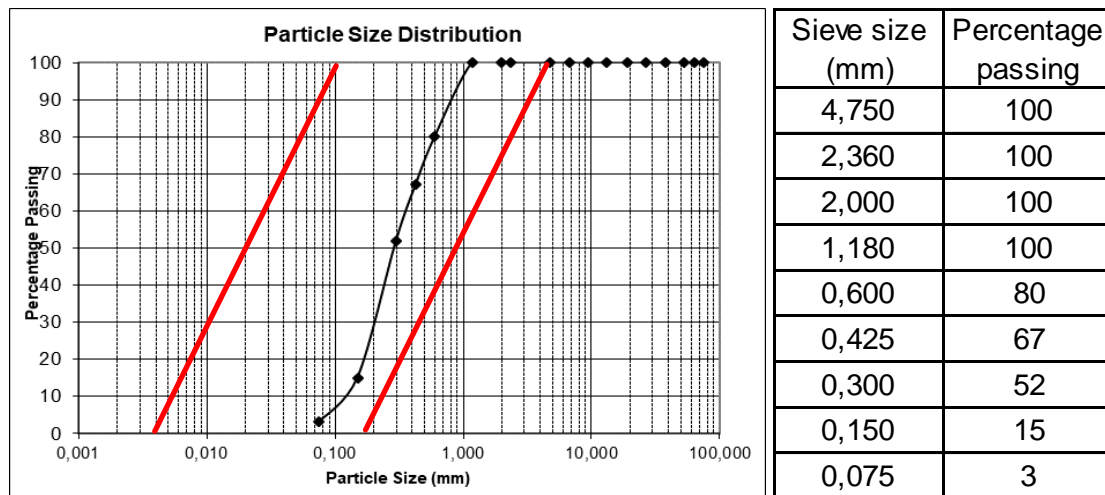
*Figure 4.17: Grading curve and sieve analysis for Langa site – Uniform graded*



| Sieve size (mm) | Percentage passing |
|---|---|
| 4,750 | 100 |
| 2,360 | 98 |
| 2,000 | 98 |
| 1,180 | 97 |
| 0,600 | 95 |
| 0,425 | 86 |
| 0,300 | 66 |
| 0,150 | 16 |
| 0,075 | 3 |
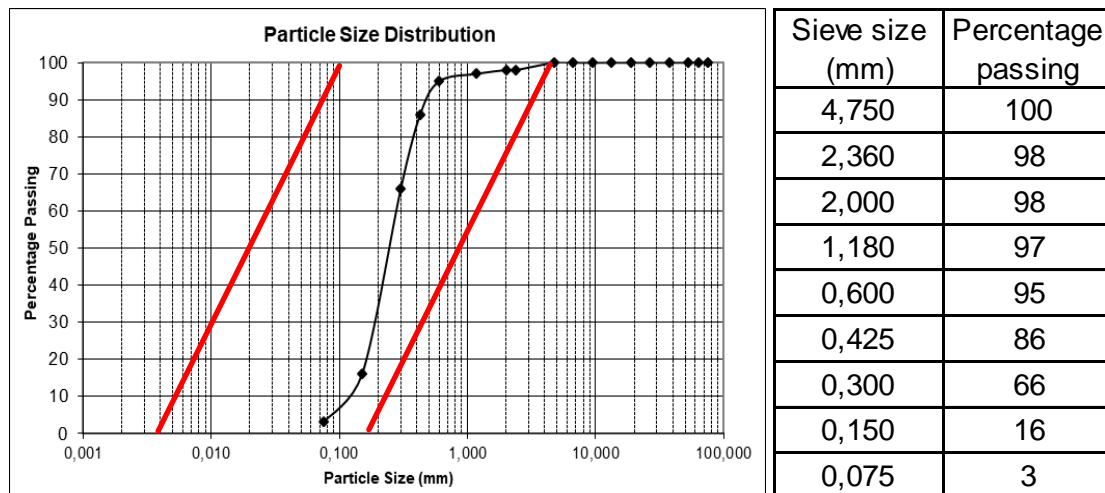
*Figure 4.18: Grading curve and sieve analysis for Talana Road site – Uniform graded*



| Sieve size (mm) | Percentage passing |
|---|---|
| 4,750 | 100 |
| 2,360 | 99 |
| 2,000 | 98 |
| 1,180 | 96 |
| 0,600 | 94 |
| 0,425 | 90 |
| 0,300 | 74 |
| 0,150 | 12 |
| 0,075 | 3 |
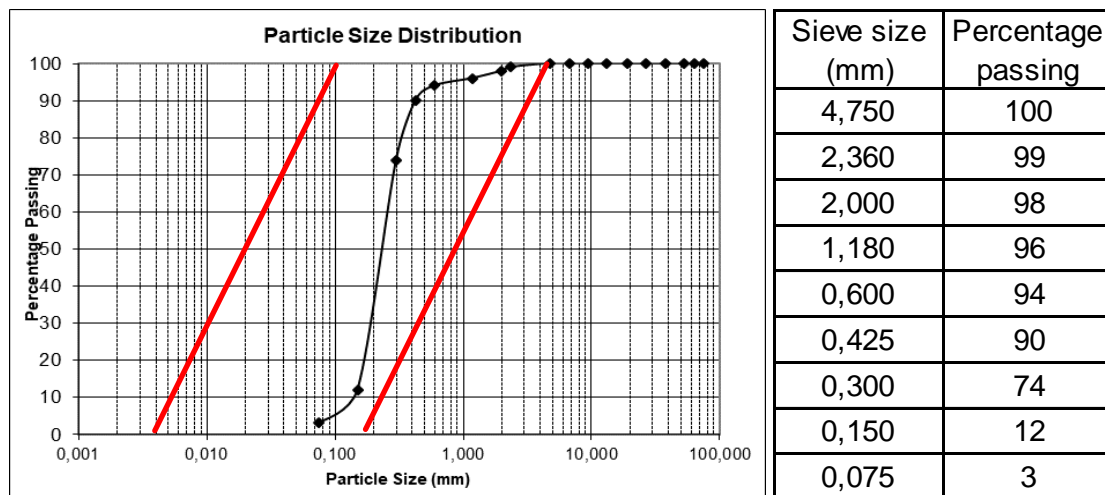
*Figure 4.19: Grading curve and sieve analysis for Bardale Village site – Uniform graded*



| Sieve size (mm) | Percentage passing |
|---|---|
| 4,750 | 100 |
| 2,360 | 100 |
| 2,000 | 100 |
| 1,180 | 98 |
| 0,600 | 85 |
| 0,425 | 75 |
| 0,300 | 71 |
| 0,150 | 10 |
| 0,075 | 5 |
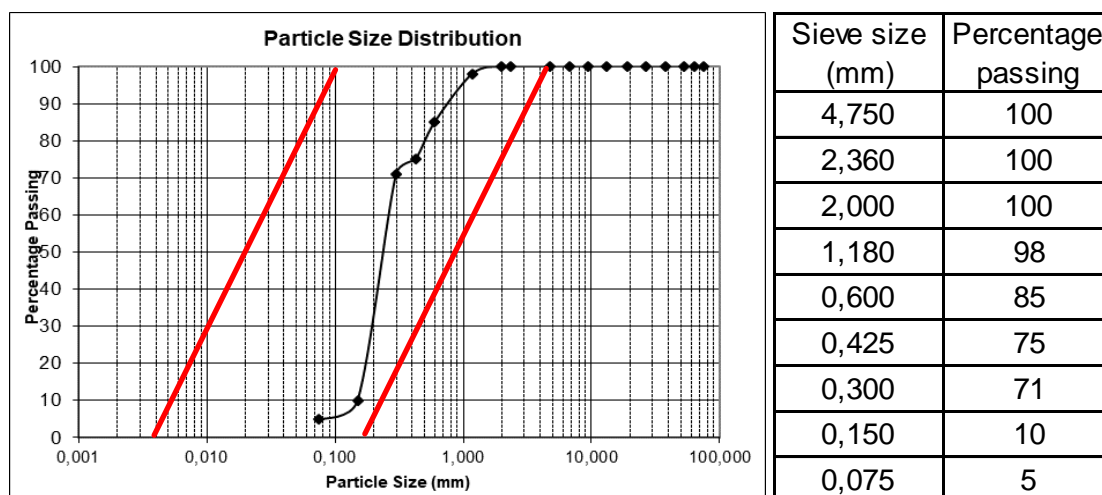
*Figure 4.20: Grading curve and sieve analysis for Mitchells Plain site – Uniform graded*



| Sieve size (mm) | Percentage passing |
|---|---|
| 4,750 | 100 |
| 2,360 | 100 |
| 2,000 | 100 |
| 1,180 | 100 |
| 0,600 | 100 |
| 0,425 | 100 |
| 0,300 | 100 |
| 0,150 | 0 |
| 0,075 | 0 |
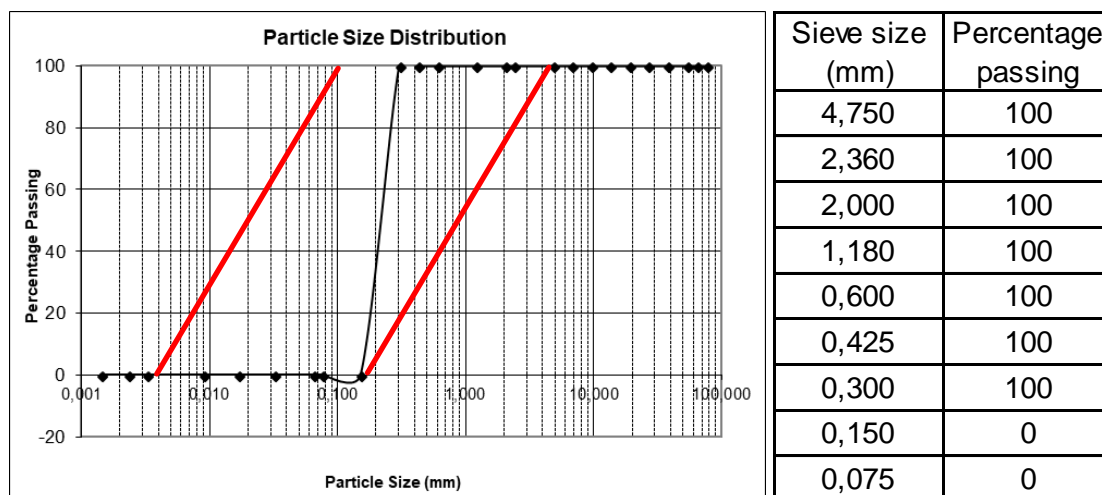
*Figure 4.21: Grading curve and sieve analysis for pre-graded 0.150 sample – Uniform graded*



| Sieve size (mm) | Percentage passing |
|---|---|
| 4,750 | 100 |
| 2,360 | 100 |
| 2,000 | 100 |
| 1,180 | 100 |
| 0,600 | 100 |
| 0,425 | 0 |
| 0,300 | 0 |
| 0,150 | 0 |
| 0,075 | 0 |
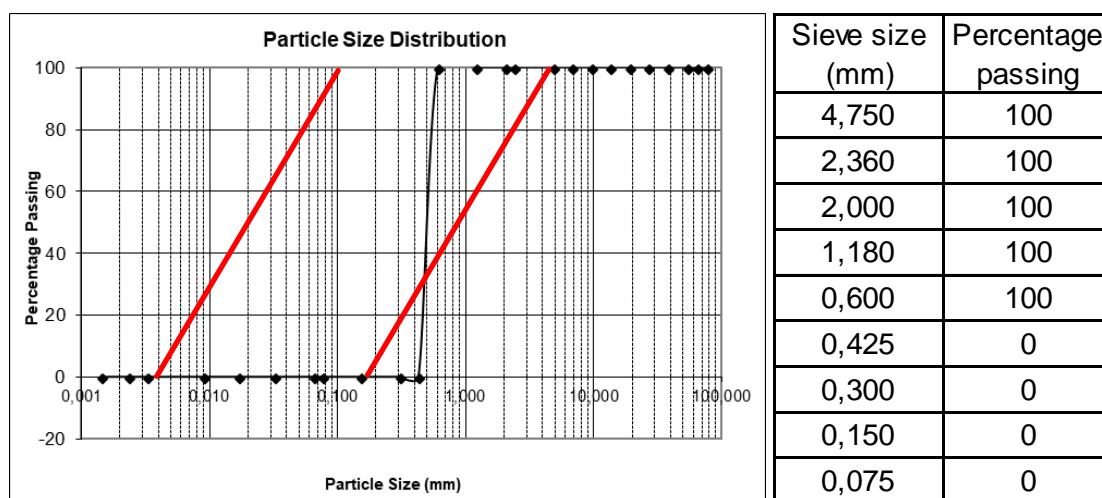
*Figure 4.22: Grading curve and sieve analysis for pre-graded 0.425 sample – Uniform graded*

91

#### 4.4.4   Grading results for manually mixed samples (second phase)



| Sieve size (mm) | Percentage passing |
|---|---|
| 4,750 | 100 |
| 2,360 | 100 |
| 2,000 | 100 |
| 1,180 | 100 |
| 0,600 | 65 |
| 0,425 | 45 |
| 0,300 | 25 |
| 0,150 | 5 |
| 0,075 | 0 |
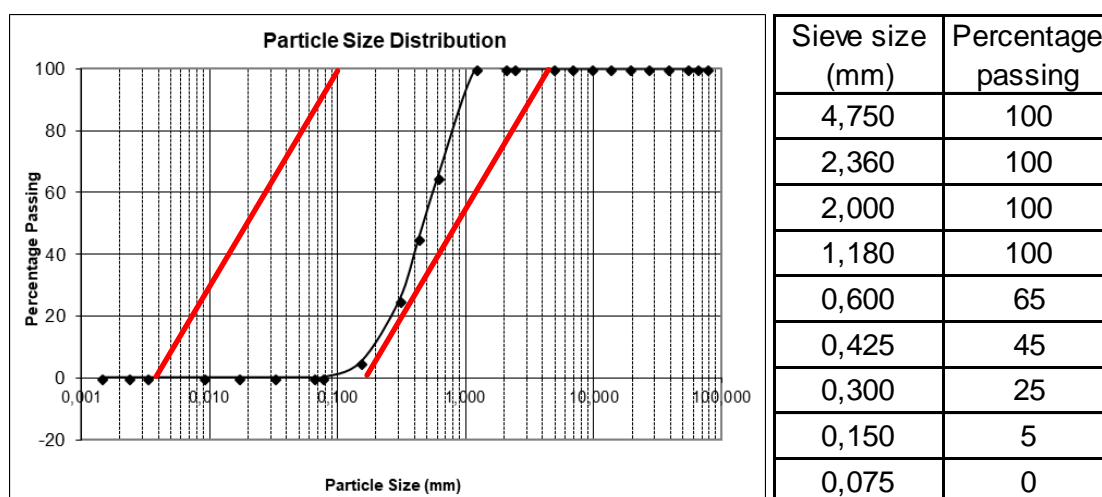
*Figure 4.23: Grading curve and sieve-analysis for second phase sample 1 – Uniform graded*



| Sieve size (mm) | Percentage passing |
|---|---|
| 4,750 | 100 |
| 2,360 | 100 |
| 2,000 | 55 |
| 1,180 | 55 |
| 0,600 | 55 |
| 0,425 | 55 |
| 0,300 | 50 |
| 0,150 | 50 |
| 0,075 | 5 |
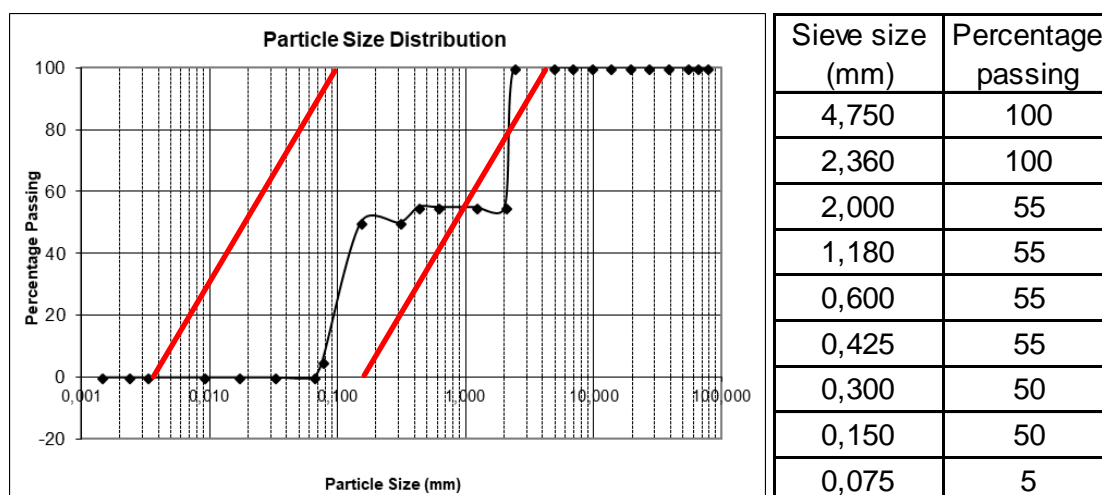
*Figure 4.24: Grading curve and sieve-analysis for second phase sample 2 – Gap graded*



| Sieve size (mm) | Percentage passing |
|---|---|
| 4,750 | 90 |
| 2,360 | 75 |
| 2,000 | 65 |
| 1,180 | 55 |
| 0,600 | 45 |
| 0,425 | 35 |
| 0,300 | 25 |
| 0,150 | 15 |
| 0,075 | 5 |
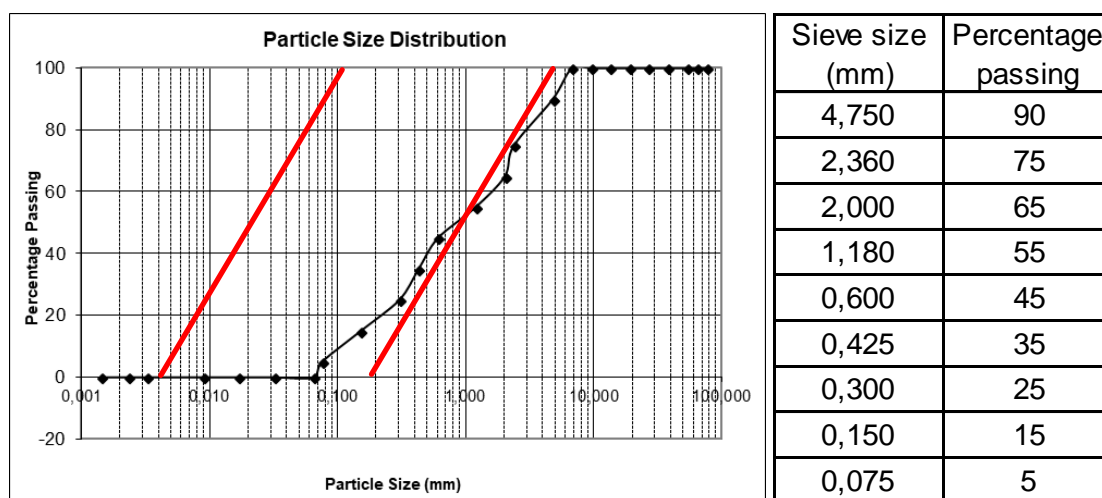
*Figure 4.25: Grading curve and sieve-analysis for second phase sample 3 – Uniform/Gap graded*

92

| Sieve size (mm) | Percentage passing |
|---|---|
| 4,750 | 90 |
| 2,360 | 90 |
| 2,000 | 90 |
| 1,180 | 90 |
| 0,600 | 90 |
| 0,425 | 50 |
| 0,300 | 50 |
| 0,150 | 50 |
| 0,075 | 5 |
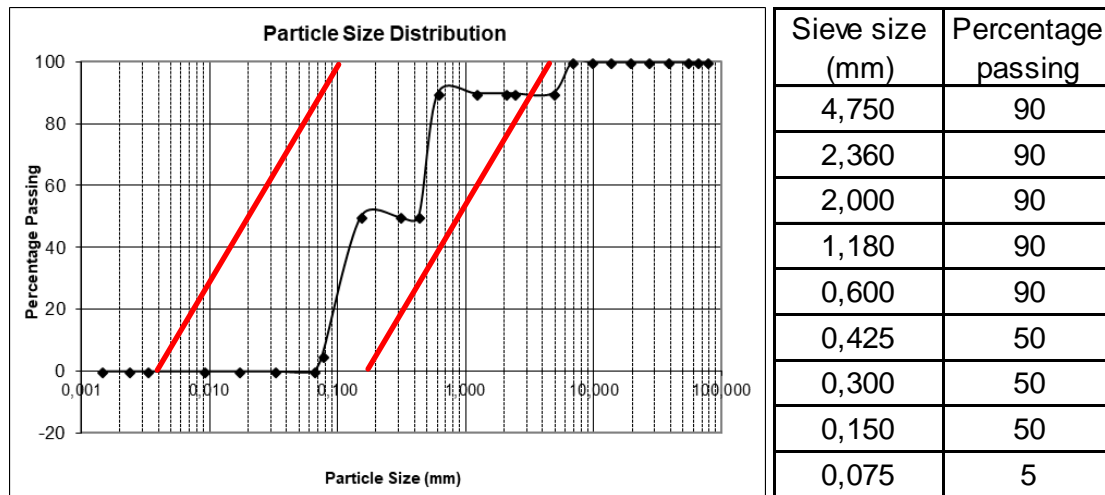
*Figure 4.26: Grading curve and sieve-analysis for second phase sample 4 – Gap graded*



| Sieve size (mm) | Percentage passing |
|---|---|
| 4,750 | 50 |
| 2,360 | 50 |
| 2,000 | 50 |
| 1,180 | 50 |
| 0,600 | 50 |
| 0,425 | 25 |
| 0,300 | 25 |
| 0,150 | 25 |
| 0,075 | 25 |
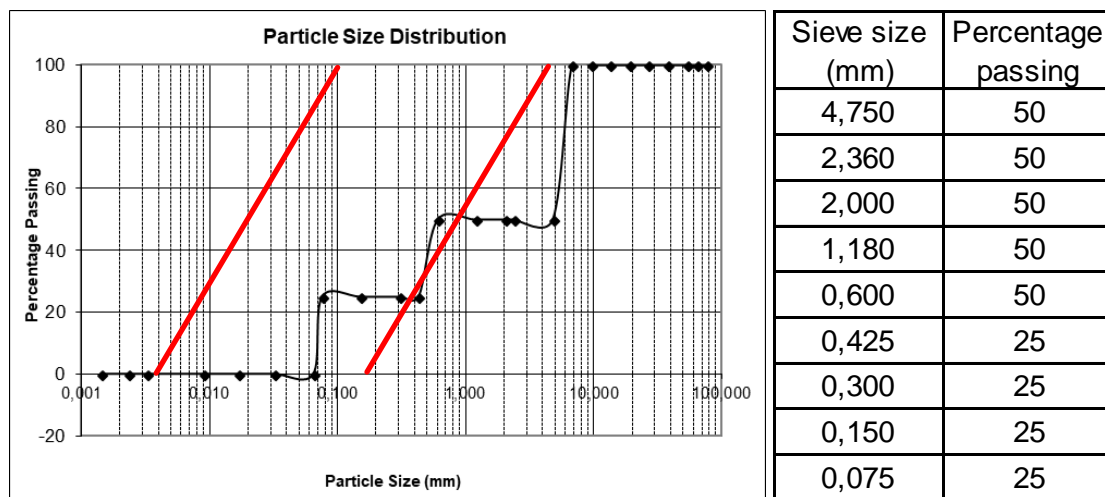
*Figure 4.27: Grading curve and sieve-analysis for second phase sample 5 – Gap graded*



| Sieve size (mm) | Percentage passing |
|---|---|
| 4,750 | 50 |
| 2,360 | 50 |
| 2,000 | 50 |
| 1,180 | 50 |
| 0,600 | 50 |
| 0,425 | 50 |
| 0,300 | 50 |
| 0,150 | 50 |
| 0,075 | 50 |
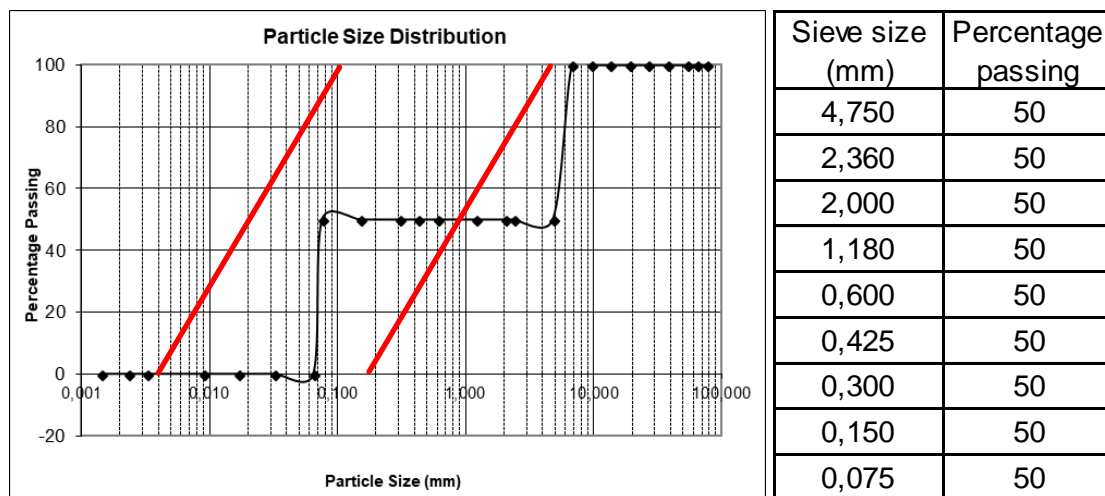
*Figure 4.28: Grading curve and sieve-analysis for second phase sample 6 – Gap graded*

| Sieve size (mm) | Percentage passing |
|---|---|
| 4,750 | 100 |
| 2,360 | 100 |
| 2,000 | 50 |
| 1,180 | 50 |
| 0,600 | 50 |
| 0,425 | 50 |
| 0,300 | 50 |
| 0,150 | 10 |
| 0,075 | 5 |
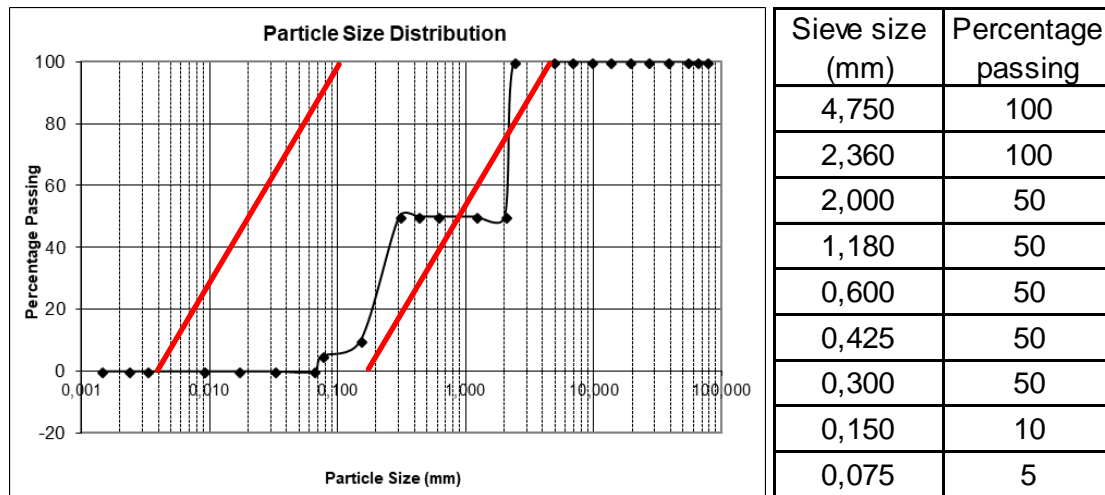
*Figure 4.29: Grading curve and sieve-analysis for second phase sample 7 – Gap graded*



| Sieve size (mm) | Percentage passing |
|---|---|
| 4,750 | 100 |
| 2,360 | 75 |
| 2,000 | 65 |
| 1,180 | 55 |
| 0,600 | 45 |
| 0,425 | 35 |
| 0,300 | 25 |
| 0,150 | 15 |
| 0,075 | 5 |
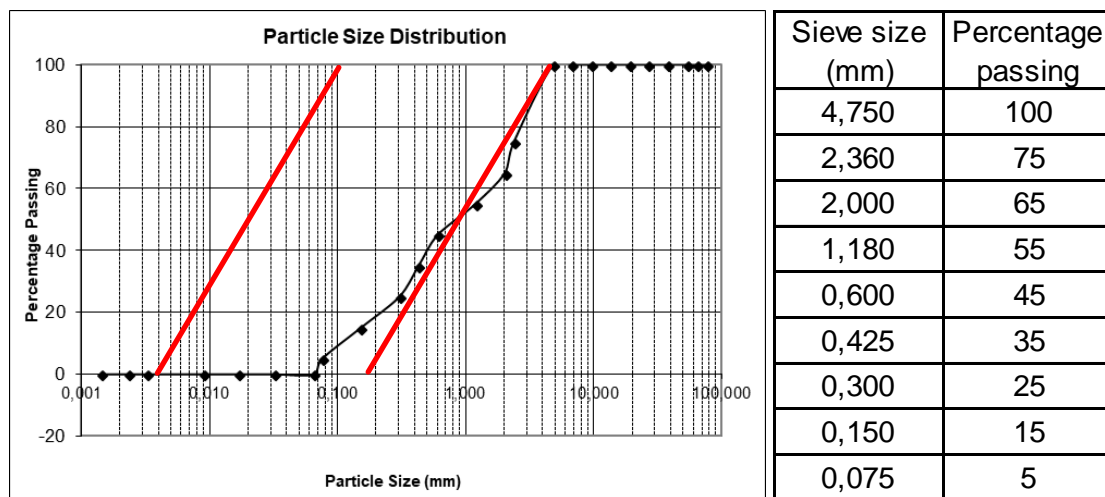
*Figure 4.30: Grading curve and sieve-analysis for second phase sample 8 – Gap/Uniform graded*



| Sieve size (mm) | Percentage passing |
|---|---|
| 4,750 | 100 |
| 2,360 | 100 |
| 2,000 | 100 |
| 1,180 | 95 |
| 0,600 | 52 |
| 0,425 | 52 |
| 0,300 | 50 |
| 0,150 | 50 |
| 0,075 | 5 |
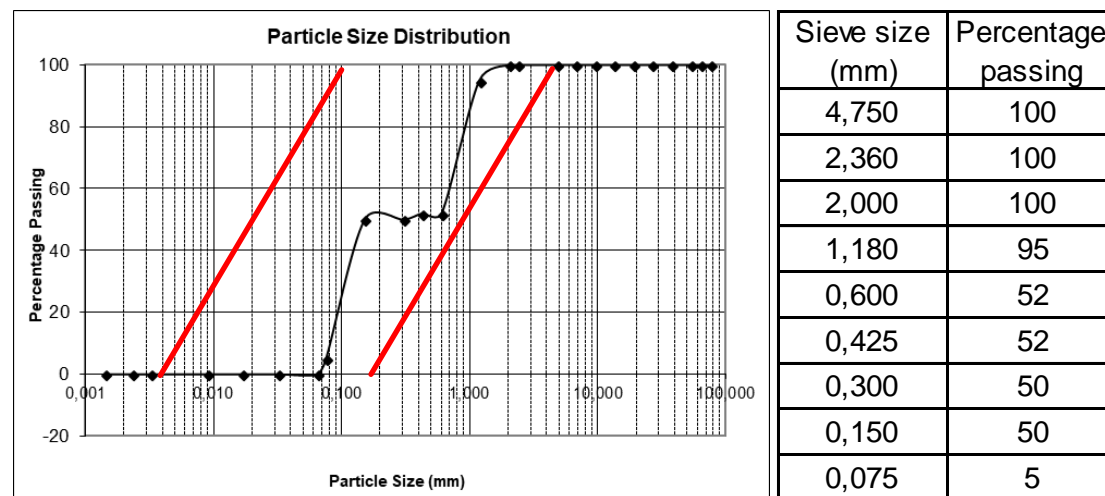
*Figure 4.31: Grading curve and sieve-analysis for second phase sample 9 – Gap graded*

94

| Sieve size (mm) | Percentage passing |
|---|---|
| 4,750 | 70 |
| 2,360 | 65 |
| 2,000 | 60 |
| 1,180 | 55 |
| 0,600 | 50 |
| 0,425 | 45 |
| 0,300 | 40 |
| 0,150 | 35 |
| 0,075 | 30 |
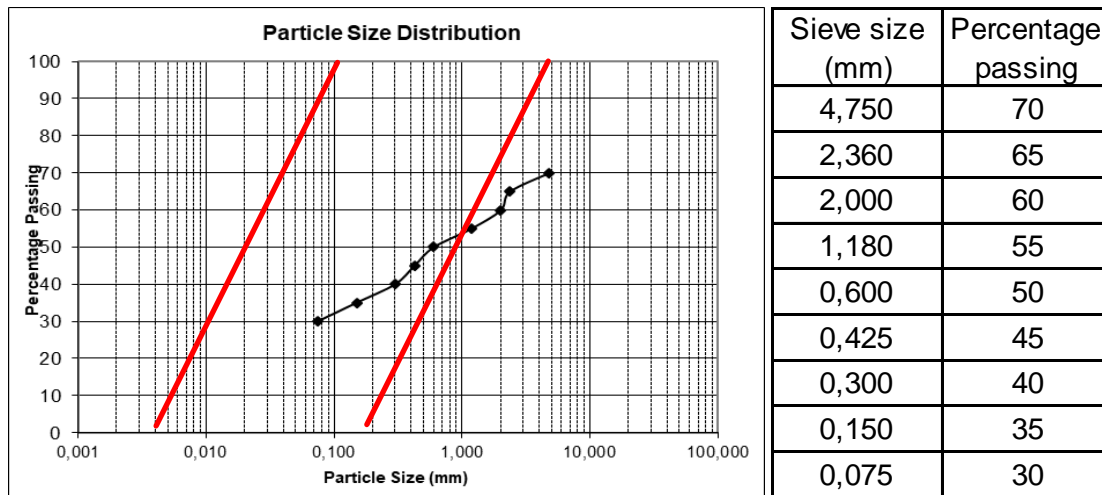
*Figure 4.32: Grading curve and sieve-analysis for second phase sample 10 – Well graded*



| Sieve size (mm) | Percentage passing |
|---|---|
| 4,750 | 85 |
| 2,360 | 80 |
| 2,000 | 75 |
| 1,180 | 70 |
| 0,600 | 65 |
| 0,425 | 60 |
| 0,300 | 55 |
| 0,150 | 50 |
| 0,075 | 45 |
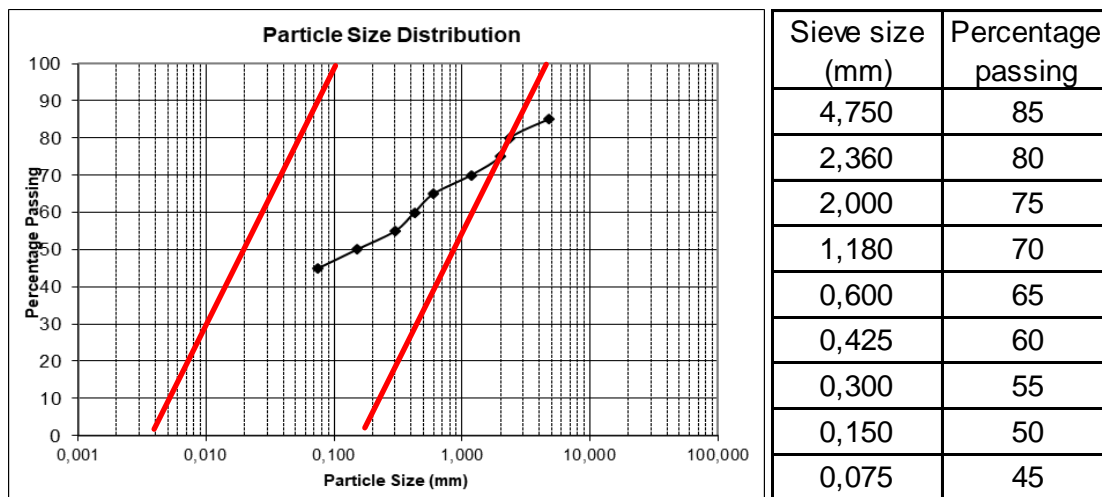
*Figure 4.33: Grading curve and sieve-analysis for second phase sample 11 – Well graded*

## 4.5    Vibration Table Results

### 4.5.1    Introduction

A total of 72 vibration table tests have been conducted. As mentioned before, samples were divided into two phases. Phase one includes seven samples from the following areas:

1.    University of the Western Cape
2.    Langa Shopping Centre
3.    Talana Road, Sacks Circle, Bellville
4.    Bardale Village
5.    Mitchells Plain Station
6.    Pre-graded 0.150 sand
7.    Pre-graded 0.425 sand

Each sample was tested at four different phases. Each sample was tested at 0.15g, which is the expected PGA value for soils from the Cape Town area, as well as 0.25g, which provides a maximum and worst-case scenario for southern Africa. In addition, each sample was tested at a loose, un-compacted state, as well as a dense compacted state, totalling 28 results. Results from the first phase led to the testing of a second phase. Nine more samples were tested, all at 0.15g. Each sample was tested at a loose, uncompacted state and then at a dense, compacted state. This was done twice for each sample to provide four result sets for each sample in the second phase, totalling 44 results. Table 4.3 display all phase one's data for density, initial water content of each sample, and data used in calculating the amount of water required to saturate the sample after compaction. Samples were either compacted, or not. The un-compacted samples were however also placed in the same way as the compacted samples, with the funnel. The densities for all samples were measured from within the plastic containers and listed in the table.

Table 4.5 indicates the measured height of the brick, as explained in the methodology section. The initial height, indicated as height 1, is the height from the top of the brick to the top of the plastic container. Height 2 is the measured distance after 60 seconds of vibration. The difference between height 1 and 2, known as the settlement, is also listed. Liquefaction was said to have occurred if water raised to such a level that none of the underlying sand was visible, and the brick experienced large settlement. In some cases, no liquefaction occurred within the 60 second test frame. In these cases, vibration was continued and acceleration was increased. The time it took for liquefaction to occur, was noted. The test was stopped if no liquefaction occurred within 120 seconds.

96

*Table 4.3: Basic properties and water content needed for first phase*

| Test # | 1 | 2 | 3 | 4 | 1 | 2 | 3 | 4 | 1 | 2 | 3 | 4 | 1 | 2 | 3 | 4 |
|---|---|---|---|---|---|---|---|---|---|---|---|---|---|---|---|---|
| Site | UWC | | | | Langa Shopping Centre | | | | Talana Road Bellville | | | | Bardale Village | | | |
| Soil Description | Light greyish brown sand | | | | Light greyish brown sand | | | | Light brown and buff sand | | | | Yellowish brown sand | | | |
| Sample Weight Kg | 20 | 20 | 20 | 20 | 20 | 20 | 20 | 20 | 20 | 20 | 20 | 20 | 20 | 20 | 20 | 20 |
| Initial Moisture Content (%) | 3 | 3 | 3 | 3 | 4.4 | 4.4 | 4.4 | 4.4 | 10.5 | 10.5 | 10.5 | 10.5 | 4 | 4 | 4 | 4 |
| | 0.03 | 0.03 | 0.03 | 0.03 | 0.04 | 0.04 | 0.04 | 0.04 | 0.11 | 0.11 | 0.11 | 0.11 | 0.04 | 0.04 | 0.04 | 0.04 |
| Compacted? | No | Yes | No | Yes | No | Yes | No | Yes | No | Yes | No | Yes | No | Yes | No | Yes |
| Density kg/m3 | 1539 | 1695 | 1601 | 1709 | 1555 | 1805 | 1570 | 1795 | 1520 | 1699 | 1505 | 1702 | 1605 | 1761 | 1618 | 1755 |
| Gs | 2.67 | 2.67 | 2.67 | 2.67 | 2.67 | 2.67 | 2.67 | 2.67 | 2.67 | 2.67 | 2.67 | 2.67 | 2.67 | 2.67 | 2.67 | 2.67 |
| Water kg/m$^3$ | 1000 | 1000 | 1000 | 1000 | 1000 | 1000 | 1000 | 1000 | 1000 | 1000 | 1000 | 1000 | 1000 | 1000 | 1000 | 1000 |
| Void ratio e | 0.73 | 0.58 | 0.67 | 0.56 | 0.72 | 0.48 | 0.70 | 0.49 | 0.76 | 0.57 | 0.77 | 0.57 | 0.66 | 0.52 | 0.65 | 0.52 |
| Sr Required | 1.00 | 1.00 | 1.00 | 1.00 | 1.00 | 1.00 | 1.00 | 1.00 | 1.00 | 1.00 | 1.00 | 1.00 | 1.00 | 1.00 | 1.00 | 1.00 |
| Water content required | 0.28 | 0.22 | 0.25 | 0.21 | 0.27 | 0.18 | 0.26 | 0.18 | 0.28 | 0.21 | 0.29 | 0.21 | 0.25 | 0.19 | 0.24 | 0.20 |
| After initial moisture | 0.25 | 0.19 | 0.22 | 0.18 | 0.22 | 0.14 | 0.22 | 0.14 | 0.18 | 0.11 | 0.18 | 0.11 | 0.21 | 0.15 | 0.20 | 0.16 |
| % | 24.5 | 18.5 | 22.0 | 18.1 | 22.5 | 13.5 | 21.8 | 13.9 | 17.8 | 10.9 | 18.5 | 10.8 | 20.9 | 15.3 | 20.4 | 15.5 |
| Liter water needed | 4.90 | 3.71 | 4.40 | 3.61 | 4.49 | 2.71 | 4.37 | 2.77 | 3.57 | 2.18 | 3.70 | 2.16 | 4.17 | 3.07 | 4.07 | 3.11 |

97

*Basic properties and water content needed for first phase (continue)*

| Test # | 1 | 2 | 3 | 4 | 1 | 2 | 3 | 4 | 1 | 2 | 3 | 4 |
|---|---|---|---|---|---|---|---|---|---|---|---|---|
| Site | Mitchells Plain Station | | | | Pre graded 0,150 | | | | Pre graded 0,425 | | | |
| Soil Description | Light brown and buff sand | | | | Yellowish sand | | | | Yellowish sand | | | |
| Sample Weight Kg | 20 | 20 | 20 | 20 | 20 | 20 | 20 | 20 | 20 | 20 | 20 | 20 |
| Initial Moisture Content (%) | 5.8 | 5.8 | 5.8 | 5.8 | 2.5 | 2.5 | 2.5 | 2.5 | 2.2 | 2.2 | 2.2 | 2.2 |
| | 0.058 | 0.058 | 0.058 | 0.058 | 0.025 | 0.025 | 0.025 | 0.025 | 0.022 | 0.022 | 0.022 | 0.022 |
| Compacted? | No | Yes | No | Yes | No | Yes | No | Yes | No | Yes | No | Yes |
| Density kg/m3 | 1580 | 1790 | 1605 | 1788 | 1622 | 1690 | 1635 | 1685 | 1610 | 1666 | 1614 | 1682 |
| Gs | 2.67 | 2.67 | 2.67 | 2.67 | 2.67 | 2.67 | 2.67 | 2.67 | 2.67 | 2.67 | 2.67 | 2.67 |
| Water kg/m$^3$ | 1000 | 1000 | 1000 | 1000 | 1000 | 1000 | 1000 | 1000 | 1000 | 1000 | 1000 | 1000 |
| Void ratio e | 0.69 | 0.49 | 0.66 | 0.49 | 0.65 | 0.58 | 0.63 | 0.58 | 0.66 | 0.60 | 0.65 | 0.59 |
| Sr Required | 1.00 | 1.00 | 1.00 | 1.00 | 1.00 | 1.00 | 1.00 | 1.00 | 1.00 | 1.00 | 1.00 | 1.00 |
| Water content required | 0.26 | 0.18 | 0.25 | 0.18 | 0.24 | 0.22 | 0.24 | 0.22 | 0.25 | 0.23 | 0.25 | 0.22 |
| After initial moisture | 0.20 | 0.13 | 0.19 | 0.13 | 0.22 | 0.19 | 0.21 | 0.19 | 0.22 | 0.20 | 0.22 | 0.20 |
| % | 20.0 | 12.6 | 19.1 | 12.7 | 21.7 | 19.2 | 21.2 | 19.4 | 22.5 | 20.4 | 22.3 | 19.8 |
| Liter water needed | 4.01 | 2.52 | 3.81 | 2.54 | 4.34 | 3.84 | 4.24 | 3.88 | 4.49 | 4.07 | 4.46 | 3.96 |

98

### 4.5.2   Results from first phase of testing

Table 4.4 summarises the grading results, Atterberg Limits and compaction characteristics obtained for the first phase of samples. Physical properties such as the sample depth and water table is also indicated, if known/present.

*Table 4.4 Gradings and other soil data from tested sites and pre-graded sands*

| Site | | UWC Chem Building | Langa Shopping Centre | Sacks Circle Talana Road | Bardale Village | Mitchells Plain | Pre graded 0,150 | Pre graded 0,425 |
|---|---|---|---|---|---|---|---|---|
| Soil Description | | Light greyish brown sand | Light greyish brown sand | Light brown and buff sand | Yellowish brown sand | Light brown and buff sand | Yellowish sand | Yellowish sand |
| Depth of sample (meters below ground) | | 1,0 - 1,5 | 0,5 - 1,0 | 0,5 - 1,0 | 1,0 - 1,5 | 0,5 - 1,0 | - | - |
| Initial Moisture Content (%) | | 6,50 | 7,50 | 12,00 | 5,00 | 6,50 | 2,50 | 2,00 |
| Plastic Index | | Non Plastic | Non Plastic | Non Plastic | Non Plastic | Non Plastic | Non Plastic | Non Plastic |
| Max DD | | 1785 | 1822 | 1717 | 1768 | 1810 | - | - |
| Water Table meters below ground | | 1,9 | 1,7 | 1,4 | 2,1 | 1,4 | - | - |
| O.M.C (%) | | 11,7 | 9,8 | 12,2 | 11,8 | 10,5 | - | - |
| Sieve Analysis | Sieve Size (mm) | Percent Passing | | | | | | |
| | 4,750 | 100 | 100 | 100 | 100 | 100 | 100 | 100 |
| | 2,360 | 100 | 100 | 98 | 99 | 100 | 100 | 100 |
| | 2,000 | 100 | 100 | 98 | 98 | 100 | 100 | 100 |
| | 1,180 | 98 | 100 | 97 | 96 | 98 | 100 | 100 |
| | 0,600 | 90 | 80 | 95 | 94 | 85 | 100 | 100 |
| | 0,425 | 82 | 67 | 86 | 90 | 75 | 100 | 0 |
| | 0,300 | 65 | 52 | 66 | 74 | 71 | 100 | 0 |
| | 0,150 | 15 | 14 | 16 | 12 | 10 | 0 | 0 |
| | 0,075 | 5 | 3 | 3 | 3 | 5 | 0 | 0 |

The results that were obtained after vibration tests were done for the first phase, are presented in Table 4.5. The amount of settlement is indicated as well as whether or not liquefaction occurred. The time it took for a soil to liquefy, if it did, is also indicated. Other important data such as the amount of water required to saturate the sample and density of the tested sample is also indicated.

*Table 4.5: Vibration Table Results For all Samples Tested*

| Test # | 1 | 2 | 3 | 4 | 1 | 2 | 3 | 4 |
|---|---|---|---|---|---|---|---|---|
| Site | UWC | | | | Langa Shopping Centre | | | |
| Soil Description | Light greyish brown sand | | | | Light greyish brown sand | | | |
| Sample Weight Kg | 20 | 20 | 20 | 20 | 20 | 20 | 20 | 20 |
| Initial Moisture Content (%) | 3 | 3 | 3 | 3 | 4,4 | 4,4 | 4,4 | 4,4 |
| | 0,03 | 0,03 | 0,03 | 0,03 | 0,044 | 0,044 | 0,044 | 0,044 |
| Compacted? | No | Yes | No | Yes | No | Yes | No | Yes |
| Density kg/m3 | 1539 | 1695 | 1601 | 1709 | 1555 | 1805 | 1570 | 1795 |
| Gs | 2,67 | 2,67 | 2,67 | 2,67 | 2,67 | 2,67 | 2,67 | 2,67 |
| Gamma Water | 1000 | 1000 | 1000 | 1000 | 1000 | 1000 | 1000 | 1000 |
| Void ratio e | 0,73 | 0,58 | 0,67 | 0,56 | 0,72 | 0,48 | 0,70 | 0,49 |
| Sr Required | 1,00 | 1,00 | 1,00 | 1,00 | 1,00 | 1,00 | 1,00 | 1,00 |
| Water content required | 0,28 | 0,22 | 0,25 | 0,21 | 0,27 | 0,18 | 0,26 | 0,18 |
| After initial moisture | 0,25 | 0,19 | 0,22 | 0,18 | 0,22 | 0,14 | 0,22 | 0,14 |
| % | 24,52 | 18,54 | 22,01 | 18,06 | 22,46 | 13,55 | 21,84 | 13,86 |
| Liter water needed | 4,90 | 3,71 | 4,40 | 3,61 | 4,49 | 2,71 | 4,37 | 2,77 |
| Height 1 (mm) | 20 | 26 | 23 | 28 | 18 | 25 | 28 | 29 |
| Height 2 (mm) | 65 | 40 | 62 | 45 | 64 | 33 | 80 | 71 |
| Settle Amount | 45 | 14 | 39 | 17 | 46 | 8 | 52 | 42 |
| Tested at 'g' | 0,15 | 0,15 | 0,25 | 0,25 | 0,15 | 0,15 | 0,25 | 0,25 |
| **Liquefaction?** | **Yes** | **Yes** | **Yes** | **Yes** | **Yes** | **No** | **Yes** | **Yes** |
| At what time? Seconds | 10 | 15 | 12 | 16 | 8 | - | 12 | 20 |
| If not, did it liquefy after 60sec? | | | | | | **Yes** | | |
| At what g'? | | | | | | 0,15 | | |
| After how long? Seconds | | | | | | 72 | | |

*Vibration Table Results Continue*

| Test # | 1 | 2 | 3 | 4 | 1 | 2 | 3 | 4 | 1 | 2 | 3 | 4 |
|---|---|---|---|---|---|---|---|---|---|---|---|---|
| Site | Talana Road Bellville | | | | Bardale Village | | | | Mitchells Plain Station | | | |
| Soil Description | Light brown and buff sand | | | | Yellowish brown sand | | | | Light brown and buff sand | | | |
| Sample Weight Kg | 20 | 20 | 20 | 20 | 20 | 20 | 20 | 20 | 20 | 20 | 20 | 20 |
| Initial Moisture Content (%) | 10,5 | 10,5 | 10,5 | 10,5 | 4 | 4 | 4 | 4 | 5,8 | 5,8 | 5,8 | 5,8 |
| | 0,105 | 0,105 | 0,105 | 0,105 | 0,04 | 0,04 | 0,04 | 0,04 | 0,058 | 0,058 | 0,058 | 0,058 |
| Compacted? | No | Yes | No | Yes | No | Yes | No | Yes | No | Yes | No | Yes |
| Density kg/m3 | 1520 | 1699 | 1505 | 1702 | 1605 | 1761 | 1618 | 1755 | 1580 | 1790 | 1605 | 1788 |
| Gs | 2,67 | 2,67 | 2,67 | 2,67 | 2,67 | 2,67 | 2,67 | 2,67 | 2,67 | 2,67 | 2,67 | 2,67 |
| Gamma Water | 1000 | 1000 | 1000 | 1000 | 1000 | 1000 | 1000 | 1000 | 1000 | 1000 | 1000 | 1000 |
| Void ratio e | 0,76 | 0,57 | 0,77 | 0,57 | 0,66 | 0,52 | 0,65 | 0,52 | 0,69 | 0,49 | 0,66 | 0,49 |
| Sr Required | 1,00 | 1,00 | 1,00 | 1,00 | 1,00 | 1,00 | 1,00 | 1,00 | 1,00 | 1,00 | 1,00 | 1,00 |
| Water content required | 0,28 | 0,21 | 0,29 | 0,21 | 0,25 | 0,19 | 0,24 | 0,20 | 0,26 | 0,18 | 0,25 | 0,18 |
| After initial moisture | 0,18 | 0,11 | 0,18 | 0,11 | 0,21 | 0,15 | 0,20 | 0,16 | 0,20 | 0,13 | 0,19 | 0,13 |
| % | 17,84 | 10,90 | 18,49 | 10,80 | 20,85 | 15,33 | 20,35 | 15,53 | 20,04 | 12,61 | 19,05 | 12,68 |
| Liter water needed | 3,57 | 2,18 | 3,70 | 2,16 | 4,17 | 3,07 | 4,07 | 3,11 | 4,01 | 2,52 | 3,81 | 2,54 |
| Height 1 (mm) | 22 | 26 | 24 | 30 | 20 | 22 | 23 | 26 | 19 | 22 | 21 | 29 |
| Height 2 (mm) | 67 | 40 | 70 | 42 | 44 | 28 | 65 | 31 | 48 | 26 | 62 | 38 |
| Settle Amount | 45 | 14 | 46 | 12 | 24 | 6 | 42 | 5 | 29 | 4 | 41 | 9 |
| Tested at 'g' | 0,15 | 0,15 | 0,25 | 0,25 | 0,15 | 0,15 | 0,25 | 0,25 | 0,15 | 0,15 | 0,25 | 0,25 |
| **Liquefaction?** | **Yes** | **Yes** | **Yes** | **Yes** | **Yes** | **Yes** | **Yes** | **Yes** | **Yes** | **No** | **Yes** | **Yes** |
| At what time? Seconds | 10 | 15 | 8 | 12 | 10 | 14 | 7 | 9 | 15 | - | 18 | 55 |
| If not, did it liquefy after 60sec? | | | | | | | | | | **Yes** | | |
| At what g'? | | | | | | | | | | 0,15 | | |
| After how long? Seconds | | | | | | | | | | 65 | | |

*Vibration Table Results Continue*

| Test # | 1 | 2 | 3 | 4 | 1 | 2 | 3 | 4 |
|---|---|---|---|---|---|---|---|---|
| Site | Pre graded 0,150 | | | | Pre graded 0,425 | | | |
| Soil Description | Yellowish sand | | | | Yellowish sand | | | |
| Sample Weight Kg | 20 | 20 | 20 | 20 | 20 | 20 | 20 | 20 |
| Initial Moisture | 2,5 | 2,5 | 2,5 | 2,5 | 2,2 | 2,2 | 2,2 | 2,2 |
| Content (%) | 0,025 | 0,025 | 0,025 | 0,025 | 0,022 | 0,022 | 0,022 | 0,022 |
| Compacted? | No | Yes | No | Yes | No | Yes | No | Yes |
| Density kg/m3 | 1622 | 1690 | 1635 | 1685 | 1610 | 1666 | 1614 | 1682 |
| Gs | 2,67 | 2,67 | 2,67 | 2,67 | 2,67 | 2,67 | 2,67 | 2,67 |
| Gamma Water | 1000 | 1000 | 1000 | 1000 | 1000 | 1000 | 1000 | 1000 |
| Void ratio e | 0,65 | 0,58 | 0,63 | 0,58 | 0,66 | 0,60 | 0,65 | 0,59 |
| Sr Required | 1,00 | 1,00 | 1,00 | 1,00 | 1,00 | 1,00 | 1,00 | 1,00 |
| Water content required | 0,24 | 0,22 | 0,24 | 0,22 | 0,25 | 0,23 | 0,25 | 0,22 |
| After initial moisture | 0,22 | 0,19 | 0,21 | 0,19 | 0,22 | 0,20 | 0,22 | 0,20 |
| % | 21,70 | 19,22 | 21,21 | 19,39 | 22,46 | 20,37 | 22,30 | 19,80 |
| Liter water needed | 4,34 | 3,84 | 4,24 | 3,88 | 4,49 | 4,07 | 4,46 | 3,96 |
| Height 1 (mm) | 25 | 28 | 24 | 26 | 28 | 33 | 30 | 32 |
| Height 2 (mm) | 30 | 30 | 31 | 28 | 68 | 35 | 72 | 47 |
| Settle Amount | 5 | 2 | 7 | 2 | 40 | 2 | 42 | 15 |
| Tested at 'g' | 0,15 | 0,15 | 0,25 | 0,25 | 0,15 | 0,15 | 0,25 | 0,25 |
| **Liquefaction?** | **No** | **No** | **No** | **No** | **Yes** | **No** | **Yes** | **Yes** |
| At what time? Seconds | - | - | - | - | 25 | - | 22 | 30 |
| If not, did it liquefy after 60sec? | **No** | **No** | **No** | **No** | | **Yes** | | |
| At what g'? | 0,35 | 0,35 | 0,35 | 0,35 | | 0,25 | | |
| After how long? Seconds | No after 120 | No after 120 | No after 120 | No after 120 | | 95 | | |

### 4.5.3 Results from second phase of testing

Results from the first phase led to the manual grading of eleven more samples. These samples have also been tested on the vibrating table and the resulting data are presented in Table 4.6. All the tests were conducted at 0.15g and at a duration of 60 seconds. The settlement is also noted at the end of the 60 seconds.

*Table 4.6: Vibration table results for second phase of testing*

| Test # | 1 | 2 | 3 | 4 | 1 | 2 | 3 | 4 | 1 | 2 | 3 | 4 |
|---|---|---|---|---|---|---|---|---|---|---|---|---|
| Sample # | 1 | | | | 2 | | | | 3 | | | |
| Gradation | Uniformly graded | | | | Gap graded | | | | Gap graded | | | |
| Soil Description | Light greyish brown sand | | | | Light greyish brown sand | | | | Light greyish brown sand | | | |
| Sample Weight Kg | 20 | 20 | 20 | 20 | 20 | 20 | 20 | 20 | 20 | 20 | 20 | 20 |
| Initial Moisture Content (%) | 2,4 | 2,4 | 2,4 | 2,4 | 3,1 | 3,1 | 3,1 | 3,1 | 2 | 2 | 2 | 2 |
| | 0,024 | 0,024 | 0,024 | 0,024 | 0,031 | 0,031 | 0,031 | 0,031 | 0,02 | 0,02 | 0,02 | 0,02 |
| Compacted? | No | No | Yes | Yes | No | No | Yes | Yes | No | No | Yes | Yes |
| Density kg/m3 | 1522 | 1538 | 1810 | 1818 | 1608 | 1624 | 1989 | 2008 | 1588 | 1611 | 1977 | 1986 |
| Gs | 2,67 | 2,67 | 2,67 | 2,67 | 2,67 | 2,67 | 2,67 | 2,67 | 2,67 | 2,67 | 2,67 | 2,67 |
| Gamma Water | 1000 | 1000 | 1000 | 1000 | 1000 | 1000 | 1000 | 1000 | 1000 | 1000 | 1000 | 1000 |
| Void ratio e | 0,75 | 0,74 | 0,48 | 0,47 | 0,66 | 0,64 | 0,34 | 0,33 | 0,68 | 0,66 | 0,35 | 0,34 |
| Sr Required | 1,00 | 1,00 | 1,00 | 1,00 | 1,00 | 1,00 | 1,00 | 1,00 | 1,00 | 1,00 | 1,00 | 1,00 |
| Water content required | 0,28 | 0,28 | 0,18 | 0,18 | 0,25 | 0,24 | 0,13 | 0,12 | 0,26 | 0,25 | 0,13 | 0,13 |
| After initial moisture | 0,26 | 0,25 | 0,15 | 0,15 | 0,22 | 0,21 | 0,10 | 0,09 | 0,24 | 0,23 | 0,11 | 0,11 |
| % | 25,85 | 25,17 | 15,40 | 15,15 | 21,64 | 21,02 | 9,72 | 9,25 | 23,52 | 22,62 | 11,13 | 10,90 |
| Liter water needed | 5,17 | 5,03 | 3,08 | 3,03 | 4,33 | 4,20 | 1,94 | 1,85 | 4,70 | 4,52 | 2,23 | 2,18 |
| Height 1 (mm) | 20 | 24 | 18 | 17 | 25 | 22 | 30 | 33 | 19 | 23 | 25 | 28 |
| Height 2 (mm) | 59 | 50 | 29 | 36 | 48 | 43 | 32 | 39 | 59 | 48 | 29 | 37 |
| Settle Amount | 39 | 26 | 11 | 19 | 23 | 21 | 2 | 6 | 40 | 25 | 4 | 9 |
| Tested at 'g' | 0,15 | | | | 0,15 | | | | 0,15 | | | |
| Liquefaction? | Yes | Yes | Yes | Yes | Yes | Yes | No | No | Yes | Yes | No | No |
| At what time? Seconds | 11 | 14 | 28 | 40 | 10 | 8 | - | - | 15 | 21 | - | - |

103

*Vibration table results for second phase of testing (continue)*

| Test # | 1 | 2 | 3 | 4 | 1 | 2 | 3 | 4 | 1 | 2 | 3 | 4 |
|---|---|---|---|---|---|---|---|---|---|---|---|---|
| Site | 4 | | | | 5 | | | | 6 | | | |
| Gradation | Gap graded | | | | Gap graded | | | | Gap graded | | | |
| Soil Description | Light greyish brown sand | | | | Light greyish brown sand | | | | Light greyish brown sand | | | |
| Sample Weight Kg | 20 | 20 | 20 | 20 | 20 | 20 | 20 | 20 | 20 | 20 | 20 | 20 |
| Initial Moisture Content (%) | 1,8 | 1,8 | 1,8 | 1,8 | 2,2 | 2,2 | 2,2 | 2,2 | 2,8 | 2,8 | 2,8 | 2,8 |
| | 0,018 | 0,018 | 0,018 | 0,018 | 0,022 | 0,022 | 0,022 | 0,022 | 0,028 | 0,028 | 0,028 | 0,028 |
| Compacted? | No | No | Yes | Yes | No | No | Yes | Yes | No | No | Yes | Yes |
| Density kg/m3 | 1562 | 1579 | 1902 | 1898 | 1628 | 1620 | 1856 | 1861 | 1613 | 1599 | 1814 | 1844 |
| Gs | 2,67 | 2,67 | 2,67 | 2,67 | 2,67 | 2,67 | 2,67 | 2,67 | 2,67 | 2,67 | 2,67 | 2,67 |
| Gamma Water | 1000 | 1000 | 1000 | 1000 | 1000 | 1000 | 1000 | 1000 | 1000 | 1000 | 1000 | 1000 |
| Void ratio e | 0,71 | 0,69 | 0,40 | 0,41 | 0,64 | 0,65 | 0,44 | 0,43 | 0,66 | 0,67 | 0,47 | 0,45 |
| Sr Required | 1,00 | 1,00 | 1,00 | 1,00 | 1,00 | 1,00 | 1,00 | 1,00 | 1,00 | 1,00 | 1,00 | 1,00 |
| Water content required | 0,27 | 0,26 | 0,15 | 0,15 | 0,24 | 0,24 | 0,16 | 0,16 | 0,25 | 0,25 | 0,18 | 0,17 |
| After initial moisture | 0,25 | 0,24 | 0,13 | 0,13 | 0,22 | 0,22 | 0,14 | 0,14 | 0,22 | 0,22 | 0,15 | 0,14 |
| % | 24,77 | 24,08 | 13,32 | 13,43 | 21,77 | 22,08 | 14,23 | 14,08 | 21,74 | 22,29 | 14,87 | 13,98 |
| Liter water needed | 4,95 | 4,82 | 2,66 | 2,69 | 4,35 | 4,42 | 2,85 | 2,82 | 4,35 | 4,46 | 2,97 | 2,80 |
| Height 1 (mm) | 18 | 20 | 26 | 31 | 22 | 24 | 28 | 29 | 18 | 20 | 24 | 25 |
| Height 2 (mm) | 33 | 41 | 30 | 41 | 28 | 37 | 30 | 35 | 39 | 38 | 34 | 33 |
| Settle Amount | 15 | 21 | 4 | 10 | 6 | 13 | 2 | 6 | 21 | 18 | 10 | 8 |
| Tested at 'g' | 0,15 | | | | 0,15 | | | | 0,15 | | | |
| **Liquefaction?** | **Yes** | **Yes** | **No** | **No** | **No** | **Yes** | **No** | **No** | **Yes** | **Yes** | **Yes Partially** | **No** |
| At what time? Seconds | 12 | 8 | - | - | - | 33 | - | - | 14 | 22 | 29 | - |

104

*Vibration table results for second phase of testing (continue)*

| Test # | 1 | 2 | 3 | 4 | 1 | 2 | 3 | 4 | 1 | 2 | 3 | 4 |
|---|---|---|---|---|---|---|---|---|---|---|---|---|
| Site | 7 | | | | 8 | | | | 9 | | | |
| Gradation | Gap graded | | | | Gap - Uniformly graded | | | | Gap graded | | | |
| Soil Description | Light greyish brown sand | | | | Light greyish brown sand | | | | Light greyish brown sand | | | |
| Sample Weight Kg | 20 | 20 | 20 | 20 | 20 | 20 | 20 | 20 | 20 | 20 | 20 | 20 |
| Initial Moisture Content (%) | 2,5 | 2,5 | 2,5 | 2,5 | 2,4 | 2,4 | 2,4 | 2,4 | 1,9 | 1,9 | 1,9 | 1,9 |
| | 0,025 | 0,025 | 0,025 | 0,025 | 0,024 | 0,024 | 0,024 | 0,024 | 0,019 | 0,019 | 0,019 | 0,019 |
| Compacted? | No | No | Yes | Yes | No | No | Yes | Yes | No | No | Yes | Yes |
| Density kg/m3 | 1798 | 1811 | 1991 | 2002 | 1600 | 1651 | 1819 | 1833 | 1712 | 1650 | 1912 | 1897 |
| Gs | 2,67 | 2,67 | 2,67 | 2,67 | 2,67 | 2,67 | 2,67 | 2,67 | 2,67 | 2,67 | 2,67 | 2,67 |
| Gamma Water | 1000 | 1000 | 1000 | 1000 | 1000 | 1000 | 1000 | 1000 | 1000 | 1000 | 1000 | 1000 |
| Void ratio e | 0,48 | 0,47 | 0,34 | 0,33 | 0,67 | 0,62 | 0,47 | 0,46 | 0,56 | 0,62 | 0,40 | 0,41 |
| Sr Required | 1,00 | 1,00 | 1,00 | 1,00 | 1,00 | 1,00 | 1,00 | 1,00 | 1,00 | 1,00 | 1,00 | 1,00 |
| Water content required | 0,18 | 0,18 | 0,13 | 0,12 | 0,25 | 0,23 | 0,18 | 0,17 | 0,21 | 0,23 | 0,15 | 0,15 |
| After initial moisture | 0,16 | 0,15 | 0,10 | 0,10 | 0,23 | 0,21 | 0,15 | 0,15 | 0,19 | 0,21 | 0,13 | 0,13 |
| % | 15,66 | 15,26 | 10,27 | 10,00 | 22,65 | 20,72 | 15,12 | 14,70 | 19,06 | 21,25 | 12,95 | 13,36 |
| Liter water needed | 3,13 | 3,05 | 2,05 | 2,00 | 4,53 | 4,14 | 3,02 | 2,94 | 3,81 | 4,25 | 2,59 | 2,67 |
| Height 1 (mm) | 19 | 23 | 26 | 30 | 21 | 20 | 24 | 29 | 17 | 22 | 26 | 30 |
| Height 2 (mm) | 56 | 58 | 32 | 40 | 60 | 57 | 38 | 47 | 58 | 54 | 38 | 46 |
| Settle Amount | 37 | 35 | 6 | 10 | 39 | 37 | 14 | 18 | 41 | 32 | 12 | 16 |
| Tested at 'g' | 0,15 | | | | 0,15 | | | | 0,15 | | | |
| Liquefaction? | Yes | Yes | No | No | Yes | Yes | Yes | Yes | Yes | Yes | Yes Partially | Yes |
| At what time? Seconds | 5 | 13 | - | - | 11 | 7 | 44 | 38 | 15 | 12 | 18 | 47 |

*Vibration table results for second phase of testing (continue)*

| Test # | 1 | 2 | 3 | 4 | 1 | 2 | 3 | 4 |
|---|---|---|---|---|---|---|---|---|
| Site | 10 | | | | 11 | | | |
| Gradation | Well graded | | | | Well graded | | | |
| Soil Description | Light greyish brown sand | | | | Light greyish brown sand | | | |
| Sample Weight Kg | 20 | 20 | 20 | 20 | 20 | 20 | 20 | 20 |
| Initial Moisture Content (%) | 2 | 2 | 2 | 2 | 1,7 | 1,7 | 1,7 | 1,7 |
| | 0,02 | 0,02 | 0,02 | 0,02 | 0,017 | 0,017 | 0,017 | 0,017 |
| Compacted? | No | No | Yes | Yes | No | No | Yes | Yes |
| Density kg/m3 | 1588 | 1601 | 1885 | 1914 | 1614 | 1592 | 1798 | 1810 |
| Gs | 2,67 | 2,67 | 2,67 | 2,67 | 2,67 | 2,67 | 2,67 | 2,67 |
| Gamma Water | 1000 | 1000 | 1000 | 1000 | 1000 | 1000 | 1000 | 1000 |
| Void ratio e | 0,68 | 0,67 | 0,42 | 0,39 | 0,65 | 0,68 | 0,48 | 0,48 |
| Sr Required | 1,00 | 1,00 | 1,00 | 1,00 | 1,00 | 1,00 | 1,00 | 1,00 |
| Water content required | 0,26 | 0,25 | 0,16 | 0,15 | 0,25 | 0,25 | 0,18 | 0,18 |
| After initial moisture | 0,24 | 0,23 | 0,14 | 0,13 | 0,23 | 0,24 | 0,16 | 0,16 |
| % | 23,52 | 23,01 | 13,60 | 12,79 | 22,80 | 23,66 | 16,46 | 16,10 |
| Liter water needed | 4,70 | 4,60 | 2,72 | 2,56 | 4,56 | 4,73 | 3,29 | 3,22 |
| Height 1 (mm) | 18 | 20 | 27 | 29 | 22 | 19 | 28 | 27 |
| Height 2 (mm) | 33 | 40 | 35 | 39 | 29 | 30 | 34 | 31 |
| Settle Amount | 15 | 20 | 8 | 10 | 7 | 11 | 6 | 4 |
| Tested at 'g' | 0,15 | | | | 0,15 | | | |
| Liquefaction? | Yes | Yes | No | Yes Partially | No | Yes Partially | No | No |
| At what time? Seconds | 17 | 22 | - | 30 | - | 26 | - | - |

106

### 4.5.3.1    Analysis of first phase of testing

The first phase of testing clearly indicate that soils with a higher density were more resistant to liquefaction compared to soils with lower densities. In addition, liquefaction occurred much sooner at a higher PGA.

### 4.5.3.2    University of the Western Cape

All the bulk samples from UWC experienced liquefaction and a large amount of settlement. Liquefaction occurred within 10-12 seconds for the looser samples at both 0.15g and 0.25g, and within 15 – 16 seconds for the denser, more compacted samples. There was also considerably less settlement for the compacted, denser samples.



*Figure 4.34: Liquefied soils for the UWC site*

### 4.5.3.3    Langa Shopping Centre

The Langa soil samples had gradings similar to that of UWC, and evidently more or less the same outcome in terms of liquefaction. One sample did however resist liquefaction for a relatively long time, up to 72 seconds. The sample was compacted to $1805kg/m^3$ and was continuously vibrated at 0.15g. However, settlement of 8 mm occurred within the first 60 seconds. The second compacted sample for Langa had a density of $1795kg/m^3$ and were exposed to an acceleration of 0.25g from the start. The second sample failed and experienced liquefaction within 20 seconds. This is much shorter than the 72 seconds exposed to 0.15g but at a somewhat denser state.

### 4.5.3.4    Talana Road, Bellville

The samples from Talana Road all experienced liquefaction. The gradings were once again similar to that of UWC and Langa. There is also a small percentage of larger grain sizes within the Talana Road sample. However, this did not seem to influence the resistance of the soil to liquefy during shearing. All samples experienced large amounts of settlement and failed within 15 seconds.

### 4.5.3.5    Bardale Village

All samples from Bardale village liquefied within 14 seconds. Considerably less settlement was noted for the lower acceleration compacted sample compared to the higher acceleration compacted sample. The gradings from the Bardale Village site can be compared to the gradings of Talana Road, as they have a more or less similar sieve distribution.

### 4.5.3.6    Mitchells Plain Station

Samples from the Mitchells Plain Station had some resistance to liquefaction initially. The un-compacted samples for this site experienced liquefaction only after 15 and 18 seconds for the accelerations of 0.15g and 0.25g, respectively. This is an increase of approximately 50% in liquefaction resistance time for the Mitchells Plain Station area. The compacted samples had a longer resistance time to liquefaction. The compacted samples exposed to 0.15g and 0.25g only experienced liquefaction after 65 and 55 seconds, respectively. This is interesting, as the Mitchells Plain Station sample has a grading similar to that of Langa, which also had some resistance initially.

### 4.5.3.7    Pre – Graded Sands of 0.150

The pre-graded samples of 0.150 (uniformly graded) experienced no liquefaction. It was also difficult to compact the samples to more than 1685kg/m$^3$. Samples that were placed in the loose state, were also relatively dense compared to other samples. The test sample with the lowest density in this pre-graded soil sample was 1622kg/m$^3$. The difficulty in compaction can probably be due to the same-size of the grains that made compaction difficult. The sample with the lowest density in the entire first phase test series was that Talana Road, Bellville, with a density of 1505kg/m$^3$. The highest density sample in the first phase of testing was that of the Langa sample that had a density of 1805kg/m$^3$ and resisted liquefaction for some time.

The acceleration on the 0.150 pre-graded sands were gradually increased until an acceleration level of 0.35g's were reached. Liquefaction still did not occur, and this can probably be explained by the smaller grain sizes (uniformly graded) that are packed more tightly than that of larger grains, leaving less space for internal settlement and water to accumulate. The sample was also exposed to two bricks next to each other, to determine if this will have any effect on surface loading. The result was almost similar to that of the first test with the same soil type. No real significant observation was made.

*Figure 4.35: Sample of sand that resisted liquefaction*

### 4.5.3.8   Pre – Graded Sands of 0.450

The pre-graded soils of 0.425 indicated some resistance to liquefaction. However, all samples experienced liquefaction eventually. The un-compacted samples resisted liquefaction for 25 and 22 seconds at 0.15g and 0.25g, respectively.

The compacted sample at an initial acceleration of 0.15g did not liquefy and only 2 mm of settlement was registered within the first 60 seconds. The sample was continuously vibrated, not stopping after 60 seconds, and eventually experienced liquefaction after 95 seconds at 0.25g. The compacted sample exposed to an initial 0.25g's experienced liquefaction after 30 seconds of continuous shearing.

### 4.5.4   Summary – first phase of testing

Observations made from the vibration table testing shows that compaction and finer sand grains have a positive effect towards soil liquefaction resistance. The settlement of the brick during shearing was recorded and is plotted with the density of the sample and acceleration of the shearing event. The results from the first phase was somewhat insufficient and no real conclusion could be made with regards to the number of fines and the result thereof on liquefaction resistance.

### 4.5.5   Second phase of testing analysis

The 11 additional samples indicated a similar trend where an increase in density provided more resistance to liquefaction compared to looser samples. No conclusive observation could be made with regards to the number of fines. Samples 2, 3, 4, 5, 6, 7, 10 and 11 resisted liquefaction at a compacted state. From the grading curves in the soil property section, all these samples have some part of the grading curve that lie outside of the red boundary lines and all the samples are either gap graded or well graded. The only exception was that of sample 3 that is partially uniformly graded and partially well graded. Sample 9 is however also gap graded, well compacted but did experience liquefaction. The only difference was that sample 9 contains 50% of fine to very fine sand. It can perhaps be said that the

109

number of fine sands in the grading range of 0.425-0.150mm could be a key factor to liquefaction resistance.

### 4.5.6    Combined analysis from phase one and two

To prove the previous statements regarding the number of fine sand and liquefaction resistance, a series of scatter plots were created. The effect of density and settlement of the brick is displayed in Figure 4.36. The graph indicates all 64 results, with symbols indicating each bulk sample. As mentioned before, each sample has four tests, hence four symbols per sample. Refer to the grading results and grading curves for each of these samples (Section 4.4.3).
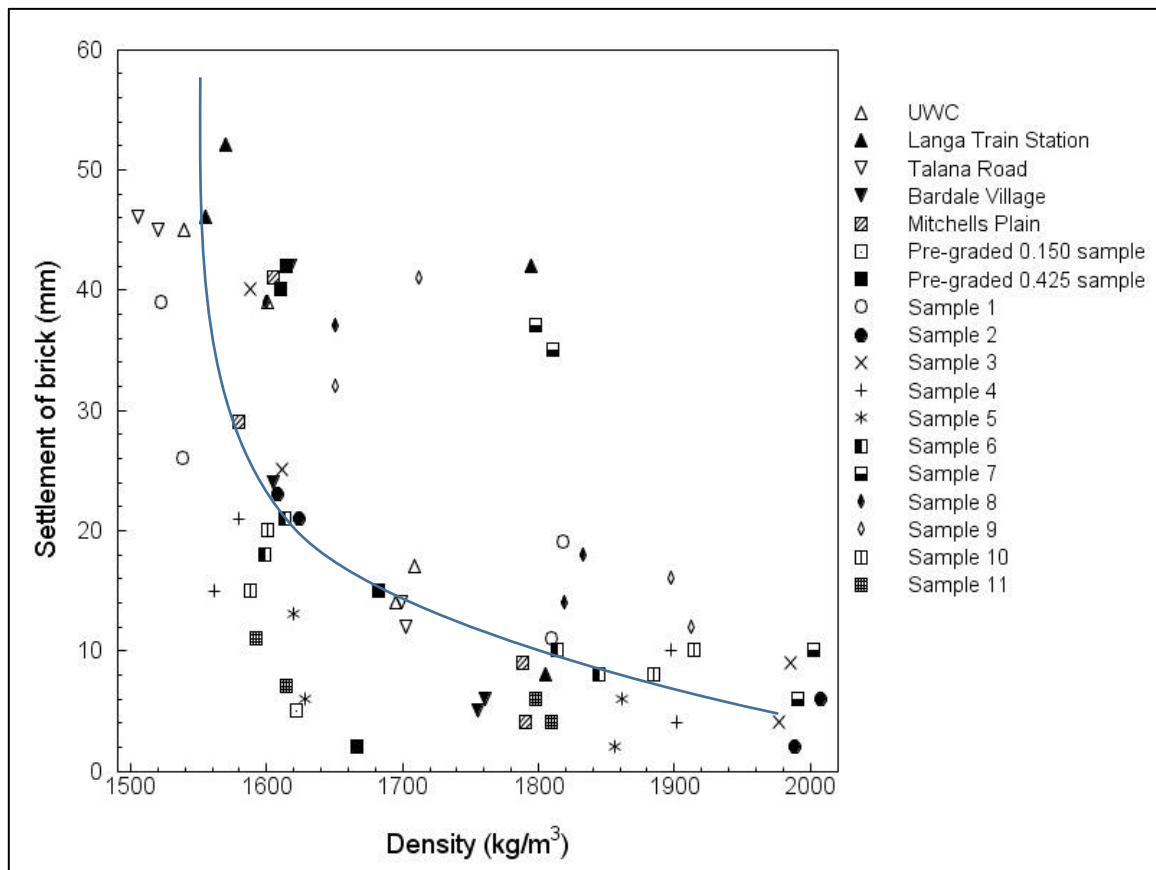


*Figure 4.36: Settlement vs Density of Sample*

The settlement to density graph proves the first assumption of an increase in density having more resistance to liquefaction, or in this case settlement, compared to lower density samples. The majority of the samples lie near the trendline and appear to follow the same pattern. Some results, such as the uncompacted sample 7, lie outside of this trendline. Sample 7 is a gap graded soil with a higher uncompacted density compared to that of the other uncompacted samples that experienced much lower settlement. This could be because of the electrical motor in the vibration table being unable or inaccurate in maintaining a consistent speed. Samples that lie outside of the trendline, with similar soil gradings to other samples, should preferably be discarded as results. Samples 10 and 11 are both well graded soil

samples. The denser samples either resisted liquefaction entirely or partially, whereas the looser samples from sample 10 experienced liquefaction. Sample 11 resisted liquefaction in the compacted state and partially resisted liquefaction in the loose, uncompacted state. Sample 11 had a smaller amount of gravels and larger amount of fine sand compared to that of sample 10.

Three additional graphs were created (Figure 4.37) to plot the percentage passing through each of the three different sieve sizes (4.75, 0.425 and 0.075mm), compared to the settlement. At first, no particular amount of settlement stands out with a certain grading when comparing the three graphs. Of particular interest is that of settlement noted with the number of fines (percentage passing the 0.075mm sieve). Samples with a fines content of up to 50% experienced more or less the same amount of settlement compared to samples of approximately 5% fines. The same can be said for the other two graphs (a and b), where no specific grading percentage led to more or lower settlement.
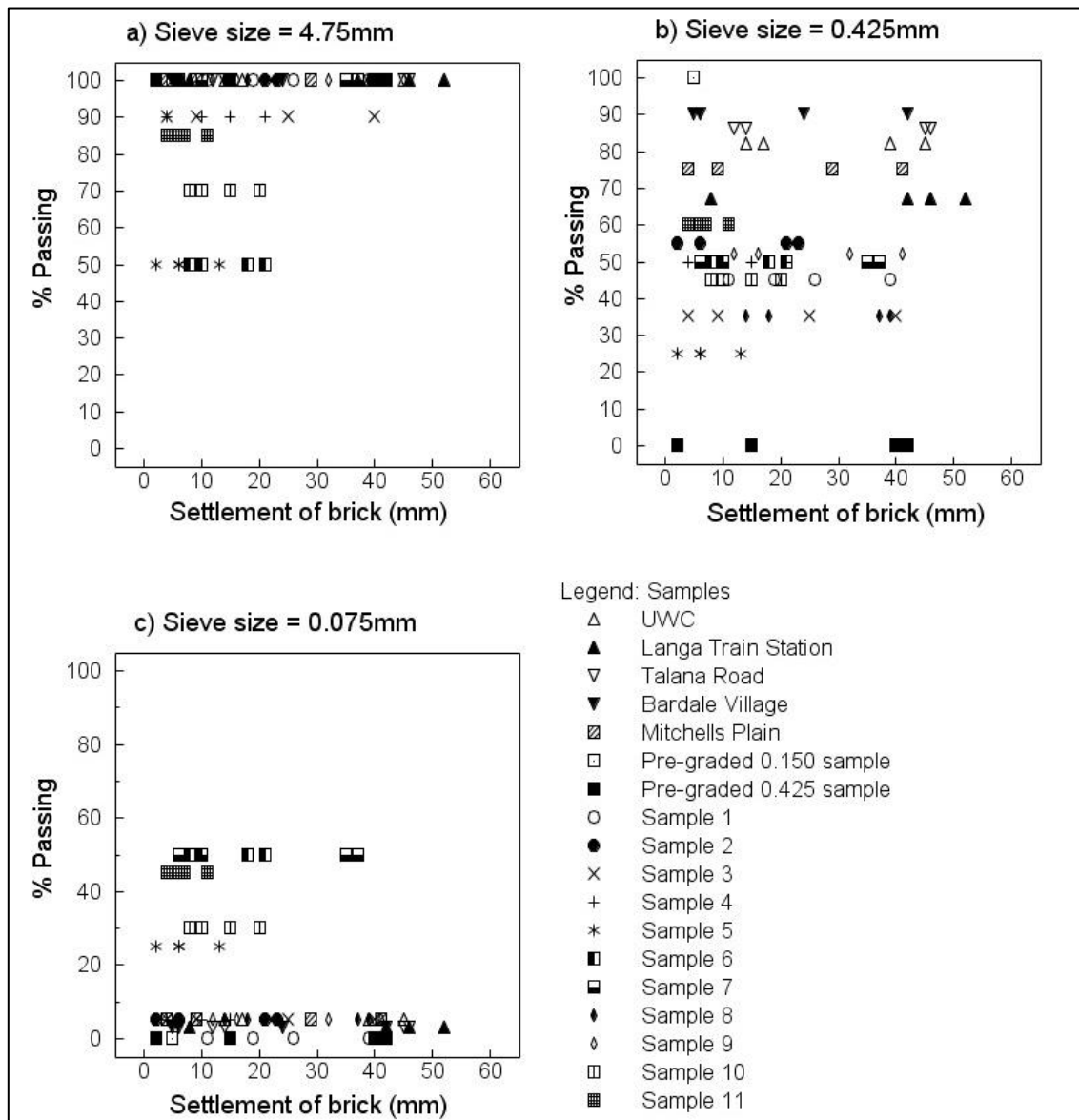


*Figure 4.37: Grading vs settlement of sample*

Figure 4.36 shows a clear, almost linear relation of density and settlement. This can be seen by the trendline. Furthermore, the range in settlement variations is due to different initial densities and acceleration. Finally, one proven assumption made was that compaction increases liquefaction resistance and lowers settlement. Samples that experienced liquefaction and large settlement can probably be said to have contracted during shear, while samples that resisted liquefaction exhibited dilatant properties.

112

# 5   Conclusions and Recommendations

## 5.1   To conclude

Liquefaction has been proven to be a high-risk geotechnical problem for the lower lying areas of the greater Cape Peninsula, especially the Cape Flats. Areas with a shallow water table and relatively loose sands are especially vulnerable. Results from SPT testing and DPSH derived testing generally indicate that the tested soils are dense enough to resist liquefaction at an expected PGA of 0.15g and a magnitude of M=6. If the same data is analysed at a PGA of 0.25g and M=8, liquefaction will occur in all of the tested locations. This basically means that the tested area has some resistance to liquefaction at low PGA's and would be more susceptible to liquefaction if a higher magnitude earthquake occurred.

Essentially, piezocone penetrometer results indicate results similar to those of the SPT results, stating that soils are generally dense enough to resist liquefaction. The two tested areas will rather dilate than contract during shear. At the Geoscience Laboratories site loose and contractive zones were encountered and could perhaps form small localised sand boils during shear, considering they are at depth, approximately two to three and four to six meters below ground level. If the potentially contractive horizon is spread out over an area, then large scale liquefaction could occur in this area. The SPT graphs created with the Gregg Software tool indicates that some of the soils at Geoscience Laboratories are very loose, some below a SPT-N value of 10. Liquefaction can be possible in this area if the results are compared to the SPT factor of safety graphs, even at a PGA of only 0.15g and a magnitude of M=6. Furthermore, flow liquefaction and cyclic liquefaction can occur if the soils contract, and cyclic liquefaction can occur in areas that are characterized as dilative.

The gradings of 46 samples across the Cape Town Metropolitan area were plotted on a bar diagram, Figure 4.15, and compared to liquefied samples from case studies, Figure 3.12. A total of 16 bulk samples were also tested on a vibration table, and grading curves were created for these samples. If one only compares soil characteristics to that of liquefied case studies, then one can argue that almost all of the samples will experience liquefaction. The literature and case studies could not confirm that any specific number of fines will be more prone to liquefaction. The number of fines in a given soil had no influence on liquefaction resistance on the vibration table. No conclusive evidence or assumptions could be made regarding soil structure or the size of grains. Instead the only conclusion made was that soils with a higher density resisted liquefaction either entirely or longer. The density prior to liquefaction was determined and could perhaps be used to determine the ideal density for soils to resist liquefaction or excessive settlement during seismic activity. These densities could be used in conjunction with the minimum SPT-N value required to resist liquefaction.

## 5.2    Measures to limit potential for liquefaction

Liquefaction proved to be possible on the Cape Flats during a large seismic event, such as an earthquake. Various methods do however exist to increase a soil's capability to resist liquefaction. The primary and most obvious is that of compaction. From the case studies, medium dense soils with a SPT-N value of approximately N=10 should resist liquefaction. If one were to design for a higher PGA and earthquake magnitude, then one would need a SPT-N value of at least N=10. Liquefaction is of no risk in areas where a deep-water table is present. Excessive settlement could still occur, and this should be approached differently. If only the first 1-2m is loose, then conventional compaction could be used to densify the soils. Foundations can also be founded slightly deeper onto these denser underlying soils. Conventional compaction such as vibratory rollers will not work if deep layers of loose soils are present

Three primary conditions can be improved to reduce the risk of liquefaction:

1. Increase the soil strength (CRR)
    a. Deep compaction methods such as rapid impact compaction or dynamic compaction. These are methods that physically compact the underlying soil layers by using a high-energy drop-weight or diesel-powered hammer.
    b. Deep soil mixtures and installation of stone columns and aggregate piers. Stone columns can be installed in loose soil horizons and are generally installed by drilling a large diameter hole into the ground and filling it with stone aggregate. These stones are vibrated while being placed, effectively densifying the soil body around the stone column.
    c. Grouting of large areas. A cement slurry or grout is pumped into the ground to fill open pores and voids to cement and densify the area. This method is however not very effective.
2. Decrease the driving shear (CSR)
    a. Installing stiffer stronger material at pre-defined locations across the site to limit the horizontal stress, such as a material that will absorb or reduce any shear or ground movements.
3. Decrease the excess pore water pressure quickly during shear
    a. Installing drainage lines in the form of permeable layers and any method that can drain excess pore water pressure away quickly enough during shearing.

## 5.3    Recommendations for future studies

The biggest limitation in this study was the vibration table. A future study should perhaps obtain a larger vibration table with a more sensitive and accurate electrical motor to better control acceleration. One could perhaps also use active pore pressure sensors within the containers to accurately measure pressure and determine the critical state of the soil during shear.

SPT and DPSH samples were sufficient for the purpose of this study. More data is however needed to accurately identify potential high-risk liquefaction areas and perhaps create a liquefaction potential map of the greater Cape Town Metropolitan area. The CPT samples were also sufficient for use in this thesis. The testing procedure is however very expensive and trained personnel is required in both operating and analysing of the results. More of these tests on the Cape Flats will only contribute to our limited CPT data for study area.

The use of other laboratory testing methods could also be considered. The triaxial shear test could perhaps be used to determine the critical state of a soil sample and how it behaves at this point. This data can then be compared to literature data and empirical correlations.

# 6   References

Allaby, M., 2008. *Dictionary of Earth Sciences.* 3rd ed. Oxford: Oxford University Press.

Andrews, D. C. & Martin, G. R., 2000. *Criteria for liquefaction of silty soils.* Hong Kong, 12WCEE.

Andrus , R. D. & Stokoe, K. H., 2000. Liquefaction Resistance of Soils from Shear-Wave Velocity. *Journal of Geotechnical and Geoenvironmental Engineering ,* 126(11), pp. 1015-1025.

Atkinson, J., 2000. *University of the West of England.* [Online]
Available at: http://environment.uwe.ac.uk/geocal/SoilMech/classification/default.htm
[Accessed 29 July 2018].

Byrne, G., Berry, A. & Braatvedt, I., 2008. *A guide to practical geotechnical engineering in South Africa.* Fouth ed. Johannesburg: VIVO Design.

Chamber of Mines, 1994. *Chamber of Mines.* [Online]
Available at: http://www.chamberofmines.org.za/industry-news/we-care-we-remember/324-we-remember-merriespruit
[Accessed 04 June 2017].

Chih-Chieh, L., Jin-Hung, H. & Shang-Yi, H., 2017. The impact evaluation of soil liquefaction on low-rise building in the Meinong earthquake. *Earth, Planets and Space,* 109(69), p. 16.

Cichowicz, A. & Kijko, A., 2006. *Origin, Intensity and Damage Potential of Tectonic and Mining Seismic Events,* Johannesburg: Seismological Unit, Council for Geoscience.

City of Cape Town, 2011. *Spatial Development Plan and Environmental Management Framework,* Cape Town: City of Cape Town.

Craig, R. F., 2010. *Craig's Soil Mechanics.* Seventh ed. New York: Spon Press.

Davids, J., 2001. *PEER.* [Online]
Available at: http://peer.berkeley.edu/publications/nisqually/geotech/liquefaction/distribution/
[Accessed 22 March 2017].

De La Harpe, C. W., 2015. *The development of a seismic risk reduction procedure for the prioritization of low cost, load bearing masonry buildings,* Stellenbosch: Stellenbosch University .

Earthquaketrack, 2016. *Earthquake track.* [Online]
Available at: http://earthquaketrack.com/za-11-ceres/recent
[Accessed 18 February 2016].

Fabbrocino, G., Dipendra, G. & de Magistris, F. S., 2017. Soil liquefaction in Kathmandu valley due to 25 April 2015 Gorkha, Nepal earthquake. *Elsevier,* 97(97), pp. 37-47.

Gandomi, A. H., Fridline, M. M. & Roke, D. A., 2013. Decision Tree Approach for Soil Liquefaction Assessment. *The ScientificWorld Journal*, 30 August, p. 9.

GeoLogismiki, 2007. *GeoLogismiki,* California: Gregg Drilling and Testing.

Guzman, . J. A. & Fernandez, L. M., 1978. *Seismic History of Southern Africa,* s.l.: Council for Geoscience.

Hartnady, C. J. H., 2003. Cape Town Earthquakes: Review of the Historical Record. p. 16.

Hutchings, M., 2015. *The Daily Meverick.* [Online]
Available at: https://www.dailymaverick.co.za/article/2015-06-01-right-of-response-cape-town-spends-hundreds-of-millions-of-rand-on-informal-settlement-sanitation/#.WNIQ9FWGMdU
[Accessed 22 March 2017].

Idriss, I. M. & Boulanger, R. W., 2010. *SPT-BASED LIQUEFACTION TRIGGERING PROCEDURES,* California: UNIVERSITY OF CALIFORNIA.

Jefferies, M. & Shuttle, D., 2011. *Understanding Liquefaction Through Applied Geo Mechanics.* Santiago, 5th International Conference on Earthquake Geotechnical Engineering, pp. 1-33.

MacRobert, C. & Beales, P., 2011. Correlating Standard Penetration Test and Dynamic Probe Super Heavy penetration resistance values in sandy soils. *Journal of the South African Institution of Civil Engineers,* 53(1), pp. 46-55.

Mengfen, S. et al., 2016. Predicting liquefaction probability based on shear wave velocity. *Springer*, 18 April, pp. 1199-1214.

National Science Foundation (U.S.), 1985. *Liquefaction of Soils During Earthquakes.* Washington, D.C.: National Academy Press.

Nichols, G., 2009. *Sedimentology and Stratigraphy.* 2nd ed. Oxford: Blackwell Pupblishing.

NKuna, B., 2016. *West Cape News.* [Online]
Available at: http://westcapenews.com/?p=159
[Accessed 22 March 2017].

Norman, N. & Whitfield, G., 2006. *Geological Journeys.* 1st ed. Cape Town: Struik Nature.

Parker, R. J., 1991. *A study of the liquefaction potential of sandy soils with speacial reference to the cape flats.* First ed. Stellenbosch: Stellenbosch University.

Puri, V. K. & Kostecki, T. R., 2013. *Liquefaction of Mine Tailings.* Chicago, University of Carbondale, pp. 1-12.

Rauch, A. F., 1997. *An Empirical Method for Prediciting Surface Displacements Due to Liquefaction-Induced Lateral Spreading in Earthquakes.* [Online]
Available at: https://theses.lib.vt.edu/theses/available/etd-219182249741411/unrestricted/Etd.pdf
[Accessed 18 May 2017].

Roberts, D. L., Botha, G. A., Maud, R. R. & Pether, J., 2006. Coastal Cenozoic Deposits. In: M. R. Johnson, C. R. Anhaeusser & R. J. Thomas, eds. *The Geology Of South Africa.* Johannesburg: The Geological Society of South Africa, pp. 605-628.

Robertson, P. K., 2010. Evaluation of flow liquefaction and liquefied strength using the cone penetration test. *Journal of geotechnical and environmental engineering @ ASCE,* pp. 842-853.

Robertson, P. K. & Cabal, K. L., 2012. *Cone Penetration Testing for Geotechnical Engineering.* 5th ed. Signal Hill: Cregg Drilling.

Rothe, J. P., 1969. *USGS.* [Online]
Available at:
https://web.archive.org/web/20100128105443/http://earthquake.usgs.gov/earthquakes/world/events/1964_06_16.php
[Accessed 04 June 2017].

Sarsby, R., 2000. *Environmental Geotechnics.* London: Thomas Telford Publising.

Schofield, A. & Wroth, P., 2005. *Critical State Soil Mechanics.* 1st ed. Cambridge : Cambridge Press.

Seed, R. B. et al., 2003. *Recent advances in soil liquefaction engineering,* Berkeley: College of Engineering University of California.

Segun, A., Yongxin, X. & Vrbka, P., 2010. *South African Water Research Comission.* [Online]
Available at: www.wrc.org.za
[Accessed 14 May 2017].

Terzaghi, K., Peck, R. B. & Mesri, G., 1996. *Soil mechanics in engineering practice.* Third ed. New York: John Wiley & Sons Inc.,.

Thamm, A. G. & Johnson, M. R., 2009. The Cape Supergroup. In: M. R. Johnson, C. R. Anhaeusser & R. J. Thomas, eds. *The Geology of South Africa.* Johannesburg: The Geological Society of South Africa, pp. 443-457.

Theron, J. N., Gresse, P. G., Siegfried, H. P. & Rogers, J., 1992. *The Geology of the Cape Town Area.* 1st ed. Pretoria: Geological Survey.

Toerien, H., 2014. *Wanneer Suid Afrika deur aardbewings geskud word.* [Online]
Available at: http://maroelamedia.co.za/nuus/nuuskommentaar/nuuskommentaar-wanneer-suid-afrika-deur-aardbewings-geskud-word/
[Accessed 29 January 2016].

Totani, G. & Calabrese, M., 2001. *The Flat Dilatometer Test in soil investigations ,* L'Aqula: ISSMGE Committee TC16.

Wei, X. & Yang, J., 2015. *The Effects of Initial Static Shear Stress on Liquefaction Resistance of Silty Sand.* Christchurch, 6th International Conference on Earthquake Geotechnical Engineering.

Wium, J., 2010. Background to draft sans 10160 (2009): Part 4 seismic loading. *South African Institute of Civil Engineering ,* 52(1), pp. 20-27.

Yamaguchi, A., Mori, T., Kazama, M. & Yoshida, N., 2012. *Liquefaction in Tohoku district during the 2011 off the Pacific Coast of Tohoku Earthquake,* Tokyo: Elsevier.